Design and applications of protein delivery systems in nanomedicine and tissue engineering

Joëlle Bizeau, Damien Mertz

Design and Applications of Protein Delivery Systems in Nanomedicine and Tissue Engineering

Joëlle Bizeau[1] and Damien Mertz[1]

[1]Institut de Physique et Chimie des Matériaux de Strasbourg (IPCMS), UMR-7504 CNRS-Université de Strasbourg, 23 rue du Lœss, BP 34 67034, Strasbourg Cedex 2, France
Corresponding e-mail : damien.mertz@ipcms.unistra.fr

Abstract

Proteins are biological macromolecules involved in a wide range of biological functions, which makes them very appealing as therapeutics agents. Indeed, compared to small molecule drugs, their endogenous nature ensures their biocompatibility and biodegradability, they can be used in a large range of applications and present a higher specificity and activity. However, they suffer from unfolding, enzymatic degradation, short half-life and poor membrane permeability. To overcome such drawbacks, the development of protein delivery systems to protect, carry and deliver them in a controlled way have emerged importantly these last years. In this review, the formulation of a wide panel of protein delivery systems either in the form of polymer or inorganic nanoengineered colloids and scaffolds are presented and the protein loading and release mechanisms are addressed. A section is also dedicated to the detection of proteins and the characterization methods of their release. Then, the main protein delivery systems developed these last three years for anticancer, tissue engineering or diabetes applications are presented, as well as the major *in vivo* models used to test them. The last part of this review aims at presenting the perspectives of the field such as the use of protein-rich material or the sequestration of proteins. This part will also deal with less common applications and gene therapy as an indirect method to deliver protein.

Keywords

Protein therapeutics, Drug delivery systems, Nanoengineered carriers, Scaffolds, Growth factors, RNase, Insulin, Tissue Engineering, Cancer, Diabetes

Highlights

- A wide range of delivery systems was recently developed to control protein release
- Delivery systems consist typically of polymer or inorganic colloids and scaffolds
- Various experimental and theoretical methods allow to characterize the protein release

- Main applications of these systems are cancer, tissue engineering and diabetes

I Introduction

Proteins are biomacromolecules existing in a very broad range of biological processes and displaying remarkable functions such as biocatalysis, high affinity molecular recognition, activation/inhibition of cell pathways [1], which makes them very interesting therapeutics agents. Indeed, they present a unique therapeutic richness compared to small molecule drugs, with higher spectra of specificity and activity [2]. Thus, they have been studied for decades in various applications: for instance, ribonuclease A (RNAse A) has been studied for the treatment of cancer, growth factors are widely used for tissue engineering and insulin is still the molecule of choice to treat diabetes. Another advantage of using proteins as therapeutic agents rather than other molecules is their endogenous nature which makes them biocompatible and biodegradable. It is also important to notice that their degradation products are already known and eliminated by the body, which also has the advantage to limit importantly any potential toxicity of the treatment.

However, proteins are fragile conformational macromolecular structures, susceptible to unfolding and to enzymatic degradation and they present a short half-life. Combined with poor membrane permeability limiting their cellular internalization, it necessitates frequent administrations [1,2]. To overcome these challenges, protein delivery systems have been developed these last years to protect, carry and release therapeutic proteins in a sufficient dose and only at specific sites without altering their bioactivity. These systems can be formulated in a wide range of dimensions, from nanocolloid to macroscopic scaffold sizes, with tailored shapes and physicochemical features and they can be designed to control the protein release thanks to local or external stimuli. Such control is essential to bring a longer efficiency of the treatment but also to avoid a burst release leading to the loss of the majority of the cargo and to a locally high concentration of protein which can potentially induce detrimental effects [3,4]. If this control usually aims at providing a continuous release, it is interesting to notice that some research works are also performed to design delivery systems responding to external fields (light, magnetic field) endowed with a pulsatile release, aiming at triggering in time and location adjusted amounts of drug released in the body [5,6].

In this review article, we detail the recent design and applications of protein delivery systems in nanomedecine and tissue engineering, which has been very few reviewed these last years, by providing an up-date of various impacting works (non-exhaustive list) achieved these last years in this area. In the first section of this review, the fabrication techniques of the different protein delivery systems are presented: microparticles (MPs), nanoparticles (NPs), hydrogels (HGs), fibers, films, patches and macroporous scaffolds (MacPSs). This section also describes the various loading and release possibilities by giving insights into the release mechanism from drug delivery systems including natural diffusion, hydrolytic erosion or local biochemical stimuli (pH, redox, enzymes). In a second section, the characterization techniques and mathematical models commonly used to detect and quantify proteins and to study the release mechanism are presented. Then, the three

following sections present the protein delivery systems split into three categories: circulating, implantable and covering systems that are mainly used for anticancer, tissue engineering and diabetes applications. The *in vivo* models used to evaluate the efficiency of these systems, as well as the main experimental results, are presented in a dedicated section while the last one will present emerging designs of proteins delivery systems. The **Figure 1** gives a global view into the kind of delivery systems presented in this review as well as their most common applications.

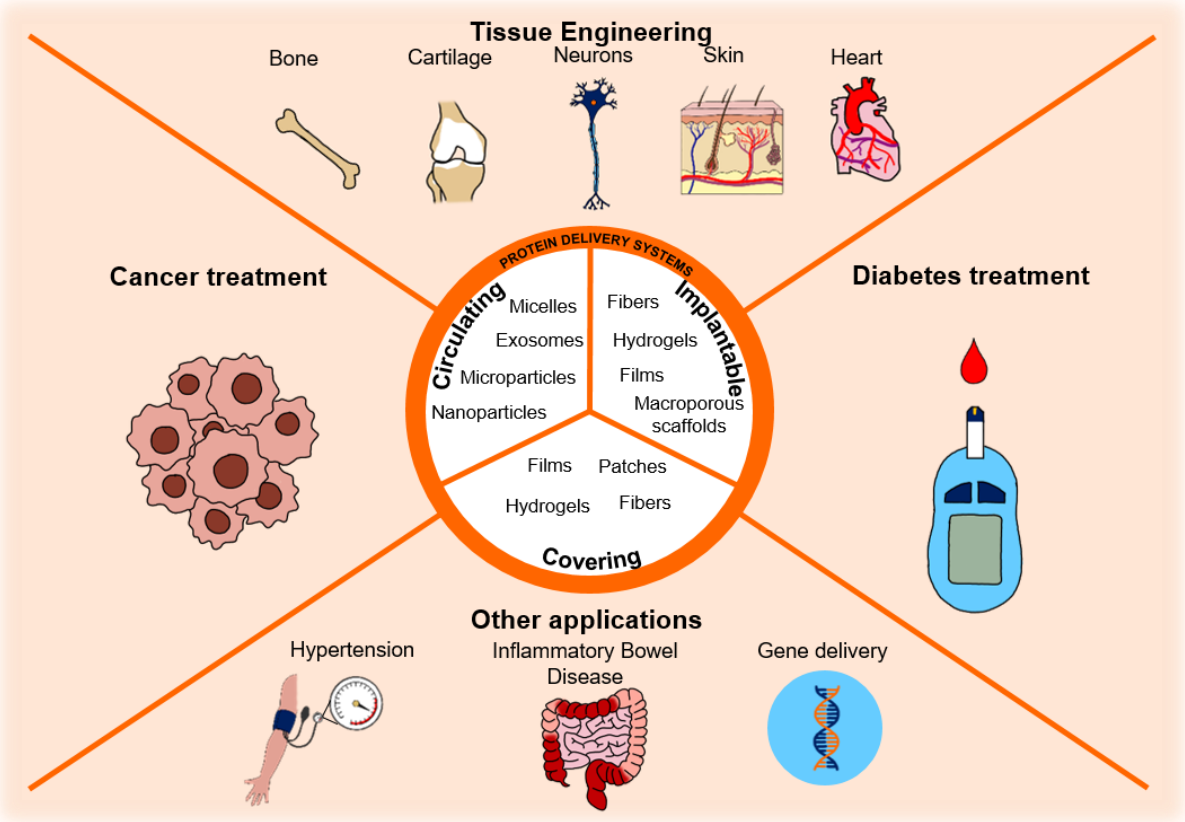

Figure 1: Overview of the different protein delivery devices and their applications

II Formulation and physico-chemistry

II.1 Fabrication techniques

Protein delivery systems are designed with range of dimensions and shapes –MPs orNPs, HGs, films or patches, fibers, MacPSs – as represented in **Figure 2**. Whatever the chosen formulation, it is also possible to load a macroscopic scaffold with MPs or NPs to improve its mechanical strength or to trigger drug release by local or external stimuli when using stimuli responsive MPs/NPs. In this section, the common fabrication techniques are reviewed for the different delivery devices.

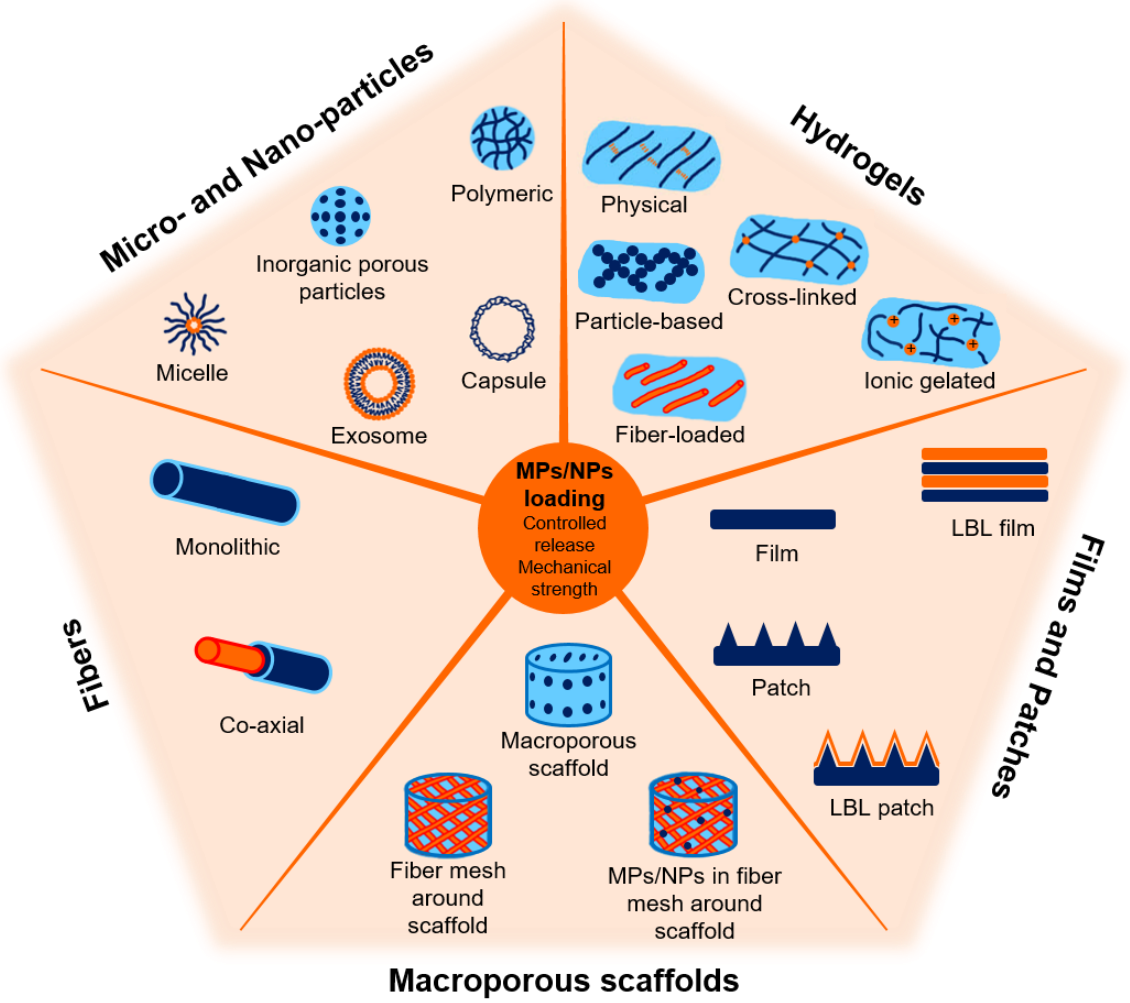

Figure 2: Overview of the different protein delivery devices

II.1.1 Micro- and nano- particles

MPs and NPs are promising tools to deliver proteins as they have the adequate size to be internalized by cells and can then directly deliver proteins to the intracellular environment. Besides, these systems are highly tunable by chemical or physical processes. They can be made with organic or inorganic materials, in the form of plain particles or capsules, or even in more complex assemblies such as micelles or exosomes.

II.1.1.1 Emulsification

The emulsion solvent evaporation is a simple and rapid fabrication method allowing the synthesis of MPs and NPs. The basic principle of an emulsion is to form droplets by mixing a first phase in a second immiscible one and then to eliminate the solvent. An emulsifier, such as polysorbate, can be added to the preparation to stabilize the emulsion. Even if this technique is very common to obtain poly(lactic-co-glycolic acid) (PLGA) [7] or chitosan (CHI) [8] particles, it can also be extended to many biological macromolecules as building blocks. For example, Rinker *et al.* reported the synthesis of heparin MPs by mixing an aqueous solution of heparin in corn oil, which is the classic water-in-oil emulsion technique [9]. More interestingly, they used it again to entrap these heparin MPs in bigger MPs mainly composed of poly(ethylene glycol) (PEG). Conversely, oil-in-water emulsion is also used to obtain particles. Recently, this technique has been reported to be useful to obtain Eudragit S100 polymer hollow MPs with pH-sensitive pores [10]. One big advantage of this technique is the easy loading of drugs by simply blending it in the adequate phase. For example, Galliani *et al.* reported the synthesis of PLGA/poly(ethylene imine) (PEI) NPs loaded with cross-linked aggregates (CLAs) made of bovine serum albumin (BSA) or cross-linked enzymes aggregates (CLEAs) made of superoxide dismutase (SOD). These CLAs or CLEAs were mixed with PLGA and PEI to obtain the oil phase that was further added dropwise to a poly(vinyl alcohol) (PVA) aqueous solution to obtain the NPs [11].

Single emulsion can be used as it is or in combination with other processes such as cross-linking [8,12] or external gelation [13]. Cross-linking CHI MPs is widely used with the nature and amount of cross-linker being important parameters to control. Recently, a study reported the chain length influence of dicarboxylic acid linkers on the properties of CHI MPs [8]. The results showed that the increase of the carbon chain length induces an increase in size, swelling ratio, erosion, encapsulation efficiency and loading capacity. For the release, the increase of the chain length increased the initial burst release and cumulative release of BSA, which is in agreement with the higher swelling ratio and erosion associated with the corresponding carbon chain length. Cross-linking has also been used to obtain polypeptide-based gel particles to combine the features of NPs and HGs [12]. A wide range of gel particles has been synthesized using water-in-oil emulsion further cross-linked with genipin, a much less toxic cross-linker as compared to the conventional glutaraldehyde. Upon their characteristics, the study notably showed the efficient encapsulation of BSA, myoglobin and lectoferrin and most importantly, it was reported that their bioactivity was retained. The use of a disulfide cross-linking agent showed the possibility to release BSA in the presence of glutathione, a naturally reducing agent of the cytoplasm. Single emulsion can also be used in combination with polymerization. As an example, Zhang *et al.* used the reverse emulsion polymerization technique to obtain hydroxypropyl-β-cyclodextrin microspheres [14]. More precisely, they emulsified the hydroxypropyl-β-cyclodextrin which then polymerized to form the microspheres.

Double emulsion technique is also operated to obtain MPs and NPs with the water-in-oil-in-water being the most used procedure and PLGA being the most commonly used polymer. A recent study aimed at tailoring PLGA MPs to obtain a controlled delayed release of the cytokine CCL25, a chemoattractant of mesenchymal stem cells (MSCs), by playing on the polymer molecular weight, chemical functionalization, emulsion type and amount of BSA excipient [15]. Another study reported the combination of lipids and PLGA to encapsulate and release

lysozyme, showing a better encapsulation efficiency and reduction of burst release of this enzyme with a higher content of PLGA [16]. This technique has also been used to integrate superparamagnetic iron oxide NPs (SPIONs) in the PLGA shell in core-shell particles encapsulating BSA [17]. The goal of this study was to exploit the superparamagnetic properties of SPIONS to obtain a better cellular uptake and immune response. This double emulsion process has been modified by Chen *et al.* as solid-in-oil-in-water process to encapsulate BSA-loaded lecithin NPs in PLGA MPs [7]. The term "solid" used here refers to the anhydrous reverse micelle made of BSA surrounded by lecithin.

As said before, the advantages of the emulsion technique are its easy handling and the possibility to load the therapeutics by blending it within the phase of interest. Unfortunately, this can lead to denaturation because the therapeutics can be in contact with an unfavourable phase or can be damaged by the mechanical stress induced by the emulsion creation process (vortex, sonication) [10].

II.1.1.2 Polymer self-assembly

Another well-known technique to obtain MPs and NPs is the self-assembly based on intra- or intermolecular interactions. In such formulations, the protein can be trapped in the self-assembled system due to interactions with the polymer material or the protein is one of the material that self-assembles to form the delivery system. Lv *et al.* used this technique in a recent study where they reported the synthesis of a library of dendrimers functionalized with fluoroalkyls and fluoroaromatics. The objective was to obtain an efficient fluorodendrimer able to self-assemble via fluorophilic effect, to entrap proteins through ionic interaction and to deliver it to the cytosol [18]. More recently, a study reported the use of the self-assembling technique to obtain metal-organic frameworks (MOFs) by mixing zinc ion with imidazole-2-carboxaldehyde and proteins. The study notably showed the effective intracellular delivery of two enzymes involved in genetic material reactions: RNase A and genome-editing Cas9 nuclease [19].

The cross-linking can also be part of the self-assembling process as in the ionic gelation process. This technique is widely used to obtain CHI particles. Briefly, the cationic form of CHI is mixed with anionic cross-linker, the most common one being tripolyphosphate (TPP), and the ionic complexation leads to CHI gelation and precipitation in particle form. Thus, the cross-linking of CHI by cationic/anionic interaction is the self-assembling phenomenon leading to the formation of CHI particles. CHI can be used as it is [20] or after functionalization, as reported by Song *et al.* who synthesized carboxymethyl-β-cyclodextrin grafted CHI NPs (CMCD-g-CHI) [21]. Another example of ionic gelation is the synthesis of gellan gum MPs with aluminium ions [22].

Finally, self-assembly is the driving mechanism to obtain micelles which consists in the spatial arrangement of amphiphilic species into a core-shell system where the hydrophobic parts segregate within the core and the hydrophilic parts locate in the shell. Meng *et al.* reported the synthesis of Pluronic F127 (PF127)/D-α-tocopheryl polyethylene glycol succinate (TPGS) micelle by thin-film hydration to specifically deliver proteins to the brain [23]. In another study, Gao *et al.* reported the stabilization of recombinant human growth hormone (rhGH) by sugar glass NPs obtained from inverse micelles [24].

II.1.1.3 Extrusion and spraying

Extrusion is a general technique in which the precursor solution is forced to go through a nozzle whose cross-section dictates the dimensions of the final material. This process has been used to obtain CHI/polyphosphoric acid (PPA) beads to encapsulate several proteins including BSA, insulin, casein hydrolysate and whey protein isolate (WPI) [25].

Spray drying is the extrusion way allowing the fabrication of drug powders. It consists of mixing the interesting therapeutics with an excipient and to spray it through an atomizer into a chamber where it will be dried by hot gas and precipitated into nanopowder. Several factors influence the final product such as the composition of initial solution and its temperature at several points of the process [26]. Wu *et al.* specifically studied the effect of excipients on the encapsulation and release properties of solid/lipid MPs obtained by spray drying. Insulin-phospholipid were then formulated with several excipients: glycerol monostearate, distearate, tribehenate and tristearate. The results showed that the spray drying process does not impact insulin conformation and that triglycerides with long chain reduces the burst release in a significant way compared to PLGA [26]. A possibility to play on the solvent is the use of supercritical fluid-assisted spray drying (SASD), and notably supercritical CO_2 ($scCO_2$)-assisted spray drying, as it is supposed to reduce organic solvent quantities and temperatures. This technique has been used to synthesize PLGA particles containing BSA and L-leucine, which role was to enhance the dispersion of the powder, for vaccine delivery to the lung [27].

The electrospraying process, also known as electrodynamic spraying, is another spraying method where a high electrical potential is applied to the atomizer, leading to the formation of charged droplets that dry before reaching the collector. This technique does not require chemical modifications and allows high encapsulation efficiency, notably of sensitive molecules such as proteins as it does not expose them to unfavourable solvents or shear stress as required in emulsions. As an example, Chen *et al.* operated coaxial electrospraying to obtain murabutide and ovalbumin (OVA)-loaded acetalated dextran MPs with several degradation profiles [28].

II.1.1.4 Microfluidics

Microfluidics is a pioneering technique to fabricate micro- and nano-materials presenting several advantages. The mixing is notably changed compared to conventional reactors as it is faster and more intensive, which leads to increased reaction kinetics and allows fast screening of experimental conditions. Besides, the surface-to-volume ratio can be tuned by changing the microchannel size and shape and the operations can be automatized, which reduces variations between experiments [29]. It can then be used to obtain inorganic particles as well as polymeric particles. For example, Hao *et al.* used this technique to synthesize hollow spherical silica with sponge-like pores with a system containing two inlets [29] while Foster *et al.* reported the use of microfluidics-based polymerization to obtain PEG microgels [30]. More recently, Yu *et al.* designed a four inlets microfluidics systems to synthesize PEI/CHI-coated alginate MPs [31]. The first two inlets were used to form water/protein core-alginate shell MPs, with $CaCO_3$ present in the alginate phase. The third inlet contained only a mineral oil to drag the particles while the fourth inlet contained the same mineral oil mixed with acetic acid. The acetic acid released the calcium ions from $CaCO_3$, leading to the internal gelation of the alginate shell. The particles were then collected in a calcium chloride ($CaCl_2$) solution to have an external gelation of the alginate. The advantage of having the four inlets was then to

have a high control of the particle size and to introduce an internal gelation of alginate prior to the external gelation, the combination of both improving the stability of the particles.

II.1.1.5 Synthesis and functionalization of inorganic colloids

Mesoporous silica nanoparticles (MSNs) are widely used in biomedical applications. The silica synthesis was historically reported by Stöber *et al.* in 1968 [32], also known as the sol-gel process while the introduction of mesopores was pioneered in the 1990's by Mobil Corporation laboratories. The sol-gel reaction consists in the hydrolysis and condensation of a silica source, mostly tetraethoxysilane (TEOS), in the presence of a catalyst in a water/ethanol/ammonia mixture. More precisely, this process leads to the formation of silica particles, and the pores are obtained by the addition of a surfactant such as cetyltrimethylammonium bromide (CTAB) [33]. The reaction is influenced by the composition of the solvent mixture, the surfactant used and the temperature. The process can also be adapted in order to obtain different shape. For example, Deng *et al.* reported the synthesis of silica nanotubes using the emulsion linear-merging growth technique [34]. More precisely, they operated the reaction in 1-pentanol, exploiting the formation and assembly of water droplets to obtain the nanotube shape. An additional feature of this work is that the authors could obtain an asymmetric chemical surface by using different silane molecules for the reaction. The use of a specific organosilane for the synthesis to add a chemical function to silica material has also been reported by Shao *et al* [35]. Of course, the chemical functionality can also be added after the synthesis [36]. These last years in our groups, we have notably deeply investigated the potential of isobutyramide binders grafted on silica surface [37,38] to non-covalently immobilize various types of proteins films for drug delivery [39] and bioimaging [40,41]. It is also noteworthy that mesoporous particles can be used as material without chemical modification. For example, Wang *et al.* used MSNs as a building block to obtain supraparticles and used it as a BDNF delivery system for hearing loss therapy [42].

$CaCO_3$ MPs also attracted attention in biomedical applications due to several properties and notably the easy synthesis. Indeed, these particles can be obtained by simple co-precipitation of $CaCl_2$ and sodium carbonate (Na_2CO_3) [43]. The use of $scCO_2$ has also been developed, bringing better control of the MPs size [44].

Another technique to formulate mineral particles is ion etching. More precisely, it can be used as perforation etching to form porous particles [45,46] or as ion etching, as reported by Bae *et al*., who used calcium ion etching to enlarge pores in cubic MSNs [47].

Finally, metallic or metal oxide particles are other kinds of particles presenting interesting properties for the delivery of drugs such as proteins. For example, iron oxide NPs were synthesized by annealing temperature directly inside the pores of MSNs to add a magnetic responsive property to the protein delivery system [33]. In another study, arginine-functionalized gold NPs were synthesized by phase-exchange reaction before being mixed with E-tagged protein to form nano-assemblies [48].

II.1.1.6 Template assisted method

Another common technique to obtain particles and capsules is the use of a sacrificial template. The well-known technique to obtain capsules is the layer-by-layer (LBL) assembly, where several layers of polymers are deposited around a template thanks to intermolecular interactions. The strength of the assembly can be based only on the force of the interactions, can be reinforced by cross-linking and additionally tailored to be responsive to a local stimulus. This idea has been operated by Yang *et al.* who added a thiol function to hyaluronic acid (HA) and CHI before using them as LBL materials. The layers were then cross-linked by oxidation of the thiol groups by horseradish peroxidase (HRP), leading to the formation of disulphide bonds which are redox-responsive [43]. In this case, the sacrificial template was $CaCO_3$ MPs, a material of choice to be used as template to formulate protein-loaded particles or even protein particles as developed since decades by D.V. Volodkin *et al.* [49,50].

Silica particles are also a very common sacrificial template. For example, Tan *et al.* used mesoporous silica to synthesized poly(L-glutamic acid) (PGA) particles [51]. In this case, the PGA material infiltrated in the mesoporous silica before removal of the template, resulting in the obtention of porous particles. The isobutyramide functionalization of silica developed in our group has also been used to produce nano/micro protein capsules for different applications: drug delivery [52], biocatalysis [53] and siRNA delivery [54].

An interesting study also reported the use of proteins as a core template for the surrounding assembly of polymers, forming a kind of shell that was further cross-linked [55]. This approach is similar to the layer-by-layer self-assembly technique, This template can be removed to obtain hollow capsules. Similarly, the on calcium carbonate ($CaCO_3$) MPs sacrificial template..

II.1.1.7 Cell exosome production

Cell production is the technique used to obtain exosomes, as they are nanosized extracellular vesicles and are produced by most of the cells. Usually, the cell line is transfected with the desired plasmid to produce exosome with specific functionalization. For example, HEK293T cells have been transfected with a plasmid encoding for PH20 hyaluronidase [56] in a study and with signal regulatory protein α (SIRPα) plasmid in another one [57]. The PH20 hyaluronidase and SIRPα were then included in the structure of the exosome.

II.1.2 Hydrogels

HGs are three-dimensional hydrophilic networks able to absorb a large amount of water. They are also highly tunable, notably on the viscoelastic point of view, making them very interesting in tissue engineering as they can be formulated to have the same mechanical properties of the damaged tissue. In this section, the different HG cross-linking strategies will be described.

II.1.2.1 Self-polymerized hydrogels

Self-polymerized HGs refer to HGs that are formed through polymerization of monomers or macromonomers with the creation of chemical cross-linking points. This technique has for example been used by Lima *et al.* who modified alginate with glycidyl methacrylate for further radical copolymerization with sodium acrylate and N-vinyl-pyrrolidone [58]. The technique can also be used with a pre-formed polymer as

developed by the group of Wei Dong. This group used salecan as one of the building blocks of HGs and polymerized 2-(dimethylamino) ethyl methacrylate (DMAEMA) in a solution containing salecan to obtain a salecan/PDMAEMA interpenetrating HG [59] or grafted 2-acrylamido-2-methyl-1-propanesulfonic acid (AMPS) directly to salecan to polymerize it and obtain salecan-g-PAMPS HG [60].

II.1.2.2 Covalent cross-linking of pre-formed polymers

Here, the polymers are already formed and the cross-linking is induced. Two possibilities appear: the addition of a cross-linker or the self-cross-linking of the polymer. The work of Olthof *et al.* illustrates the first possibility as they used UV irradiation of a mixture of oligo[(polyethylene glycol) fumarate]/ N-vinyl pyrrolidinone/ bis[2-(methacryloyloxy) ethyl] phosphate to obtain chemical cross-linking [61]. The main drawback of this technique is the possible toxicity and the reactivity of the chemical cross-linker. The second possibility can be illustrated by the work of McAvan *et al*. , who used the deprotection of cysteine at the end of each arm of a 4-armed PEG to form intermolecular disulfide bonds by exposition of the thiol groups [62]. In addition, Ma *et al*. reported the use of Schiff base reaction to obtain HA/ γ-PGA HG [63] and Koshy *et al*. the use of the inverse electron demand Diels-Alder reaction to have the spontaneous cross-linking between alginate-norbornene and alginate-tetrazine [64].

II.1.2.3 Physical hydrogels

Physical HGs are cross-linked by physical interactions, such as hydrogen bonding [65,66], hydrophobic [67], electrostatic [65], van der Waals or even π- [66] interactions. This physical cross-linking can occur spontaneously or can be induced by the change of environmental conditions, the most common one being the change in temperature. This is the common conditions used to obtain whey protein HGs, as the heating partially denatures the protein, leading to exposure of non-polar moieties and then to the aggregation of the protein in the form of HG [68]. More recently, the use of thermoresponsive particles that self-assemble into HG upon hydrophobic interaction through heating has also been reported [69]. Another possibility to induce physical cross-linking is a change of light intensity. For example, Wang *et al.* used the ability of the C-terminal adenosylcobalamin binding domain (CarHC) of CarH protein to tetramerize in the dark when binding to adenosylcobalamin ($AdoB_{12}$) to obtain an HG [70]. When exposed to light, the tetramer is disrupted and thus the HG formulation loses its integrity.

II.1.2.4 Ionic gelation

Finally, HGs can be obtained through ionic gelation, which here means that the cross-linker is an ion. This technique is the one already described to obtain some CHI particle. It has been used by Hettiaratchi *et al.* to obtain alginate HG cross-linked with calcium sulfate [71] and also by Lokhande *et al.* to obtain κ-carrageenan HG cross-linked with potassium ions [72].

II.1.3 Fibers

Fibers are interesting drug delivery devices (DDS) notably in tissue engineering as their interconnected porous structure can mimic the fibrous one of extracellular matrix

(ECM) or even of neurons. They also have a high surface area and the ability to load several types of drugs and, more importantly, biological molecules.

II.1.3.1 Single electrospinning

Electrospinning is the most widely used technique to produce fibers due to many advantages such as the simplicity, the cost-effectiveness and the adaptability to a wide range of polymers either natural or synthetic [20,73]. In this fabrication technique, an electrical potential is applied to a polymer solution by forcing it to move through a charged needle. The electrostatic force between the charged needle and the grounded collector leads to the formation of a jet called a Taylor cone, and this jet dries before reaching the collector, forming a fiber [74]. The parameters influencing the results are mainly the polymer properties (molecular weight, conductivity, viscosity), the voltage, the distance between the needle and the collector, and the size of the needle. This technique can be used with a single polymer solution [20] or with a mixture of polymers [73]. The fibers can then be used as they are or treated after synthesis. For example, oxygen plasma treatment can be used to increase the hydrophilicity of the fibers or to functionalize it with chemical functions [20,75].

The shape of the collector is another interesting parameter to change. Most of the time, fibers are collected on a grounded plate or a cylinder, but it is also possible to collect them between two negatively charged plates or piers (spheres). This is reported as the two-pole air gap electrospinning [76,77]. This way of synthesis allows, for example, the fabrication of nerve conduit with the fibers aligned in the same direction of the conduit, which can help to direct axons growth [77].

Although electrospinning is easy to handle, it has a major disadvantage: it generally necessitates the use of an organic solvent to dissolve the polymer, which is not a good environment for sensitive molecules such as proteins [46].

II.1.3.2 Coaxial electrospinning

Coaxial electrospinning allows the synthesis of core-sheath fibers. Even though it is more difficult to operate, it brings some advantages compared to single electrospinning: first of all, it allows the use of different solvents, such as hydrophobic and hydrophilic, allowing the loading of a wide range of molecules. Then, when a therapeutic is loaded in the core fiber, the sheath can protect it from the environment, allowing the loading of sensitive molecules. This kind of fiber is very interesting as it impacts the release profile of the drug loaded in the core, but it also allows the loading of different drug in the core and the sheath with different release kinetics [78,79]. As for monolithic fibers, core-sheath fibers can be functionalized after synthesis, as reported by Wang *et al.* who treated the fibers with cold atmospheric plasma to increase the pore size and the hydrophilicity to improve cell attachment and proliferation [80].

The integration of particles in such fibers has been reported in different ways: they have been blended in the core solution [79] or they have been electrosprayed on the fibers during the coaxial electrospinning process [81].

II.1.3.3 Other techniques

A quite new method to synthesize fibers is the rotary jet spinning. This technique uses high-speed rotation to obtain aligned fibers. More precisely, the polymer is injected to a reservoir fixed on the shaft of a motor. When the motor is rotating, the polymer is extruded through a hole in the reservoir by centrifugal force, leading to the

formation of a jet from which the solvent evaporates, forming a fiber. The properties of the fibers can then be controlled by the properties of the polymer solution itself, the diameter of the hole and the rotation speed [74,82]. As an example, this technique has notably been used to synthesize soy protein/cellulose nanofibers [82]. Compared to electrospinning, this technique has the advantage to not need an electrical field, which removes a stress applied to the polymer and its cargo [74].

Finally, fibers can also be synthesized by spray nebulization, as reported by Zuidema *et al.* to avoid the electrical field needed for electrospinning and the resulting stress induced to the loaded therapeutics [46].

II.1.4 Films and microneedle patches

Films are thin layers of material and are very interesting in the field of transdermal delivery as they can replace classical subcutaneous injections and notably reduce pain. Microneedles (MNs) patches are in the same family but present an array of micron-sized needles able to penetrate the epidermis with low depth, reducing pain and damages to the subcutaneous tissue.

II.1.4.1 Layer-by-layer assembly

The LBL process is a very suitable technique to incorporate proteins in a drug delivery film as it is operated in soft conditions and on any template, whatever the size, shape, porosity or surface chemistry, notably allowing a very high tunability of the system [83–85]. The operation principle is to alternatively adsorb two materials on a surface thanks to complementary interactions. Most of the time, two polymers are adsorbed on a surface by alternative immersion in the polymer solutions. Regarding these interactions, if electrostatic ones are the most common, the integrity of the assembly can be due to other non-covalent (H-bond, van der Waals, hydrophobic), covalent or even, bio-specific bonds [86,87].

Regarding materials, and especially in the scope of this review, proteins can also be used as a layer type of the system without any modification [85,88,89] or after functionalization, as reported by Zhao *et al.* who PEGylated salmon calcitonin (PEGsc) before use with tannic acid to obtain hydrogen-bonded LBL film [87]. In addition, they can be used in combination with another polymer, as developed by Straeten *et al*. Indeed, they reported the use of protein-polyelectrolyte complex, more precisely lysozyme-poly(styrene sulfonate) (PSS) complex, as building block to synthesize an LBL film in combination with poly(allylamine hydrochloride) (PAH) [83,84].

Regarding the fabrication technique, adsorption by dipping method is almost the only one used, but inkjet-printing has also been reported with some advantages: it is a non-contact technique, meaning that the therapeutic is not in contact with the second material solvent or surfactant. Besides, it brings a high control of the coating through the formation of the droplets and this brings an economical feature as it can reduce the quantities of expensive therapeutics needed [89].

The LBL easily allows the tunability of the film properties, notably by the strength of the interactions, by the number of layers and by the possible cross-linking between layers [86].

II.1.4.2 Solvent evaporation

Solvent evaporation is a very easy way to prepare films. The desired solution is simply poured on a surface, or even in a mold to have a specific shape, and dried

[90–92]. This is mainly reported as the solvent casting method [91] but can also be referred as the dry phase-inversion when the main component is a polymer, as this means that the polymer solution turns into a gel phase by solvent evaporation [92].

II.1.4.3 Molding

The molding process, which can also be referred as the casting process, is mainly operated to fabricate MNs patches. The first male mold can be bought or fabricated to obtain a specific MN shape and is usually done with poly(methylmethacrylate) (PMMA), but metallic male mold has also been reported [93]. This male mold is used to fabricate a female mold, sometimes named inverse MNs patch, most often with polydimethylsiloxane (PDMS) and this mold is finally used to fabricate the final MNs patch with the desired polymer materials. During the process, high-speed centrifugation can be used to ensure a complete filling of the mold with the polymer solution [93–95]. These MNs patches can be done with only one polymer material or several. For example, Liu *et al.* reported the fabrication of poly(vinylpyrrolidone) (PVP) MNs patches in two steps: first the filling of the inverse MNs of the mold with $CaCO_3$ MPs-loaded PVP solution, second the formation of the top layer with only PVP solution [94]. In another hand, Seong *et al.* reported the fabrication of double-layer MNs patch with a swellable poly(styrene)-block-poly(acrylic acid) (PS-PAA) external layer and a non-swellable PS internal layer [93].

II.1.4.4 Other techniques

Films and MNs patches can be obtained by other methods. For example, the use of cross-linking allows the formation of films from another kind of device. This has been used by Zhang *et al.* who cross-linked a chitosan HG solution into a mold to obtain a CHI HG film [96]. The cross-linking technique has also been operated by Qi *et al.* who first prepared zein fibers by electrospinning and then cross-linked the matrix to obtain a fibrous film [97]. Films can also be naturally synthesized by bacterial culture. For example, this has been exploited by Cacicedo *et al.* to obtain a bacterial cellulose film, produced by *Komagataeibacter hansenii* as Levofloxacin (Levo) delivery system [98].

At last, the use of 3D printing has also been reported to fabricate MNs patches with pyramid or spear MNs shape, further coated with insulin-sugar film by inkjet-printing [99].

II.1.5 Macroporous scaffolds

MacPSs are 3D interconnected porous structures highly used in bone tissue regeneration due to their strength and ability to support cell migration and proliferation.

II.1.5.1 Freeze-drying

Freeze-drying, also known as lyophilisation, is the most used technique to fabricate MacPSs. The principle is to freeze the material and then to eliminate the solvent by sublimation, which is the direct transition from solid state to gas state. Quite obviously, the procedure is influenced by the pressure and temperature in the freeze-drying chamber. The freeze-drying of materials can be done in a mold [100,101] or not and with only one polymer material [102–105] or several [100,101,106,107]. The incorporation of particles can easily be done on this kind of scaffold [100,101,105–107], but the integration of fibers has also been reported [104].

Here again, freeze-drying can be combined with other techniques used in device fabrication. Cross-linking is notably used to reinforce the final scaffold, and it can be done before the freeze-drying treatment [102,106] or after it [104,108]. Other interesting combinations have been reported. For example, Li *et al.* fabricated a device by freezing alternate layers of silk fibroin solution and silk fibroin MPs through an LBL process before freeze-drying [105]. Another example is the one reported by Wang *et al*. In their work, they first prepared a gelatin scaffold by freeze-drying and cross-linking with glutaraldehyde. The scaffold was then functionalized with bacterial cellulose by incubation in bacterial culture and with heparin via EDC/NHS reaction [108].

II.1.5.2 Template assisted method

Template assisted method refers to a technique in which a template is used to give a specific structure to the scaffold and is then removed, leading to the other designation: template-leaching technique. The template can be of any type as long as they can be removed without affecting the fabricated scaffold. A very common type of template is spheres to obtain highly porous scaffold. For example, the use of sugar spheres has been reported to fabricate a hydroxyapatite (HAP) scaffold [14] by extruding the HAP solution to a cylindrical mold containing the sugar spheres. The resulting scaffold were then immersed in water and the sugar spheres were slowly dissolved while the HAP sol gelated. The use of paraffin spheres has also been reported to obtain a 3D gelatin nanofibrous scaffold by combining thermally induced phase separation (TIPS) and this template-leaching technique [109]. In this case, the spheres were removed by immersion in hexane. The template can be more complex, as reported by Bastami *et al.* who used a polyurethane (PU) foam as template, cut in a cubic shape with two orthogonal canals in the interior, to obtain a β-tricalcium phosphate (β-TCP) scaffold [110].

II.1.5.3 3D printing

Finally, 3D printing is also used to fabricate MacPSs as it allows good control of the structure and good reproducibility. The synthesis of protein delivery devices made of poly(lactic acid) (PLA) [111] or polycaprolactone (PCL) [112] using this technique has been reported. Here again, the use of a mixture of material is also possible. As an example, J. Lee and G. Kim reported the synthesis and characterization of α-TCP/collagen (COL) scaffolds made by low-temperature printing and room-temperature printing [113].

II.2 Loading of protein and control of the release

II.2.1 Integration of proteins in the system

The loading of proteins in a delivery system can be done by three techniques: blending, adsorption or covalent immobilization.

The blending technique consists of mixing the protein with the raw material constituting the scaffold (polymer, molecules, sol-gel precursor etc..) and then to formulate this material in the desired shape. If this technique is easy, it necessitates however having a good solubility of the protein in the material and a main drawback is the possible denaturation of the protein due to the fabrication process. For instance, the electrical stress induced by electrospinning when fabricating fibers is reported to induce such effect [46].

The adsorption technique is also very easy to operate. It only consists of incubating the DDS in the protein solution or to pipette the protein solution onto the system, and to let it diffuse and being adsorbed by the DDS. The main drawback linked to this technique is that the adsorption is a physical phenomenon which can be too weak to retain a large amount of proteins. In addition, burst release is often observed due to the desorption of proteins present at the surface of the DDS, which can induce locally high drug concentration and lead to side effects.

Finally, the immobilization process consists of the covalent linking of the protein to the material. This allows a very good anchor of the protein but it has also its drawbacks. It is necessary needed that the protein is not denaturated by the covalent immobilization which can potentially lead to a conformational change, or that the biological function (enzymatic, receptor, etc…) site is still available and active. Besides, this technique may lead to a few anchored proteins due to a low grafting yield or even low percentage of available reactive sites on the material.

A representation of these loading technique is given in **Figure 3**.

II.2.2 Release of proteins

II.2.2.1 Generalities

Several mechanisms can be involved in the release of drugs from a delivery system, alone or in combination. The first one is the desorption of drugs from the surface, leading to a burst release. A possible solution to avoid this uncontrolled release is to add standardized washings to the fabrication protocol to remove the poorly bound proteins and only keep the strongly bound ones. The main drawback of this technique is the reduction of the loading capacity, and the possible difficulty to release the cargo. The challenge is then to design a delivery system that could release the proteins in a controlled and efficient way due to specific stimuli. The second mechanism is the diffusion of the drug through the matrix, which can be helped by the swelling of this matrix, as it introduces more solvent inside the device. The third one is the natural erosion of the system. Indeed, implantable systems are often designed to degrade with a specific speed to let the place to new tissue. This degradation rate leads to controlled delivery of the entrapped therapeutic. This erosion can occur naturally or be driven by a sensitivity of the system to specific conditions such as pH, Reactive Oxygen Species (ROS) concentration, glucose concentration, etc... referred here as local stimuli. And the final one is the degradation of the system due to external stimuli such as light (visible or near-infrared (NIR)), magnetic field or even mechanical stimuli [114].

These general mechanisms are represented in **Figure 3**.

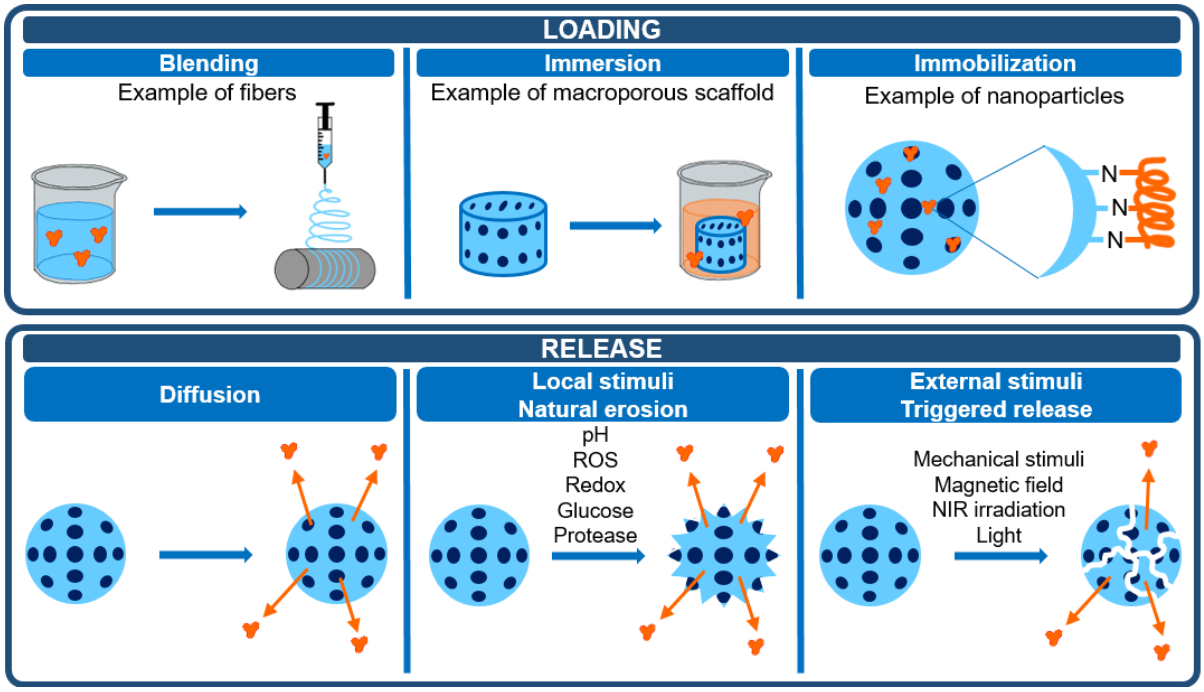

Figure 3: Protein loading and release methods

II.2.2.2 Local stimuli

Local stimuli are due to the natural change of physiological conditions, such as the difference of the pH value in gastric fluid and intestinal fluid, to give only one example. If pH is the most commonly used stimuli, it is not the only one: redox, ROS, glucose and protease sensitivity are also used to design delivery devices. We detail these local stimuli in the next paragraphs.

i) pH

The most common used local stimulus is the pH, which effect can be non-destructive or destructive. The non-destructive effect implies that the change of pH induces a change of interactions, which itself can induce a swelling/shrinking of the system. Several MPs systems have been developed using this change of interaction, notably for delivery through the intestine pathway, such as acetylated CHI/pectin MPs [115], alginate/CHI MPs [116] or even gellan gum MPs coated with retrograded starch and pectin [22]. In this last case, the authors showed very low release in acidic media and explained that it comes from the protonation of the carboxyl group of gellan gum. This protonation promotes electrostatic interactions between the polymers, making the organization tighter and then preventing insulin release. The pH sensitivity has also been used by the group of Wei Dong, who introduced pH-sensitivity to salecan-based HGs by adding PDMAEMA or PAMPS. The PDMAEMA notably brought pH-, ionic strength- and temperature-dependent swelling/shrinking [59] while the PAMPS only induced pH-sensitivity, which played on electrostatic interactions and so on swelling behaviour [60]. For the destructive effect, this means that bonds are cleaved or that the change of pH leads to the degradation of the system. For example, in Tian *et al*. work, the acidic pH cleaves the imine bond between primary amine of BSA and aldehyde function grafted to the dendritic MSNs [36]. In contrast, amino acid-modified CHI nanocapsules (NCs) and anionic carboxymethyl starch/cationic quaternary ammonium starch NCs were decomposed at pH 5.5 and 6.8 respectively [117,118]. The disruption of films has also been

reported. For example, He *et al.* reported the synthesis of an LBL film-coated MNs patch with charge-invertible micelle as first layer. When pH is increased, the micelle charge is inverted and the rest of the film is delivered from the MNs patch [88]. More recently, Straeten *et al.* reported the disruption of an LBL film due to a change of interaction when pH is changed. The film is composed of PAH as weak polycation and a complex PSS/lysozyme, with PSS being a strong polyanion. When pH is decreased under the pKa of PAH, the interaction between PSS and PAH becomes stronger and the film is disrupted, releasing lysozyme [84].

ii) Redox and ROS

Most of the time, the redox-responsivity is induced in the system by a disulfide bond. This can be added by the cross-linker itself [12] or by the addition of thiol groups to the material to obtain a disulfide cross-linking [43,62]. This was the strategy adopted by Yang *et al.* who thiolated CHI and HA prior to using them to fabricate LBL NCs. The disulfide cross-linking then occurred through the action of HRP [43]. This redox sensitivity can also be introduced by diselenide bonds as reported by Shao *et al.*, who used bis[3-(triethoxysilyl)propyl]diselenide (BTESePD) as silica source to add the diselenide bonds in MSNs [35]. Interestingly, this diselenide bond also presents ROS-sensitivity, compared to disulphide bond that is only Redox-responsive.

ROS, such as hydrogen peroxide H_2O_2, hydroxyl radical $^{\bullet}OH$ or even SOD $^{\bullet}O_2^-$, can be overproduced in some conditions like inflammation. Designing a ROS-responsive system then totally makes sense to treat some diseases. The diselenide bond-containing MSNs described above is one design example of ROS-sensitivity. Another example, which combines this ROS-responsivity to glucose-responsivity, is the one reported by Tong *et al*. They designed a tri-block copolymer made with PEG, poly(phenylboronic acid) as glucose-sensitive block and poly(phenylboronic acid pinacol ester) as H_2O_2-sensitive block. They used this triblock copolymer to form insulin and glucose oxidase (GOx)-loaded NPs. In presence of glucose, the glucose-sensitive part of the copolymer starts releasing the cargos. The GOx then interacts with glucose, producing H_2O_2 that reacts with the H_2O_2-responsive block of the polymer, enhancing the release [95]. The glucose-responsivity, which can be combined with ROS-responsivity as presented here or with other stimuli such as pH [119], is notably very used to treat diabetes.

iii) *Protease enzyme*

The last common stimulus inducing the degradation of delivery systems is the presence of proteases [30,44,118,120,121]. This sensibility to protease can come from the nature of the material, like the sensitivity of COL toward collagenase, or from specific functionality added to the material. For example, Zhang *et al.* showed that their starch-based NCs could be degraded under action of pH change in simulated gastric, intestinal and colon fluid (SGF, SIF and SCF respectively) but also under pancreatic α-amylase degradation in SIF [118]. Regarding the addition of functionality, Foster *et al.* specifically added protease degradable peptide as cross-linker to their MPs and modulated the degradation rate by modulating the ratio between degradable and non-degradable cross-link [30] while Ramalapa *et al.* added a thrombin sensitive site in their protein cargo to obtain thrombin-mediated release [44].

Of course, other kinds of stimuli can be exploited such as ionic strength [59,97], temperature [59] or even more specific ones such as adenosine triphosphate (ATP) [19], bacterial alkaline phosphatase (BAP), sodium hydrosulfite ($Na_2S_2O_4$) [66] or complementary DNA [96].

II.2.2.3 External stimuli

An external stimulus can also be used to induce the protein delivery, such as light (visible or NIR), magnetic field or even mechanical stimulus. The next paragraphs will present some examples of these stimuli.

i) Light

In this case, the exposure of the system to light is the cause of the release. For example, Wang *et al.* synthesized a light sensitive HG based on the light sensitivity of CarHc tetramer [70]. More precisely, they functionalized elastin-like polymers (ELPs) with CarHc, a protein binding domain, able to form tetramers in presence of $AdoB_{12}$ if the solution is in the dark, leading to the formation of an HG with cross-linking points: the tetramers. When the obtained HG is exposed to light, the tetramer is disrupted, which degrade the HG. In this case, the light only leads to the degradation of the HG, but it can have multiple purposes as in the work reported by He *et al.* [122]. The system described is composed of a nanocomplex of phenylboronic acid-modified RNase A (RNBC) and ketal cross-linked PEI coated with hematoporphyrin-conjugated HA. When the system is exposed to light, the irradiation of hematoporphyrin leads to a high level of H_2O_2 which kills cancer cells. In addition, this high H_2O_2 level cleaves the phenylboronic acid-RNase A bond, delivering the protein which can also kill cancer cells. Thus the exposure of light has two consequences: the production of H_2O_2 and the release of RNaseA.

In the same kind of field, NIR irradiation can also be used as a stimulus. It has for example been reported as stimulus in a transdermal delivery system. The system described is a polysaccharide HG film loaded with gold nanorods. Due to the photothermal characteristic of these nanorods, the NIR irradiation of the system leads to an increase in temperature and then to an enhancement of the transdermal delivery of protein [123]. Tuncaboylu *et al.* also used this stimulus in their work. They designed a shape-memory tube made of PCL loaded with IR-26-dye. The NIR irradiation of the tube leads to temperature increase and so to the shrinking of the tube, delivering the protein loaded inside the tube [124].

ii) Magnetic field

Another kind of external stimulus is the application of a magnetic field. This non-invasive technique, which allows deeper penetration than NIR irradiation, has been widely used to induce magnetic hyperthermia to kill cancer cells, but also as a stimulus to release several types of drugs [125]. It has for example been used by Omar *et al.* to control the release of mTFP-ferritin from silica-iron oxide NPs as a proof of concept for the delivery of large proteins [33]. The suggested release mechanism was that the application of the magnetic field leads to temperature increase, disrupting the electrostatic interaction between the protein and the NPs.

iii) Mechanical stress/action

The last kind of external stimulus presented here is still not very developed: mechanical stimulus. Even if not very used, it is easily applicable, notably in

mechanically active tissue such as cardiac tissue or cartilage tissue where it is omnipresent [126,127]. As an example of reported systems, Xu *et al.* designed a bioinspired ceramic composite sponge made of HAP and natural cornstarch and tested its delivery properties under strain using bromophenol blue, BSA and fibroblast [127]. In another hand, Zhang *et al.* reported the use of a piezoelectric-dielectric composite film to release proteins. A piezoelectric material has the ability to convert mechanical energy into electrical energy. The system developed converts the mechanical stimulus such as press or massage into electrical energy, polarizing the film and inducing shrinking or swelling of the layers, leading to an accelerated protein delivery [126]. Furthermore, aside the protein delivery, the reversible enzyme exhibition/embedding from LBL polymer films submitted to applied mechanical forces was also developed for applications towards mechanically controlled biocatalytic systems [128,129].

III. Assessment of the protein release

The characterization of the loading and release capacities of a designed protein delivery device is mandatory to present a complete characterization of the system. Thus, this section aims at reviewing the detection and characterization of proteins loading and release and at presenting the common mathematical models used to characterize the release. It is interesting to notice that there are two possibilities to quantify the loaded amount of protein: indirect quantification by measuring the unloaded amount of protein, the most commonly used, or destruction of the delivery device to recover the loaded amount of protein.

III.1 Characterization of the proteins: dosage, structure and imaging

III.1.1 UV-visible absorbance

III.1.1.1 Absorbance

UltraViolet-visible absorbance is the measurement of the quantity of light absorbed by a solution in the wavelength range of 200-800 nm. It is very easy to use and it allows the quantification of proteins in a solution thanks to the Beer-Lambert law:

$$A = \varepsilon * l * c$$

where A is the absorbance of the solution, ε is the molar extinction coefficient in $L.mol^{-1}.cm^{-1}$, l is the optical path length in cm and c is the concentration of the absorbing molecule in $mol.L^{-1}$.

Absorbance has been reported as quantifying technique for a lot of proteins: BSA (around 280 nm) [27,36,58], WPI (200-320 nm) [25], casein hydrolysate (200-320 nm) [25], OVA (280 nm) [31], mTFP-ferritin [33], RNase A (280 nm) [35], black carrot extract (530 nm, due to anthocyanins) [68], vancomycin chloride (280 nm) [73], lysozyme (295 nm) [83], insulin (276 nm) [95], GOx (450 nm) [95]. The peak at 280 nm is due to the aromatic ring in two amino acids: tryptophan and tyrosine. It is also possible to use the absorbance due to the peptide bond. This bond absorbs strongly at 190 nm, but for technical reasons, the absorbance is usually measured around 205 nm [130]. Unfortunately, the absorption phenomenon is sensitive to its environment and thus, the absorbance value can largely vary between two proteins even if they have the same molecular weight.

III.1.1.2 Bradford assay

The Bradford assay has first been reported by Marion M. Bradford in 1976 [131] and has widely been used since this moment to quantify proteins [132]. This assay relies on the absorbance maximum shift of the Coomassie Blue G250 dye: the free molecule is in a cationic red form with a maximum absorbance at 470 nm. When binding to a protein, the molecule is in its anionic bleu form and the absorbance peak is then at 595 nm. The complexation, due to electrostatic and hydrophobic interactions [133], occurs more specifically with arginine and lysine residues of proteins but it can also occur with histidine, tryptophan, tyrosine and phenylalanine due to their aromatic residues. This quantification method is very interesting as is not too sensitive to the presence of reagents or biological sample components other than proteins. However, the presence of detergents has to be controlled to avoid interferences [132]. The detection limits can vary from a commercial kit to another but are usually ranging from 100 to 1,500 $\mu g.mL^{-1}$. It has to be noticed that the detection limits can be different when the protocol is adapted to be used with microplates. It is very used to quantify BSA

[8,13,43,47] and insulin [13,59,60,93], but it is also used with other proteins such as chymotrypsin, myoglobin, HRP [13], immunoglobulin G (IgG) and OVA [47].

III.1.1.3 Bicinchoninic Acid assay

The BiCinchoninic Acid assay (BCA assay) has first been reported by Smith *et al.* in 1985 [134]. The principle is to incubate the protein solution with Cu^{2+} in alkaline solution to have the reduction of Cu^{2+} in Cu^{+} by the peptide bonds of proteins, which is a temperature-dependent reaction. Then, Cu^{+} is chelated by two BCA molecules, forming a purple complex having a maximum absorbance at 562 nm. The advantages of this process is that is occurs in a single step and that it is not that sensitive towards detergents, denaturing agents and other compounds that could be present in the sample [135]. As for the Bradford assay, the detection limits can vary from a kit to another but are usually ranging from 0.5 to 20 $\mu g.mL^{-1}$, with a possible modification when using microplates to perform the test. This technique has also been used for a wide variety of proteins: BSA [97,124], lysozyme [46,124], OVA, IgG [124], rhGH [24], human chitin binding domain-modified beta-lactamase (ChBD-BlaP) [44], PH20 hyaluronidase [56], SIRPα [57], cytochrome C [97], enhanced green fluorescent protein (eGFP) [116], GOx [119], HA-modified RNase A [136], E7-bone morphogenetic protein 2 (BMP2) [137] and rhBMP2 [138].

III.1.2 Fluorimetry

III.1.2.1 Intrinsic fluorescence

Fluorescence is an interesting property to operate to quantify proteins as it is very easy to handle. Intrinsic fluorescence of proteins notably allows a direct quantification, and this has been used for example to quantify GFP [19] and mCherry [70]. The major drawback is the potential environmental sensitivity of the fluorescence moiety. As an example, intrinsic fluorescence of BSA is due to two tryptophan residues, Trp-212 and Trp-134. However, the fluorescence of these residues is influenced by their environment [139]. Thus, it is tricky to use this property to quantify BSA in solution, but it is very interesting to characterize the interaction with other components. Fluorescence quenching of BSA has for example been used to study the interaction of BSA with tuftsin [140], wogonin [141], glutathione [142] and more recently with lipidic NPs by applying the Stern-Volmer model [139]. It has also been used by Cacicedo *et al.* to show the interaction between Levo and HSA, which impacts the Levo release from bacterial cellulose film [98].

III.1.2.2 Fluorescent labelling

To avoid any modification of the intrinsic fluorescence due to the environment or protein conformational change, it is common to covalently attach a fluorescent label to proteins and then measure the fluorescence due to this moiety. The most common label is fluorescein isothiocyanate (FITC) and it has been linked to a wide variety of proteins such as BSA [18,72], insulin [105], HRP [90], RNBC [122], OVA [123] and Concanavalin A (ConA) [143]. Advantages of this dye are an easy grafting and a low cost, however FITC is known to be highly sensitive to experimental parameters such as pH or photobleaching. Hence, other more stable labelling molecules have also been used on several proteins such as cyanine 5 on BSA, erythropoietin [69], RNBC [122], hepatocyte growth factor dimeric fragment (HGFdf) [144] and tumor necrosis factor-related apoptosis inducing ligand TRAIL [145], vivostag S750 on BMP2 [71],

Texas red [85] and fluorescein [86] on OVA, rhodamine on hirudin [145] and AlexaFluor on IgG [30].

III.1.2.3 Fluorescamine assay

Fluorescamine has first been used by Udenfriend *et al.* in 1972 for the detection of primary amines in the picomole range [146]. Fluorescamine is a non-fluorescent molecule but reacts very rapidly (hundreds of milliseconds) with primary amines to form a fluorescent molecule, while the excess reacts with water to form a non-fluorescent molecule (after some seconds). So this method is very interesting due to the specific reaction with primary amines in proteins and peptides, its fast reaction time and sensitivity [146]. In addition, a commercial protocols allows the use of only 2 µL of solution with a sensitivity ranging from 8 to 500 $\mu g.mL^{-1}$ [147]. The assay has been used by Chen *et al.* to characterize the loading of murabutide and OVA in acetalated dextran MPs as well as BSA release from these MPs [28] and J. Lee and G. Kim to characterize the release of BSA from α-TCP/COL scaffold [113].

III.1.3 Highly specific and sensitive assays

III.1.3.1 ELISA

Enzyme-Linked ImmonuSorbent Assay has been developed by E. Engvall and P. Perlmann in 1971 [148]. ELISA uses the specific binding of antigen and antibodies and the formation of colour due to enzymatic reaction. It involves several steps: first the capture of the antigen we want to detect and quantify, second the addition of a specific antibody tagged with an enzyme, third the addition of a substrate that will give a colour product by reacting with the enzyme, fourth the analysis of the colour intensity. Three main types of ELISA exist: direct ELISA, indirect ELISA and sandwich ELISA.

i) In direct ELISA, the antigen is adsorbed on the plate and an enzyme-tagged primary antibody is then linked to it before the substrate is added to obtain the colour. This technique is the simplest ELISA protocol but presents important disadvantages such as the possible modification of the primary antibody immunoreactivity due to its functionalization with an enzyme.

ii) The indirect ELISA protocol involves two antibodies: the antigen is adsorbed on the plate surface, the primary antibody is linked to it and then an enzyme-tagged secondary antibody specific to the primary antibody is added. The final steps, which are the addition of a substrate and analysis of the signal, are similar. Even if this technique has the disadvantages of adding a step in the protocol and of not suppressing the risk of cross-reactivity, it presents many advantages such the wide variety of secondary antibodies and the possibility to use different detection methods.

iii) Finally, in the sandwich ELISA, the plate used to adsorb the enzyme is coated with an antibody. The antigen is adsorbed on this antibody before the same steps than for an indirect ELISA are applied. Thus, the antigen is sandwiched between the antibody coated on the plate and a primary antibody. As for indirect ELISA, it is possible to use several detection methods. In addition, this protocol is highly sensitive, as it can detect as low as some $pg.mL^{-1}$ of protein (protein type dependant), and highly specific but more optimization is required to operate it [149,150].

In the domain of protein delivery device, ELISA is mainly used to detect sensitive proteins such as BMP2 [103,109], stromal cell-derived factor 1 (SDF-1) [14,104], chemokine CCL25 [15], neurotrophin-3 [76], vascular endothelial growth factor (VEGF) [100,108], transforming growth factor-β (TGF-β) [20,113], basic fibroblast

growth factor (bFGF) [89], β-nerve growth factor (β-NGF) [92]… It is also used for less sensitive proteins such as insulin [93,94], lysozyme [67] and OVA [92].

III.1.3.2 Radiolabeling

Radiolabeling consists of adding a radioactive label to proteins to detect and quantify them. As the ELISA technique, it provides a high specificity and a high sensitivity of the detection. The radiolabeling of proteins with ^{125}I and the use of a gamma counter is the most used technique. Authors reported the quantification of BMP2 [61], rhBMP2 [151], VEGF, FGF2 [152], BSA and ConA [143] using this radiolabeling. In all these studies, the radioactivity decay was used to determine the protein loading or *in vitro* release but *in vivo* release was also determined using ^{125}I-radiolabelled proteins. For example, D.B. Raina *et al*. used single photon emission computed tomography to image their implanted system in rats and then used the signal to quantify the release [151]. In another study, Kuttappan *et al.* chose to excise the skin where their implanted their DDS and then to quantify the release using a gamma counter [152]. Farris *et al.* also reported the labelling of pEGFP-LUC with ^{32}P α-dATP and the use of a scintillation counter to quantify the loading of this plasmid DNA [153]. In this case, the radiolabeling of the protein was used because the material constituting the DDS was autofluorescent.

III.1.4 Separative techniques

III.1.4.2 High-Performance Liquid Chromatography

High-Performance Liquid Chromatography, or High Performance Liquid Chromatography (HPLC) is based on the difference of affinity (polar/apolar) between the solutes present in the mobile phase and the stationary phase in the column. It leads to the separation of the solutes and then to their detection and also quantification if the protocol is designed to do so. In the domain of protein delivery devices, it is mainly used with a UV detector to detect the protein and then quantify them. This has been used to quantify insulin [26,99,101,115], BSA [154], lysozyme [16], antihypertensive peptide [91,155], Exendin-4 (Ex4) [119], P28 peptide [156], and PEGsc [87]. Reversed-phase HPLC can also be used. In this case, the stationary phase is non polar while the mobile phase is polar. This has been used to detect insulin [22] and liraglutide [157] for example.

III.1.4.3 SDS PAGE

SDS PAGE, the acronym for sodium dodecyl sulfate polyacrylamide gel electrophoresis, is based on the different migration of proteins in a gel under an electrical field due to their molecular weight. The principle is first to denature proteins in presence of SDS. This is a detergent that breaks the weak interactions assuring the protein assembly, so leading to a complete unfolding, and bringing a net negative charge to the proteins. Then, the samples are deposited in wells present at the top of the polyacrylamide gel and an electrical field is applied. The proteins migrate through the gel thanks to the negative charge. The migration rate and distance depend on the cross-linking density of the gel and of the protein molecular weight: the smaller the protein, the faster the migration rate and the longer the distance. A solution containing protein markers with known molecular weights allows the identification of the molecular weights of the separated proteins. This technique is mainly used to detect proteins in complex systems thanks to this molecular weight-dependent migration, but it can also be operated to quantify them when known concentrations of

the protein are deposited on the gel with the sample to analyze. In this case, after staining, the gel is imaged and the color intensity of all bands is analyzed with a software. This technique has been used by Dutta *et al.* to evaluate the release of lysozyme, RNase A and cytochrome C from polymeric particles [55] and by Shigemitsu *et al.* to evaluate the release of IgG, ConA and myoglobin from a supramolecular HG [66].

III.1.4.4 Western blot

Western blot is a technique aiming at detecting, identifying and quantifying proteins in complex samples such as cellular samples. It involves three main steps: separation, transfer to a membrane and revelation. The separation step is most often an SDS PAGE, involving all the same preparation and electrophoresis steps. Then, the proteins are transferred to a membrane, like nitrocellulose, by placing the gel close to the membrane. This “assembly” is then placed between blotting papers and an electrical field is applied, leading to the migration of proteins from the gel to the membrane. This step allows the transfer of the gel result in more solid support. The revelation is then done first by blocking all the non-specific sites of the membrane with BSA or milk proteins, for example, and then an indirect ELISA is operated to detect specific proteins. The result gives bands with different intensities related to the protein concentration. At the end of the process, the membrane gives three information: the presence or absence of the protein in the sample due to the absence or presence of the band, the molecular weight of the protein due to the proteins markers applied during the SDS PAGE step, and the concentration of the protein due to the band intensity. It has for example been used to quantify the release of proteins from bacterial inclusion body (BIB) [158], the encapsulation efficiency of neuregulin-1 (Nrg-1) from COL/poly(D-lysine) (PDL)-coated PLGA MPs [159], the OVA expression from RAW264.7 cells after DA3/pOVA transfection [160] and the expression of VEGF, notably with a transfer to a polyvinylidene difluoride (PVDF) membrane [161].

III.1.5 Imaging techniques

III.1.5.1 Fluorescence microscopy

Fluorescence microscopy is simply the use of the fluorescent property of a molecule or material for its observation with an optical microscope. The fluorescent labelling of proteins is often used to bring this fluorescence property. This technique can be used to evaluate the loading of proteins in a scaffold or its repartition within the scaffold [105,119,143,162,163] but it is also used to check *in vitro* cellular uptake [29] or even *in vivo* or *ex vivo* repartition of a protein drug in tissues or organs [71,145].

III.1.5.2 Confocal laser scanning microscopy

The confocal microscope has been described and patented by M. Minsky in 1957 [164]. This type of microscope used the fluorescence of the sample. As the source of light is mainly a laser, it is then called confocal laser scanning microscopy (CLSM). The principle is that the light source is directed to a specific point, which allows the acquisition of an image point-by-point by a scanning process. An important advantage of CLSM is that it is possible to control the depth of the field in the sample, which allows obtaining a three-dimensional image of the sample by combining the images of several planes. This imaging technique is very used to observe the cellular uptake of fluorescently-labelled proteins *in vitro* and *in vivo* after the recuperation of

the tissues and staining of cells [18,19,28,43,48,55,122,136,145,165]. But this has also been used to observe protein distribution in delivery devices [26,86,166,167] or in tissue after application of the delivery device. For example, Liu *et al.* used it to image FITC-insulin in skin after application of PVP MNs patch containing FITC-insulin loaded-$CaCO_3$ MPs [94] and Marciello *et al.* to visualize the FITC-insulin penetration into porcine vaginal mucosa after application of a sponge-like scaffold containing FITC-insulin-loaded CHI NPs [101].

III.1.6 Protein integrity

III.1.6.1 Circular dichroism

It is important to remember that the treatments applied to proteins to load them into delivery devices and then to release them may impact their integrity and activity. Most of the time, the preservation of their activity is assessed by checking their bioactivity through a specific test. For example, the bioactivity of BMP2 is assessed by measuring the alkaline phosphatase (ALP) activity as BMP2 enhances it. But to specifically check the protein integrity, so its conformation, the most common technique is circular dichroism (CD). CD is based on the fact that an optically active molecule will not absorb the right-hand and the left-hand circular polarized light in the same way. In proteins, there are several chromophores: the peptide bond, the aromatic amino acid side chain and the disulfide bond, which makes CD a very suitable technique to analyze proteins and more importantly, to obtain information on their conformation [168]. In protein delivery device domain, it is very used to compare the conformation of the native protein and the released protein from any device to check that the integrity has not been impacted by the loading and release processes. This has for example been used on eGFP [19], cytochrome C [55], BSA [43], OVA [85], PEGsc [87], insulin [101], FITC-insulin [105], Ex4 [119], hirudin and TRAIL [145].

III.1.6.2 CryoTEM

Cryogenic transmission electron microscopy (CryoTEM) is the observation by TEM of samples kept at cryogenic temperatures. It notably allows the imaging of systems in their native form in solution. Thus, it is a very interesting technique to observe systems such as lipid-based NPs [139,169], liposomes [170–172] or even lipoplexes [173]. For example, Colombani *et al.* used CryoTEM to observe the impact of the composition of lipoplexes, made of cationic liposomes and DNA, and of solvent on the lipoplexes structure [173]. Of course, it can also be used to observe polymeric NPs as reported by Dutta *et al.* who used this technique to observe CytochromeC-polymer nano-assemblies [55].

III.2. Modelization of drug release kinetics

Drug release kinetics is the application of mathematical models to the data obtained from the study of drug release. This section aims at describing the most used mathematical models and at giving some example of use.

III.2.1 Presentation of the mathematical models

III.2.1.1 Zero-order model

The zero-order release model describes a constant release which means that the same amount of drug is released per unit of time, and this release process is independent of drug concentration. The equation is:

$$M_t = M_0 + K_0 * t$$

where M_t is the amount of drug dissolved at time t, M_0 the amount of drug dissolved when t=0, so usually 0, and K_0 is the zero-order constant release. The curve to plot when using this model is the percentage cumulative drug released (%CDR) in function of time and this curve has to be linear. This model can be used to describe several types of systems such as transdermal delivery systems, matrix tablets with low soluble drugs or coated systems [174].

III.2.1.2 First-order model

The first-order model describes systems for which the release is dependent on the amount of drug remaining in the system, with a diminution of the drug released dose per unit of time. The equation describing this model is:

$$\log M_t = \log M_0 + \frac{K_1 * t}{2.303}$$

where K_1 is the first-order release constant. The curve to plot is log(M_t) in function of time, which gives a linear curve. The systems for which the release can be described by this equation are usually porous matrices containing hydrosoluble drugs [174].

III.2.1.3 Higuchi model

The Higuchi model is based on Fick's law and describes the diffusion of water-soluble drugs and low water-soluble drug out of semi-solid and solid matrices. The simplified equation of this model is:

$$M_t = K_H * \sqrt{t}$$

where K_H is the Higuchi dissolution constant. The curve to plot is the %CDR in function of the square root of time, which gives a linear curve [174].

III.2.1.4 Korsmeyer-Peppas model

The Korsmeyer-Peppas model has first been reported in 1983 by these authors to describe the release of drugs from hydrophilic polymeric matrices. The equation of this model is:

$$\frac{M_t}{M_\infty} = K * t^n$$

where M_t is the amount of drug released at time t, M_∞ is the amount of drug released at infinite time, which is the total amount of drug loaded in the system, and so M_t/M_∞ represents the fraction of drug released at time t, K is the kinetic constant and n is the release exponent. This exponent can be determined only with $M_t/M_\infty<0.6$ and represents the release mechanism. If n=0.5, the release mechanism is the Fickian diffusion (only diffusion-controlled release), if 0.5<n<1.0, it is an anomalous non-Fickian diffusion (mix of erosion-controlled release and diffusion-controlled release), if n=1.0 it is a zero-order release (Case II transport), and if n>1.0, it is a super Case II transport mechanism [175]. The curve to plot for this model is log(%CDR) in function of log(t).

The Case II transport, or Case II diffusion denomination has been introduced by T. Alfrey *et al.* in 1966 to describe a specific type of non-Fickian diffusion [176]. The concept is that, when the solvent penetrates the polymer system, a sharp boundary is created between the swollen region and the un-swollen region, and that this boundary moves with time in a linear way. So it comes from the relaxation of the polymer due to the movement of molecule in the system [177].

III.2.1.5 Ritger-Peppas model

The Ritger-Peppas model has been reported by these authors in 1987 after experiments conducted on non-swellable [178] and swellable matrices [179] such as spheres, cylinders, discs, slabs and sheets. The general equation is the same than for the Korsmeyer-Peppas, and the determination of the n value has also to be done only for M_t/M_∞<0.6, but the mechanism associated to the n value is different and reported in **Table 1**. The curve to plot is also log(%CDR) in function of log(t).

Table 1: Release exponent and associated release mechanism for several types of matrices

Release exponent n value			**Drug release mechanism**
Thin film	Cylinder	Sphere	
Non-swellable matrices			
0.50	0.45	0.43	Fickian diffusion
0.50<n<1.00	0.45<n<1.00	0.43<n<1.00	Anomalous non-Fickian transport
1.0	1.0	1.0	Zero-order (Case II transport)
Swellable matrices			
0.5	0.45	0.43	Fickian diffusion
0.5<n<1.0	0.45<n<0.89	0.43<n<0.85	Anomalous non-Fickian transport
1.0	0.89	0.85	Case II transport

III.2.1.6 Peppas-Sahlin model

The Peppas-Sahlin model has first been reported by these authors in 1989 [180] and refers to the following equation:

$$\frac{M_t}{M_\infty} = K_d * t^m + K_r * t^{2*m}$$

where K_d is the diffusion constant, K_r is the relaxation constant and m is the purely Fickian diffusion coefficient for a controlled delivery device with any geometrical shape. The K_d constant represents the contribution of Fickian diffusion and the K_r constant represents the contribution of the relaxation in the release mechanism. The values and mechanisms to be considered for m are the ones reported in Table 1 for swellable matrices. The authors gave a methodology to analyse the release study results:

1. Calculate the value of the aspect ratio=diameter/thickness of the device.
2. Determine m: if aspect ratio<0.1, m=0.45 and if aspect ratio>100, m=0.50. If m is in between, use their article as a reference to determine m.
3. Fit the first 60 % of the experimental data to the Peppas-Sahlin equation.
4. Calculate K_d and K_r.
5. Use the following equation to determine the percentage of Fickian diffusion to the release mechanism F:

$$F = \frac{1}{1 + \frac{K_r}{K_d} * t^m}$$

Although this model is more complex, it allows a finer characterization of the release mechanism.

III.2.2 How to use mathematical models?

Usually, the experimental data are fitted to the expected mathematical model, or the most relevant one or even a selection of several models. The best fit is then determined using the correlation coefficient. **Table 2** regroups some studies using mathematical models to describe their delivery device.

1143 **Table 2**: Some example of mathematical models used on protein delivery devices

System	Material	Protein/ therapeutic moeity	Mathematical model tested	Ref
MPs	Reverse micelle lecithin NPs in PLGA MPS	BSA	Zero-order, modified Ritger-Peppas	[7]
MPs	Gellan gum coated with retrograded starch and pectin	Insulin	First order, Higuchi, Korsmeyer-Peppas	[22]
MPs	CHI/alginate	Vancomycin chloride	Ritger-Peppas, Higuchi, Peppas-Sahlin, zero-order, first order	[114]
HG	HA, γ-PGA	FITC-BSA	Zero-order, first order, Higuchi, Korsmeyer-Peppas, modified Korsmeyer-Peppas, Peppas-Sahlin, modified Peppas-Sahlin	[63]
HG	TEMPO-oxidized cellulose nanofibers and cationic gar gum	BSA	Ritger-Peppas	[65]
HG	WPI, xanthan, pectin, gum tragacanth	Black carrot extract	Fick's second law as reported by Crank *et al.*	[68]
Fiber	Sodium alginate, soy protein isolate, PEO	Vancomycin chloride	Ritger-Peppas	[73]
Fiber	CHI NPs-loaded PVA core – sodium alginate, POE sheath	BSA	Higuchi, Ritger-Peppas	[79]
Fiber	PCL-HAPn core-PCL or PVAc sheath, PLGA NPs simultaneous electrospraying	BMP2, HAPn	Korsmeyer-Peppas, Peppas-Sahlin	[81]
LBL film	PEGsc, tannic acid	PEGsc	Zero-order	[87]
MacPS	CHI NPs-loaded COL HG placed in canals in porous TCP scaffold	rhBMP2	Zero-order, Higuchi	[110]

1144 MPs microparticles; NPs nanoparticles; PLGA poly(lactic-co-glycolic acid); BSA bovine serum albumin; CHI chitosan; HG
1145 hydrogel; HA hyaluronic acid; γ-PGA poly(γ-glutamic acid); FITC-BSA fluorescein isothyocianate-BSA; TEMPO 2,2,6,6-
1146 tetramethylpiperidine-1-oxyl; WPI whey protein isolate; PEO poly(ethylene oxide); PVA poly(vinyl alcohol); PCL
1147 polycaprolactone; HAPn hydroxyapatite nanorods; PVAc poly(vinyl acetate); LBL layer-by-layer; PEGsc PEGylated salmon
1148 calcitonin, COL collagen; TCP tricalcium phosphate

1149

IV Circulating systems

Circulating systems refer to protein delivery systems able to circulate in the body fluids to reach their target. They are developed for several decades for the treatment of cancer due to their ability to penetrate tumour cells and are also a good alternative to subcutaneous injection of insulin when designed for oral delivery. Some circulating systems have also been proposed for tissue engineering even if implantable systems are more common.

IV.1 Cancer treatment

IV.1.1 RNase delivery

Among the possible proteins studied to treat cancer, RNase A is interesting as it enters the cytosol and cleaves the intracellular RNA, preventing the synthesis of proteins and thus leading to cell death [181]. Several systems have then been developed to maximise the intracellular delivery of RNase A. For example, a study reported the covalent coupling of RNase A with HA to obtain two effects [136]. First, the increase of the RNase A negative charge, helping the complexation with the cationic lipid-like molecule EC16-80 to form protein/lipid-like NPs. Second, the targeting of cancer cells as HA can specifically bind to CD44 receptor, which is overexpressed in many solid tumours. The EC16-80/RNase A-HA had the best cell internalization result in A549 (lung) and MCF-7 (breast) cancer cell lines, exhibiting high and low CD44 expression respectively. An additional experiment showed the necessity of having the HA-CD44 binding to have cellular uptake and so, to have RNase A intracellular delivery and efficacy. These results are represented in **Figure 4A**.

In another study, the specific cell internalization was assured by the coating of NPs with cancer cell membrane. In this case, the selective cellular uptake was induced by the cancer cell membrane type used to coat the NPs [35].

He *et al.* also proposed an RNase A delivery system by caging this protein. As explained above in the external stimuli section, the system consists of the caging of RNase A by modifying it with H_2O_2-cleavable phenylboronic acid (RNBC). The RNBC was then encapsulated in KPEI NCs coated with hematoporphyrin-HA. The study showed that the use of HA allowed the high internalization of the system by cancer cell lines highly expressing CD44. Furthermore, the authors demonstrated the synergistic activity of the system against cancer cells: the light exposure of the system leads to the production of ROS, which induces the release of RNase A, and both leads to cancer cell death [122].

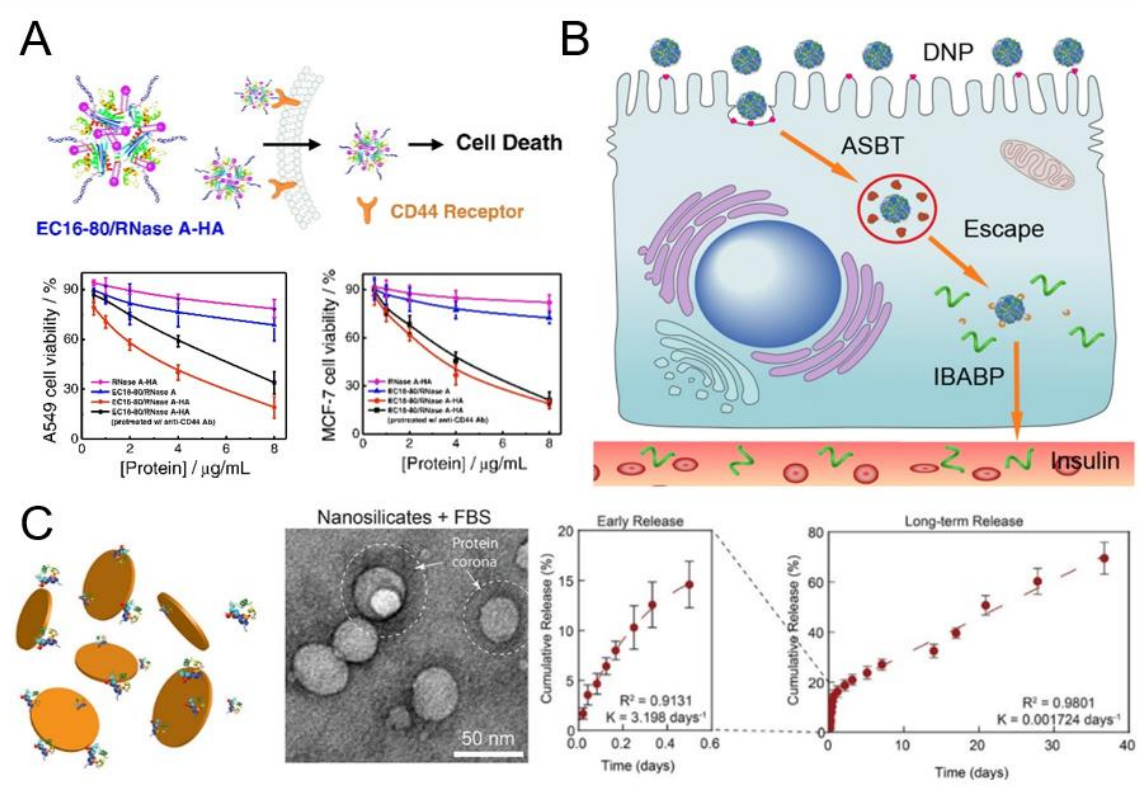

Figure 4: A. RNase A-HA/lipid-like NPs cell internalization via HA-CD44 interaction and efficiency on A459 and NCF-7 cancerous cell lines (adapted from article [136]). B. Schematic illustration of the bile acid pathways exploited by deoxycholic acid-modified nanoparticles to deliver insulin intracellularly (reproduced from article [182]). C. Interaction between nanosilicate and proteins, percent binding efficiency and protein release (adapted from article [183]).

IV.1.2 Caspase-3 delivery

Of course, RNase A is not the only interesting protein for cancer treatment. For example, Wu *et al.* developed a system for the co-delivery of paclitaxel (PTX) and recombinant human caspase-3 (Casp-3) [117]. Casp-3 is a crucial protein for the induction of apoptosis as it is able to cleave key structural proteins, leading to several phenomenon causing apoptosis such as DNA fragmentation, chromatin condensation and membrane bleeding [184]. The described system consists of linoleic acid droplet encapsulated in an amino-acid-modified CHI NC. The authors first optimized the system by functionalizing CHI with L-arginine, L-lysine or L-phenylalanine and finally chose the L-arginine due to the higher stability of the system. The PTX was then loaded inside the linoleic acid droplet and the Casp-3 was adsorbed on the NC surface. The *in vitro* tests showed a higher percentage of apoptotic cells in the samples treated with Arg-CHI-NCs-PTX/Casp-3 (53.2 %) compared to samples treated with Arg-CHI-NCs-PTX (43.7 %) and Arg-CHI-NCs-Casp-3 (20.0 %).

IV.1.3 Anticancer protein delivery mediated by exosomes

Exosomes are also systems of interest for protein delivery systems as the protein can directly be integrated into the exosome building block by transfecting cells with adequate plasmid. For example, PH20 hyaluronidase-exosome (PH20-ExSM) has been produced by HEK293T cells [56]. HA can contribute to the tumorigenesis by interaction with different receptors, such as CD44, and by accumulation in tumours,

which has notably been associated with tumour migration and chemoradioresistance. Thus, this system was expected to enhance tumour penetration via HA degradation, leading to enhanced tumour growth inhibition. The HA degradation capacity of the system has been assessed by checking the HA depletion in PC3 cells: the relative length clearly decreased in a PH20 dose-dependent manner (maximum decrease from 100% to ~ 20 %).

In another study, the use of exosome has been studied for immunotherapy, which is the stimulation of the immune system to cure a disease. More precisely, the delivery of SIRPα from exosome or ferritin nanocage has been studied for the blockage of CD47 activity, which is the inhibition of phagocytosis of tumour cells. Here again, HEK293T cells were used to produce SIRPα-ExSM [57]. A first *in vitro* experiment showed that the CD47 binding affinity on HT29 human colon adenocarcinoma cells was 5-fold higher for SIRPα-ExSM compared to SIRPα-ferritin nanocage (SIRPα-FN). In addition, the phagocytosis index of these HT29 cells was ~ 22.5 % for SIRPα-ExSM and ~ 6 % for SIRPα-FN. Altogether, these results showed that the SIRPα-ExSM was more efficient than SIRPα-FN to bind to CD47 in HT29, leading to an increase of the HT29 cells phagocytosis by inhibiting the CD47-mediated “don’t eat me” signal.

IV.2 Diabetes treatment

Insulin is almost the only protein used to treat diabetes type I with some exceptions. A quite common polymer material used to design new insulin delivery systems, and delivery systems in general, is CHI. Indeed, this biopolymer affords several advantages such as biodegradability and biocompatibility and importantly, also because it can self-assemble via electrostatic interactions with oppositely charged ions or molecules such as polysaccharides, proteins or nucleic acid. Of course, it can also be chemically modified before use.

IV.2.1 CHI as DDS material

For example, Maciel *et al.* reported the synthesis of MPs and NPs made of pectin and acetylated CHI playing on the acetylation degree (15.0 and 28.8 %) and the pectin /modified CHI ratio to act on the charge ratio [115]. After complete characterization, the release of insulin from MPs and NPs with both acetylation degrees but a unique charge ratio was evaluated in SGF (pH=1.2) and SIF (pH=6.8). The results showed no impact of the acetylation degree on the release process, which is pH-dependent: the cumulative amount of released insulin reached a maximum of 13 % in SGF and 89 % in SIF. Another study reported the modification of CHI with deoxycholic acid and then the synthesis of NPs by mixing the modified CHI, insulin and γ-PGA [182]. The authors notably studied all the insulin delivery mechanism, more precisely how it goes from the gastric system to the blood circulatory system, illustrated in Erreur ! Source du renvoi introuvable.**B**. The NPs were first internalized through apical sodium-dependent bile acid transporter (ASBT)-mediated endocytosis. Then, the endolysosomal escape of the NPs occurred leading to the crossing of the intracellular barrier. And finally, the trafficking and release of insulin were guided by the interaction between the NPs and ileal bile acid-binding protein (IBABP).

These two systems were developed for oral administration of insulin, a very interesting administration route to replace the classical subcutaneous injection.

IV.2.2 Other biopolymers for insulin delivery

Oral administration of insulin was also the objective in other studies, such as the one conducted by Meneguin *et al.* [22]. These authors synthesized gellan gum MPs coated with retrograded starch and pectin in order to enhance the insulin protection against enzymatic degradation and thus to enhance its delivery. The results showed high protection against trypsin and α-chymotrypsin with up to 80 % of insulin remaining intact when loaded inside the MPs compared to 3 % when delivered in the free form. Besides, the authors showed that the insulin permeability on Caco-2 cells was enhanced when delivered from MPs with a permeability rate between 42 and 67 % compared to free insulin for which it was 25 %. More recently, Wang *et al.* used another strategy to obtain a good oral insulin delivery [170]. They designed an insulin-loaded cationic liposome on which they adsorbed BSA to obtain a protein corona around the liposome. The resulting PcCL system, for protein corona cationic liposome, showed a very good mucus-penetrating ability and also a very good cellular uptake in presence of trypsin. Indeed, the trypsin was necessary to gradually degrade the BSA corona and then allow the cellular uptake of the remaining cationic liposome.

IV.3 Tissue engineering

IV.3.1 Bone and cartilage tissue

BMP2 is the protein drug of choice when designing a DDS for bone tissue engineering due to its osteogenesis property. Even if implantable systems are more developed to deliver this protein as it will be described in part V, some circulating systems have been reported in the literature. For example, a study reported the use of heparin NPs-loaded PEG MPs to deliver rhBMP2 after loading it by two methods: the “pre-fabrication loading” or “post-fabrication loading” which consists of loading the heparin NPs before PEG MPs formation or loading the final heparin NP/PEG MP system respectively, both done through adsorption [9]. This study showed that the pre-fabrication loading induced a similar C2C12 cell ALP activity while post-fabrication loading induced 7-fold higher ALP activity compared to free rhBMP2. As both systems presented very low protein release, the ALP activity measurement showed that the PEG-based part of the system was able to sequester proteins and then to deliver them to induce a cellular response. This sequestration ability has also been shown for SDF-1α as proof of concept for proteins with different molecular weight.

Other simplest systems have been developed, such as MPs fabricated with human COL I-based recombinant protein [120]. The authors studied the impact of several parameters on the protein release ability, such as degree of chemical cross-linking, use of dehydrothermal cross-linking (dehydration by high temperature) and the size of the MPs. For example, the initial burst release was decreased from 23 % to 17 % when increasing the chemical cross-linking. When using dehydrothermal cross-linking, this initial burst release represented 11 % of loaded protein. The measure of ALP activity in C2C12-BreLUC cells ensured the bioactivity of the released rhBMP2.

Another reported simple system is disk-shaped nanosilicate, as illustrated in Erreur ! Source du renvoi introuvable.**C** [183]. This system has been studied for the loading and release of rhBMP2 and TGF-β3 individually. The efficient differentiation of hMSCs in osteoblast cells by treatment with nanosilicate/rhBMP2 was checked by evaluating the expression of osteocalcin (OCN), as it is an osteospecific marker, and the production of COL1A1 and mineralized matrix. Regarding the treatment of hMSCs with nanosilicate/ TGF-β3, their chondrogenic differentiation has been

showed with the production of cartilage-like matrix by notably checking the amount of sulphated glycosaminoglycans (GAGs).

IV.3.2 Nerve tissue

PLGA MPs have been used to obtain protein drug delivery MPs. For example, Santhosh *et al.* optimized the PLGA MPs size and porosity to obtain an optimal release profile of rhNrg-1β1 peptide for the treatment of spinal cord injury (SCI) [185]. The goal was to deliver rhNrg-1β1 to promote the differentiation of neural precursors cells (NPCs) into myelinating olygodendrocytes as well as their survival, which could lead to cellular replacement and then to SCI repair. The *in vitro* study conducted on adult NPCs showed the successful differentiation of NPCs to oligodendrocytes. An *in vitro* study has also been performed on primary mixed astrocytes and microglia culture, as they play a key role in the central nervous system protection [186], to show that the treatment does not activate them and thus does not lead to neuroinflammation and glial scar formation.

In another study, Zeng *et al.* synthesized multiple PLGA core- CHI single shell MPs for the delivery of glial cell line-derived neurotrophic factor (GDNF) as it is able to regenerate peripheral nerves [187]. The modulation of CHI concentration allowed the reduction of the initial burst release compared to PLGA MPs and also the neutralization of PLGA degradation product acidity. Besides, *in vitro* experiments showed the preservation of GDNF bioactivity after release by assessing the neuronal differentiation of PC12 cells.

Mixed micelles made of PF127 and TPGS were also proposed for specifically deliver proteins across the blood brain barrier (BBB) [23]. An *in vitro* model of BBB using brain capillary endothelial cells (BCECs) was used to evaluate the cellular uptake of Rhodamine123 (Rho123) used as a model, notably due to its fluorescence. The CLSM analysis showed a clear enhancement of cellular uptake when using PF127/TPGS mixed micelles compared to free Rho123 and even PF127 micelles.

IV.3.3 Cardiac tissue

PLGA particles were also used for the regeneration of cardiac tissue after myocardial infarction (MI). For example, PLGA-PEG NPs have been proposed for the delivery of liraglutide [157]. Even if this protein was developed as a treatment for diabetes type II, it has multiple therapeutic effects for cardiac regeneration such as inhibition of myocardial apoptosis, attenuation of infarct size, promotion of angiogenesis and improvement of cardiac performance. The bioactivity of the released liraglutide was assessed *in vitro* by checking the phosphorylation level of AKT protein kinase in a culture of neonatal ventricular myocytes. The results showed no significant difference of AKT phosphorylation between the groups treated with liraglutide-loaded NPs and free liraglutide, showing that the bioactivity of the protein was retained.

In another study, PLGA MPs were loaded with Nrg-1 and coated with COL/PDL before adipose-derived stem cells (ADSCs) have been adhered on the MPs surface [159]. The goal was to combine the cardiac regeneration effect of both ADSCs, by their secretion of growth factors such as VEGF and HGF, and Nrg-1, by its promotion of angiogenesis, cardiomyocyte proliferation and cell survival. The MPs presented an encapsulation efficiency of 65±2 % and the released Nrg-1 was still bioactive as demonstrated by the proliferation of H9c2 cells.

IV.4 Gastrointestinal delivery

Gastrointestinal delivery is interesting to deliver proteins with enriched food to prevent some diseases or to treat diseases like inflammatory bowel disease (IBD). However, it is difficult to achieve due to several barriers such as enzymatic degradation and change of pH in the gastroinstestinal tract.

To overcome these barriers and obtain an oral delivery system for protein delivery to colon, Zhang *et al.* modified cassava starch with chloroacetic acid and 3-chloro-2-hydroxy-propyl-trimethyl ammonium chloride to obtain anionic carboxymethyl starch (CMS) and cationic quaternary ammonium starch (QAS) respectively [118]. Then, they use these new materials to produce LBL NCs and played on the degree of substitution and molecular weight of CMS to obtain several NCs. The release ability of these MPs was then tested with BSA in SGF, SIF and SCF (pH=7.2). The results showed that the NCs obtained with a lower degree of substitution and molecular weight were the best NCs for colon delivery.

CHI/PPA beads were also developed for such application and tested for BSA, WPI, insulin and casein hydrolysate encapsulation and release [25]. The authors could obtain very high encapsulation efficiency, more than 95 %, for all proteins except casein hydrolysate. The release studies showed good potential for delivery in the intestine as insulin and WPI were well retained in SGF and then delivered in SIF. More recently, Ling *et al.* studied alginate/CHI MPs for the intestinal release of bacterial effector protein AvrA/eGFP NPs for IBD treatment, as AvrA has anti-inflammatory and anti-apoptotic activity [116]. *In vitro* studies showed the MP ability to protect protein NPs in SGF and to release them in SIF as well as the cellular uptake of ~65 % of released protein NPs by HeLa cells.

IV.5 Vaccine delivery

Vaccine delivery is also an application for which MPs and NPs can be used. For example, Tavares *et al.* synthesized PLGA MPs in the form of dry powder for pulmonary vaccine delivery [27]. Their study aimed at evaluating the effect of BSA and L-leucine on the MPs characteristics, with BSA being a model antigen and L-leucine a dispersibility enhancer for the SASD process. *In vitro* studies conducted on A549 cells showed no cytotoxicity of the system.

More recently, Chatzikleanthous *et al.* studied the use of cationic liposomes made of 1, 2-distearoyl-sn-glycero-3-phosphocholine (DSPC), cholesterol and dimethyldioctadecylammonium bromide (DDA) to deliver a GBS67-CpGODN complex [172]. GBS67 is a recognized antigen of Group B *Streptococcus* (GBS) bacteria, which activity can lead to serious infections in pregnant woman and newborn. GBS67 has notably been investigated as potential vaccine candidate against GBS [188]. CpG oligodeoxynucleotide (CpGODN) is a Toll like receptor 9 (TLR9) agonist and its action leads to rapid immune responses that can inhibit or limit infections. The aim of the study was to obtain a new vaccine by covalently linking GBS67 and CpGODN prior to absorption on a liposome. The conjugation of both proteins led to a higher immune response compared to individual ones and more importantly a higher immune response with lower proteins doses.

The

Table 3 sums up some interesting circulating systems and their main *in vitro* results.

Table 3: Interesting *in vitro* results obtained with circulating systems

System/	Material	Protein /	Therapeutic ability	*In vitro* cell	Main result	Ref

Application		**therapeutic moeity**		**line model**		
NPs Cancer	Cancer cell membrane coated MSNs containing diselenide bonds	RNase A	Cleaves RNA	Hec HeLa cells, Raw 264.7, Hbc MCF-7, MEF	Selective cellular uptake	[35]
NCs Cancer	Amino acid-functionalized CHI	Casp-3 PTX	Casp-3: apoptosis of tumor cells PTX: chemotherapeutic agent	Hcc HeLa cells	Highest apoptosis with the co-delivery	[117]
ExSM Cancer	PH20-modifed exosome from HEK293T cells	Hyaluronidase PH20 DOX	PH20: Hyaluronan degradation DOX: anti-cancer	PC3 cells	Reduction of HA production by cells	[56]
MPs Diabetes	Retrograded start/ pectin-coated Gellan gum MPs	Insulin	Hypoglycemic effect	Caco-2 cells Caco-2 cells monolayer	Insulin permeability on cells increased	[22]
NPs Bone tissue eng.	Disk-shaped nanosilicate	rhBMP2 or TGF-β3	rhBMP2: osteogenesis TGF-β3 : chondrogenesis	hMSCs	Osteogenic or chondrogenic differentiation	[183]
MPs Nerve tissue eng.	PLGA particles in a single CHI MP	GDNF	Peripheral nerves regeneration	PC12 cells	Neuronal differentiation	[187]
Micelle Nerve tissue eng.	PF127 and TPGS	Rho123	Model molecule	BCECs	Enhanced cellular uptake in an *in vitro* model of BBB	[23]
MPs Cardiac tissue eng.	Adipose-derived SCs on PLGA/COL/ PDL MPs	Nrg-1	Angiogenesis, cardiomyocyte proliferation	H9c2 cells	Released Nrg-1 is bioactive	[159]

NPs nanoparticles; MSNs mesoporous silica nanoparticles; RNase A ribonuclease A; RNA ribonucleic acid; Hec HeLa cells human epithelial carcinoma HeLa cells; Raw 264.7 murine macrophages cells Raw 264.7; Hbc MCF-7 human breast cancer cell MCF-7; MEF mouse embryonic fibroblast; NCs nanocapsules, CHI chitosan; Casp-3 caspase-3; PTX paclitaxel; Hcc HeLa cells human cervical cancer HeLa cells; ExSM exosome; DOX doxorubicin; PC3 cells human PC3 prostate cancer cells; HA hyaluronic acid; MPs microparticles; Caco-2 cells Caco-2 human colon cancer cells; eng. Engineering; rhBMP2 recombinant human bone morphogenetic protein 2; TGF-β3 transforming growth factor-β3; hMSCs human mesenchymal stem cells; PLGA poly(lactic-co-glycolic acid); GDNF glial cell line derived neurotrophic factor; PC12 cells Rat pheochromocytome; PF127 Pluronic ® F127; TPGS D-α-tocopheryl polyethylene glycol succinate; Rho123 Rhodamine 123; BCECs brain capillary endothelial cells; BBB Blood Brain Barrier; SCs stem cells; COL Collagen; PDL poly-D-lysine, Nrg-1 Neuregulin-1

V Implantable matrices

Implantable matrices are mainly developed for tissue engineering, as they can be designed to mimic the tissue characteristics and thus to improve cell adhesion, migration and proliferation. Even if a huge amount of works focuses on bone tissue engineering, implantable matrices are also suitable for the regeneration of cartilage, nerve and cardiac tissues. Interestingly, implantable matrices have also emerged for the treatment of diabetes and cancer.

V.1 Bone tissue engineering

V.1.1 Macroporous scaffolds

MacPSs have been widely developed for bone tissue engineering, in response to the need of a material that could replace autologous bone graft. Indeed, this latter has several disadvantages such as the limit of donor source or the risk of rejection. As MacPSs are solids and present a porous structure, they can support cell migration and proliferation, making them very interesting in this field. As said previously, BMP2 is the therapeutic protein of choice for such application due to its ability to promote osteogenesis. The systems developed to deliver BMP2 can be separated in two categories: the first one consists of only one formulation type which can be made of organic, inorganic or a mixture organic/inorganic materials. The second category consists of the combination of several formulations such as the integration of nanostructures (MPs, NPs) into a scaffold. These ones are called nanocomposites here.

V.1.1.1 Single formulation: organic and inorganic material, alone or in combination

Organic MacPSs mainly consists of COL sponges. They have been studied for the release of BMP2, alone or with other drugs/proteins such as alendronate which promotes osteogenic cells differentiation and supresses osteoclasts [102], or osteoprotegerin which inhibits osteoclast maturation, leading to the inhibition of new bone resorption [189]. It has also been used to compare the efficiency of BMP2 and BMP9 for bone regeneration [190]. Another organic MacPSs reported recently consisted of polydopamine-coated 3D printed PLA scaffold [111]. BMP2 was then loaded on the coated surface via adsorption and the obtained MacPSs could release it, allowing proliferation and osteogenesis differentiation of hMSCs.

For inorganic-based MacPSs, Cao *et al.* proposed to use commercial α-TCP scaffold for the loading and release of a BMP2 peptide via E7 domain [137]. The E7 domain, a natural part of bone sialoprotein, was covalently linked to the BMP2 peptide KIPKASSVPTELSAISTLYL and allowed the loading via its binding to Ca^{2+} on the scaffold. Lin *et al.*, on their side, reported the synthesis of mesoporous bioactive glass scaffold for the co-delivery of BMP2 and chemokine interleukine-8 (IL-8), due to its ability to recruit stem cells [191]. The scaffold allowed the burst release of IL-8, adsorbed on the PEG-coated surface, and the sustained release of BMP2, loaded inside the mesopores.

Layered or sandwiched composite MacPSs, meaning that the final delivery system consists of a mixture of such organic and inorganic materials, have also been developed. For example, Cai *et al.* reported an HAP-COL scaffold able to release BMP2, leading to the adhesion, proliferation and differentiation of rat bone marrow-derived MSCs [103]. Another example is the formulation of a mixture of gelatin, HAP and calcium sulphate in the form of cryogel for the delivery of BMP2 and zoledronic acid, another inhibitor of new bone resorption by the killing of osteoclast [151].

The case where nanostructures are formulated into another phase, to form nanocomposites MacPSs is developed more in details in the next paragraph.

V.1.1.2 Nanocomposites: nanostructures integrated in a scaffold

A very common way to obtain such nanocomposite MacPSs is to embed MPs/NPs particles in the scaffold or on the scaffold. Here also, we can classify the delivery systems depending on the organic/inorganic nature of the material.

For example, Wang *et al.* synthesized a scaffold made of CHI, agarose and gelatin in which they loaded CHI/heparin NPs for the delivery of BMP2 and SDF-1, which is a full organic-based scaffold [106]. Full inorganic-based scaffolds can also be done, as reported by Cui *et al.* who loaded P28 peptide in enlarged pores hollow MSNs before embedding them in true bone ceramics. This system showed its ability to promote MC3T3-E1 cells proliferation and osteogenic differentiation *in vitro* due to the osteogenic activity of the BMP2 related P28 peptide [156]. Of course, the use of organic and inorganic material together is common. For example, Yao *et al.* proposed the encapsulation of BMP2 in MSNs embedded in gelatin 3D nanofibrous scaffold further coated with deferoxamine-modified CHI [109]. This allowed the delivery of deferoxamine in addition to BMP2, a molecule able to activate the hypoxia-inducible factor-α and to trigger angiogenesis. The scaffold and BMP2 release are notably illustrated in Erreur ! Source du renvoi introuvable.**A**.

The integration of the particles can be more complex. For example, Hettiaratchi *et al.* embedded heparin MPs in PCL nanofibers that were formulated as a mesh further placed around a COL sponge [192].

Of course, other material formulations can be embedded in a scaffold especially for the co-delivery of growth factors. Kuttapan *et al.* notably reinforced a gelatin scaffold containing silica-coated nanoHAP with oriented poly(L-lactic acid) (PLLA) fibrous yarns [152]. This system was studied for the co-delivery of VEGF+BMP2 and FGF2+BMP2 due to the angiogenesis property of VEGF and the ability of FGF2 to stimulate stem cell migration.

As seen above, BMP2 is not the only protein studied for bone tissue engineering: VEGF notably induces interest. It has for example been loaded in alginate MPs further embedded in a COL-HAP scaffold, combining the angiogenesis ability of VEGF and the osteoinductive property of HAP [167]. In another study, it was loaded with L-ascorbic acid 2-phosphate, a derivative of ascorbic acid which is essential for COL biosynthesis, in avidin-modified PLGA NPs [100]. These NPs were then embedded in a polymer solution made of poly(vinyl acetate) (PVAc), CHI, PLLA and biotin-modified-PEI before freeze-drying. The good integration of the NPs in the polymer solution was due to the avidin-biotin conjugation.

SDF-1 was also interesting due to its ability to promote cell migration and osteogenic differentiation. Then, Zhang *et al.* proposed an HAP scaffold coated with alginate [14]. This coating allowed the loading of SDF-1 and dexamethasone (DEX)-loaded hydroxypropyl-β-cyclodextrin microspheres. The *in vitro* experiment showed the migration of rat bone marrow MSCs inside the scaffold and their osteogenic differentiation.

High-mobility group box 1 (HMGB1), an osteogenic cytokine, was also loaded in gelatin sponge, which was combined with MSCs sheets to increase fracture healing rate [193].

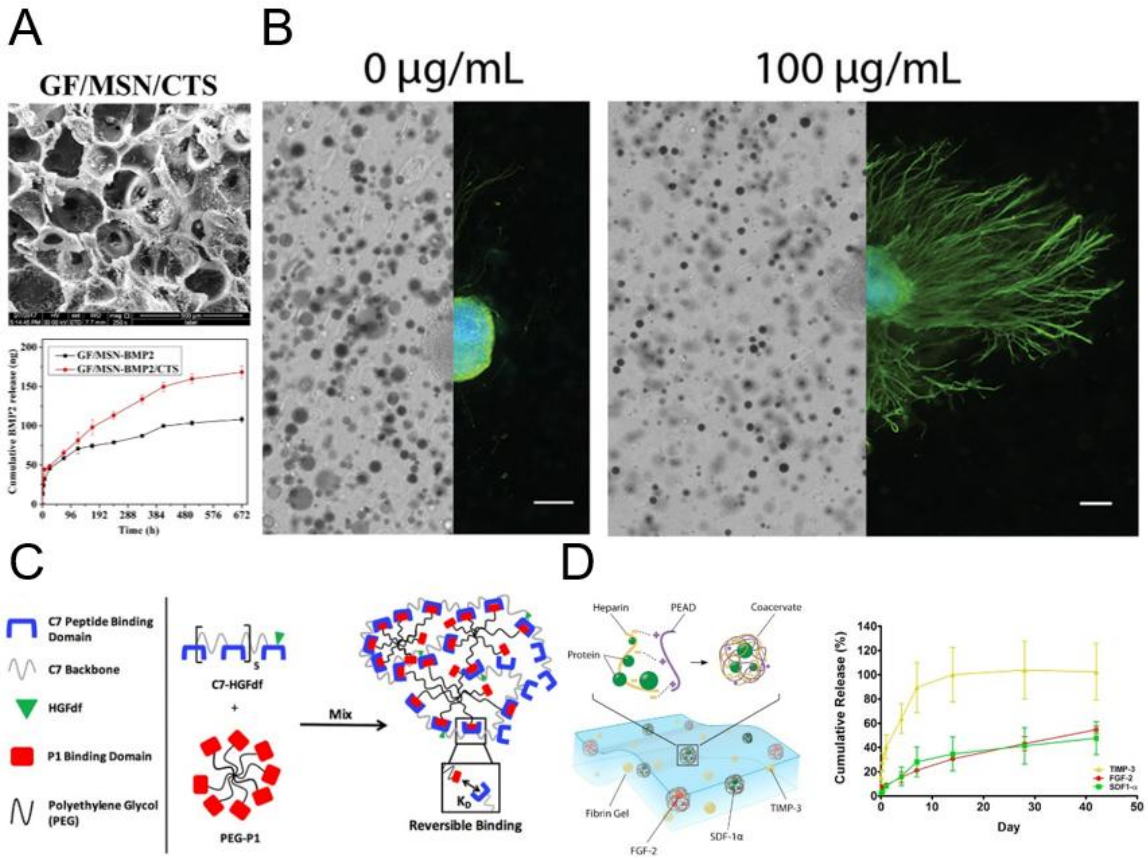

Figure 5: A. SEM pictures of the scaffold and resulting release profile of BMP-2 (adapted from article [109]). B. In vitro neurite outgrowth in presence of NGF unloaded and loaded microparticles (adapted from article [194]). C. Schematic illustration of the HG (adapted from article [144]) D. Schematic illustration of the HG and the release profile of the different proteins (reproduced from article [195])

V.1.2 Fibers

Fibers are very interesting scaffolds for tissue engineering as their structure mimics the ECM and provide good support for cell adhesion, migration and proliferation. A very used material to design fibers for bone tissue engineering is PLA, alone or in combination. For example, Bhattarai *et al.* developed PLA/BMP2 core – PLA/TUDCA sheath fibers to deliver two therapeutic agents: BMP2 and tauroursodeoxycholic acid (TUDCA), an angiogenic factor. The *in vitro* studies conducted on hMSCs and human umbilical vein endothelial cells (HUVECs) confirmed the ability of the system to promote angiogenic and osteogenic differentiation [196]. Regarding the combinations, it has notably been associated with PVA. Da Silva *et al.* notably studied the delivery of BMP2 from PVA/BMP2 core-PLA sheath fibers compared to monolithic PLA and PVA fibers [154] and Wang *et al.* evaluated the impact of cold atmospheric plasma treatment on BSA/PVA core-PLLA sheath fibers characteristics [80]. In these examples, the protein cargo was loaded only in the core of the fiber, but other possibilities have been explored. For example, Cheng *et al.* reported the synthesis of BMP2/PVA core- silk fibroin/PCL sheath fibers coated by CHI and connective tissue growth factor (CTGF), another angiogenic growth factor, via LBL [197].

At last, in another study reported by Aragón *et al.*, PCL/HAP nanorods core-PCL or PVAc sheath fibers were decorated with BMP2-loaded PLGA NPs via simultaneous electrospraying during the coaxial electrospinning [81].

V.1.3 Hydrogels

HG systems have also been proposed for the delivery of BMP2 for bone tissue engineering. Alginate HG has notably been investigated in comparison with COL sponge [198] and as a delivery system for BMP-loaded heparin MPs [71]. In both studies, the bioactivity of the released BMP2 was retained as assessed by ALP activity of MC3T3 cells and C2C12 cells respectively. Olthof *et al.* proposed another material, oligo[(polyethylene glycol) fumarate] bis[2-(methacryloyloxy) ethyl] phosphate (OPF-BP), to obtain an HG. BMP2-loaded PLGA MPs were then loaded within the HG by adsorption [61].

Some studies also reported the use of glue. For example, Huber *et al.* investigated the possibility to use commercial demineralized bone matrix (DBM) putty as BMP2 delivery system to enhance the osteinductive ability of the DBM [199]. In another study, Enezei *et al.* compared the BMP2 and VEGF expression in dental stem cells after treatment with VEGF-loaded fibrin glue or VEGF-loaded fibrin glue treated with porous biphasic calcium phosphate [200].

V.2 Cartilage tissue engineering

V.2.1 Fibers

TGF-β is a family of cytokines essential for fibrocartilage and cartilage formation, which make these cytokines proteins of choice for cartilage tissue engineering. Thus, several fibers have been designed for their delivery. Among the organic material, PCL is often used as building block due to its biocompatibility, good biodegradability and low interactions with cells (bio-inert material). For example, Qu *et al.* synthesized monolithic fibers composed of PCL, PLGA, BSA and TGF-β3 for the delivery of TGF-β3 and this system allowed the proliferation and fibrochondrogenic differentiation of synovium-derived stem cells (SDSC) [201]. PCL fibers were also used as the support for LBL coating of TGF-β3-loaded CHI nanogels and polyanions. This study notably aimed at showing the possibility to fabricate this construct and to test several polyanions for it (alginate, chondroitin sulfate, HA) [202]. Core-sheath fibers were also proposed for this protein. For example, Wang *et al.* synthesized rhTGF-β3/BSA/PBS core – P(LLA-CL)/COL sheath fibers and showed that the bioactivity of TGF-β3 was retained after release by checking the production of COL type II and GAGs by chondrocytes [203].

Inorganic nanofibers have also been studied for the delivery of TGF-β1 and growth differentiation factor-5 (GDF-5) due to their ability to induce human adipose stromal cell differentiation into intervertebral disk nucleopulpocytes. More precisely, the system was rod-shape colloidal silica nanofibers and the study assessed the bioactivity of the released proteins [204].

V.2.2 Macroporous scaffolds

A MacPS has been proposed for anterior cruciate ligament (ACL) regeneration. The scaffold consisted of silk mesh cross-linked to SDF-1-loaded COL sponge. The authors studied the effect of the SDF-1 release on ligament-derived stem/progenitor cells (LSPCs) and the results showed the SDF-1-induced recruitment of LSPCs inside the scaffold and formation of tendon tissue [104].

V.3 Nerve tissue engineering

V.3.1 Fibers

The use of fibers for nerve repair is very interesting as the structure of the fiber can direct the growth of neurons and enhance it. Whitehead *et al.* reported the synthesis of NGF-loaded PLGA MPs embedded in HA aligned fibers [194]. The system provided a mechanically good environment for dorsal root ganglia (DRG) growth. As illustrated in Erreur ! Source du renvoi introuvable.**B**, the aligned fibers enhanced the neurite outgrowth of DRG in presence of NGF-loaded MPs. A dual delivery scaffold has also been developed for such application [162]. The system consisted of PLLA fibers encapsulating β-NGF with VEGF adsorbed on its surface. This design allowed a fast release of VEGF as it was adsorbed on the surface and a slow continuous release of NGF, allowing the enhancement of neural differentiation of induced pluripotent stem cells-derived neural crest stem cells (iPSCs-NCSCs) *in vitro.*

V.3.2 Hydrogels

HG is a good system for neural regeneration, as it is a good support in which cells can migrate and proliferate, which is also used to help the transplantation of cells. HG systems delivering proteins have been developed these last five years for these reasons [205]. One interesting system combining PLA nanofibers of different sizes and self-assembling peptide-Fmoc/DIKVAV HGs in order to well mimic the ECM has been proposed [206]. The system was studied for the release of GDNF or brain-derived neurotrophic factor (BDNF) individually, both known for their ability to increase neuron survival and metabolic activity. The study tried different loading: the GDNF was embedded in the fibers by blending while the BNDF was immobilized on the fibers surface through covalent bond. This led to different release profiles, which were a burst release for GDNF and a sustained release for BDNF.

V.3.3 Macroporous scaffolds

Nguyen *et al.* proposed an hybrid scaffold delivering neurotrophin-3 (NT-3), which actions leads to neuronal survival, axonal sprouting and regeneration, and miR-222, a model microRNA which can promote severed axons regeneration by participating in the synthesis of proteins at distal axons [76]. The system consisted of poly (ε -caprolactone-co-ethyl ethylene phosphate) (PCLEEP) nanofibers embedded in a COL solution prior to freeze-drying to obtain the scaffold. NT-3 was loaded inside the COL solution while the miR-222 was loaded in micellar NPs made of PCL-PEG and PCL-PPEEA (poly(ε -caprolactone)-block-poly(2-aminoethyl ethylene phosphate)). The system notably showed positive results *in vivo*, as it will be described in section VII.

V.3.4 Films

A multifunctional film has also been proposed for the guidance of neuron growth. The study reported the synthesis of a PLLA film presenting longitudinal micropattern. The film was loaded with β-NGF on the surface following a gradient and with β-NGF-polyanhydride MPs. The surface loading allowed a fast release of the growth factor while the MPs allowed a controlled release. Altogether, it could guide and direct neurite outgrowth of PC12 cells [92].

To the best of our knowledge, this is the only example of auto-supported film delivering proteins developed these last years for implantation. However, films as protein delivery systems can be designed as coatings to be added on implants. For example, Sivak *et al.* compared the effect of silk-trehalose film loaded with

chondroitinase ABC and/or GDNF inserted in a silk nerve conduit on the regeneration of rat sciatic nerve [207].

V.4 Cardiac tissue engineering

V.4.1 Patches

The development of patches for cardiac tissue engineering is interesting due to several reasons. For example, O'Neill *et al.* developed an alginate MPs-loaded COL patch for the delivery of HGF and insulin-like growth factor-1 (IGF-1) from the MPs. These proteins induce the recruitment and proliferation of cardiac stem cells (CSCs). Then, the implantation of such system could promote the *in vivo* CSCs migration and proliferation at the infarct site and so avoid the implantation of *in vitro* cultured CSCs [208]. Fleischer *et al.*, on their site, developed a system that could mimic the structure of cardiac tissue [209]. Their system consisted of an LBL patch incorporating cells, particles and drug. More precisely, the layers were made with albumin electrospun fibers further carved with a laser. One layer presented microchannels to orient the seeded endothelial cells, one layer presented microtunnels with side cages and was loaded with endothelial cells as well and VEGF-loaded PLGA NPs, for the VEGF angiogenesis property, and the last layer was caged-like patterned and was loaded with DEX-loaded PLGA NPs, for the anti-inflammatory property of DEX.

V.4.2 Hydrogels

HGs have also been used to ensure a better delivery of growth factors after MI. Then, Steele *et al.* designed an HG for the delivery of HGFdf as it has anti-apoptotic, pro-angiogenic and cardio-protective properties [144]. More precisely, they designed a "Shear-thinning Hydrogels for Injectable Encapsulation and Long-term Delivery" named SHIELD, which is an HG able to support injection. Indeed, it turns to a solution state when submitted to shear force, and then turns back to HG state. The HG they developed is illustrated in Erreur ! Source du renvoi introuvable.**C**. The shear-thinning/self-healing ability of the HG was assured by the P1-C7 peptidic molecular recognition and reversible binding. Co-delivery of several growth factors have also been proposed by Awada *et al*. [195]. They loaded a fibrin gel with tissue inhibitor of metalloproteinases 3 (TIMP-3) and two types of coacervate made with the synthetic polycation poly(ethylene argininylaspartate diglyceride) (PEAD) and heparin/protein. The protein was either bFGF-2 or SDF-1α. This system combines the cell recruitment ability of SDF-1α, the angiogenesis property of bFGF2 and the ability of TIMP-3 to reduce ECM degradation. This system is illustrated in Erreur ! Source du renvoi introuvable.**D**.

V.5 Other applications of implantable matrices

V.5.1 Diabetes treatment

A possibility to treat diabetes type I is the use of islet transplantation, which then implies to find a good site of implantation without causing a high immune response. Thus, Liu *et al.* developed a system delivering the cytokine IL-33, which can have pro- or anti-inflammatory effect depending on its environment, to support cell transplantation in adipose tissue. The systems consisted of a disk-shape inner layer made of mannitol and IL-33-loaded PLGA MPs compressed between two outer layers of PLGA. The bioactivity of the released IL-33 was assessed by checking the production of IL-13 from naïve T cells [210].

V.5.2 Cancer treatment

An HG delivery system has been proposed for cancer treatment to provide local drug delivery and overcome the possible difficulty of circulating systems to reach their target. The system was an oligopeptide HG encapsulating hirudin for its anti-angiogenic property and TRAIL for its apoptosis property. More precisely, the HG was made of F-moc and FF-DOPA which the self-assembly was catalysed by the protease WQ9-2. The anti-angiogenic activity of the system was assessed on HUVECs and the apoptotic activity of TRAIL was assessed on human breast cancer cells MDA-MB-231 [145].

V.5.3 Internal wound healing

Lokhande *et al.* proposed an injectable HG that could be used as hemostat to treat internal haemorrhage. This HG was made with κ-carrageenan and was reinforced with 2D nanosilicates. This addition of nanosilicate increased the hMSCs adhesion and spreading on the HG. For example, with 2 % nanosilicate, the area on which cells spread was increased by 400 %. The study also showed the ability of the system to accelerate blood clotting and to deliver VEGF, which led to enhanced wound healing in a scratch assay [72].

Some implantable matrices and their major *in vitro* results are summarized in **Table 4**.

Table 4: Interesting *in vitro* results obtained with implantable matrices

System/ Application	Material	Protein / therapeutic moeity	Therapeutic ability	*In vitro* cell line model	Main result	Ref
MacPS Bone tissue eng.	PDA-coated PLA 3D printed wheel	BMP2	Osteogenesis	MG-63 hMSCs	Biocompatibility, osteogenesis	[111]
MacPS Bone tissue eng.	MesoCS NPs in PCL 3D-printed scaffold	BMP2	BMP2: osteogenesis MesoCS: bone-like apatite formation	WJMSCs	Osteogenic differentiation, calcium deposition	[112]
MacPS Bone tissue eng.	Commercial gelatin sponge	HMGB1	Osteogenesis	MSCs, MSCs sheets	STAT3-mediated osteogenic differentiation	[193]
Fiber Bone tissue eng.	PLGA-NPs on PCL/HAPn core–PCL or PVAc sheath	BMP2 and HAPn	PCL: osteoinduction and osteoconduction BMP2: osteogenesis HAPn: osteoconduction	Human osteoblasts	Enhanced bone markers expression (ALP, OCN, OPN)	[81]
HG Bone tissue eng.	Fibrin glue with or without porous BCP	VEGF	Angiogenesis	Dental stem cells	Higher osteogenesis and angiogenesis gene expression	[200]
Fiber Cartilage tissue eng.	PCL/PLGA/BSA fibers as a mesh	TGF-β3	Fibrochondrogenic differentiation, increases COL synthesis	SDSCs	Fibrocartilage-like matrix deposition	[201]
MacPS Cartilage tissue eng.	Knitted silk mesh cross-linked to COL sponge	SDF-1	Cell recruitment	LSPCs	Stem cell recruitment of the scaffold	[104]
Fiber Nerve tissue eng.	PLLA fibers used as nerve conduit	$VEGF_{165}$ β-NGF	VEGF: angiogenesis β-NGF: neurogenesis	iPSCs-NCSCs	Enhanced proliferation and neural differentiation	[162]
HG Nerve tissue eng.	PLA nanofibers in Fmoc/DIKVAV HG	GDNF BDNF	Increase neuron survival and metabolic activity	Primary CNCs culture	Increased metabolic activity	[206]
Film Nerve tissue eng.	PLLA porous film and polyanhydride MPs	β-NGF	Promote neurite outgrowth	PC12 cells	Guided neurite outgrowth	[92]
Patch Cardiac tissue eng.	Alginate MPs in COL patch	HGF IGF-1	HGF: cell migration IGF-1: cell proliferation and anti-apoptotic effect	$c\text{-}Kit^{POS}$ Cardiac Stem Cells	Cell migration and enhanced proliferation	[208]
HG Cardiac tissue eng.	SHIELD (PEG-P1 and C7-HGFdf)	HGFdf	Anti-apoptotic, pro-angiogenic and cardioprotective	NCm, HUVECs	Cell viability against hypoxia, angiogenesis	[144]

Fiber Diabete	CHI/PEO	Insulin	Hypoglycemic effect	3T3-L1	Released insulin is bioactive	[211]
MacPS Diabete	PLGA	Cytokine IL-33	Ani-inflammatory effect	Naïve T cells	Released IL-33 is bioactive	[210]
HG Cancer	Oligopeptides Fmoc-F and FF-DOPA	Hirudin TRAIL	Hirudin: anti-angiogenesis TRAIL: proapoptotic agent	MDA-MB-231, MCF-10A HUVECs	Anti-tumor activity of the co-delivering system	[145]

MacPS MacroPorous scaffold; eng. Engineering; PDA polydopamine; PLA poly(lactic acid); BMP2 bone morphogenetic protein 2; MG-63 human osteoblast-like cell line; hMSCs human mesenchymal stem cells; MesoCS mesoporous calcium silicate; NPs Nanoparticles; PCL poly(caprolactone); WJMSCs Human Wharton's Jelly mesenchymal stem cells; HMGB1 high-mobility group box 1; PLGA poly(lactic-co-glycolic acid); HAPn hydroxyapatite nanorods; PVAc polyvinyl acetate; ALP alkaline phosphatase; OCN osteocalcin; OPN osteopontin; BCP biphasic calcium phosphate; VEGF vascular endothelial growth factor; BSA bovine serum albumin; TGF-β3 transforming growth factor-β3; SDSCs synovium-derived stem cells; SDF-1 stromal cell derived factor-1; LSPCs ligament-derives stem/progenitor cells; PLLA poly(L-lactic acid); β-NGF β-nerve growth factor; iPSCs-NCSCs induced pluripotent stem cells-derived neural crest stem cells; IGF-1 insulin-like growth factor-1; BDNF brain-derived neurotrophic factor; NSCs neural stem cells; Fmoc/DIKVAV fluorenylmethyloxycarbonyl capped aspartic acid-isoleucinelysine- valine-alanine-valine; GDNF glial cell-line derived neurotrophic factor; CNCs cortical neurons cell; MPs microparticles; PC12 cells Rat pheochromocytome; HGF hepatocyte growth factor; SHIELD Shear thinning Hydrogels for Injectable Encapsulation and Long-term Delivery; HGFdf hepatocyte growth factor dimeric fragment; NCm neonatal cardiomyocytes; HUVECs human umbilical vein endothelial cells; CHI chitosan; PEO poly(ethylene oxide); 3T3-L1 preadipocyte cells; TRAIL tumor necrosis factor-related apoptosis inducing ligand; MDA-MB-231 human breast cancer cells; MCF-10A human normal breast epithelial cells

VI Covering systems

Covering systems refer to systems that are aimed at being deposited on a body surface. Such systems are mainly used to regenerate damaged skin tissue, but can also be used as transdermal delivery system to cross the skin barrier or even as transbuccal delivery systems.

VI.1 Tissue healing

VI.1.1 Fibers

As fibers mimic the ECM architecture, they are a system of choice to deliver proteins to regenerate the skin. Neovascularization is an important phenomenon to reach tissue regeneration, which makes VEGF a very good growth factor to deliver as it promotes angiogenesis.

Thus, Zigdon-Giladi *et al.* synthesized PEO/VEGF core-PCL/PEG sheath fibers to improve angiogenesis [212]. The authors notably studied the effect of PEG quantity on the pore size of the shell and release profile of VEGF. The results showed that the pore size and density increase with increased PEG quantity. The release profile presented typically a burst release followed by a sustained release. The authors showed the possibility to tune the sustained release time by playing on the PEG quantity: the continuous release increased from 4 to 18 h by decreasing the PEG amount from 3 % to 0.25 %.

VEGF has also been co-delivered with TGF-β3 [163]. In this study, PLGA nanofibers were coated with heparin/protein (VEGF or TGF)-PEAD coacervate. This coating strategy was operated to avoid the exposition of the growth factors to the electrospinning formulation conditions. The bioactivity of the released growth factors was assessed by checking the proliferation of human dermal fibroblast and tubule formation of HUVECs. The results showed the higher biological response of nanofibers loaded with the dual-drug coacervate, compared to the sample treated with VEGF-coacervate-loaded fibers and free TGF-β3 (Coa-V-Free T) and to the sample treated with TGF-β3-coacervate-loaded fibers and free VEGF (Coa-T-Free V). The capillary tubule total length was around 13 mm for the dual-drug coacervate-loaded fibers while it was around 9 mm for the Coa-V-Free T and around 7 mm for the Coa-T-Free V in the tubule formation experiment with HUVECs.

As the migration and proliferation of fibroblasts are important phenomena for wound healing, the delivery of PDGF-BB for this application is a good strategy to investigate as it can promote these phenomena. Thus, Piran *et al.* embedded PDGF-BB-loaded CHI NPs in PCL nanofibers for wound healing and evaluated its effect on fibroblast migration and proliferation [213]. The results showed a chemotaxic behaviour more pronounced toward PDGF-BB-containing scaffold and a three-fold higher expression of the Arp2 gene when cells were seeded on PDGF-BB-containing scaffold. This gene is involved in cell protrusion, a phenomenon occurring during cell migration. Altogether these results showed the ability of the PDGF-BB-containing scaffold to promote cell migration.

VI.1.2 Films

A certain interest in the design of films for wound healing is growing, notably because it can cover the wound and then protect it from the environment.

Thus, Qi *et al.* developed a zein-based film [97]. These authors notably modified zein with citric acid and acetic anhydride to modify its hydrophilicity. The fibrous film was then cross-linked with sodium hexametaphosphate, which gave it the ability to

swell in pure water and phosphate buffer solution like an HG. The obtained films were completely characterized and their protein adsorption and release ability were tested with BSA and cytochrome C due to their opposite charge. The experiments showed better results with the positively-charged cytochrome C.

On their side, Mandapalli *et al.* proposed an LBL film made of CHI and sodium alginate for the co-delivery of the growth promoting agent epidermal growth factor (EGF) and the TGF-β small interfering RNA (TGF-β siRNA) [214]. This siRNA is supposed to silent the TGF-β gene expression, which will stop the COL production. This will avoid scar formation during the healing as it is due to a surproduction of COL caused by a surpopulation of fibroblast and a decrease of collagenase within the wound site. The two therapeutics were added to the film as layers in the LBL process and the study compared their individual and co-delivery. The unloaded LBL film notably showed good cell adhesion of A431 epidermal keratinocytes without bacterial colony formation as tested with *Escherichia coli* (*E. coli*) and *Staphylococcus aureus* (*S. aureus*). The efficiency of the loaded LBL film was assessed *in vivo* and will be described in the next section.

More recently, Zhang *et al.* reported the development of a complex LBL film which is mechanically sensitive [126]. The system consists of a first layer being a piezoelectric-dielectric film, the mechano-sensitive part of the system. More precisely, this layer is made with the piezoelectric polymer poly(vinylidene fluoride-co-hexafluoropropylene) (PVDF-HFP) filled with 4-azidotetrafluorobenzoic acid (TFB)-modified rGO (graphene oxide). Then, LBL adsorption was performed on this layer, first with PAH and MSNs and second with PAH and 4,4′-Diazostilbene-2,2-disulfonic acid disodium salt (DAS). This PAH/DAS part was further cross-linked under UV light and the system was then loaded with positively charged methylene blue (MB), negatively charged sodium fluorescein (SF), zwitterionic peptide RhB-SGSGRGD or the enzyme catalase (CAT). The results showed the ability of the film to accelerate the drug release under mechanical stimuli, whatever the cargo as it can be seen in **Figure 6A**. More importantly, the CAT activity, which is the disruption of H_2O_2 into H_2O and O_2, was retained. Indeed, the viability of human lung fibroblast cells (HLFCs) exposed to H_2O_2 was increased by 10-30 % after treatment with the CAT-loaded film.

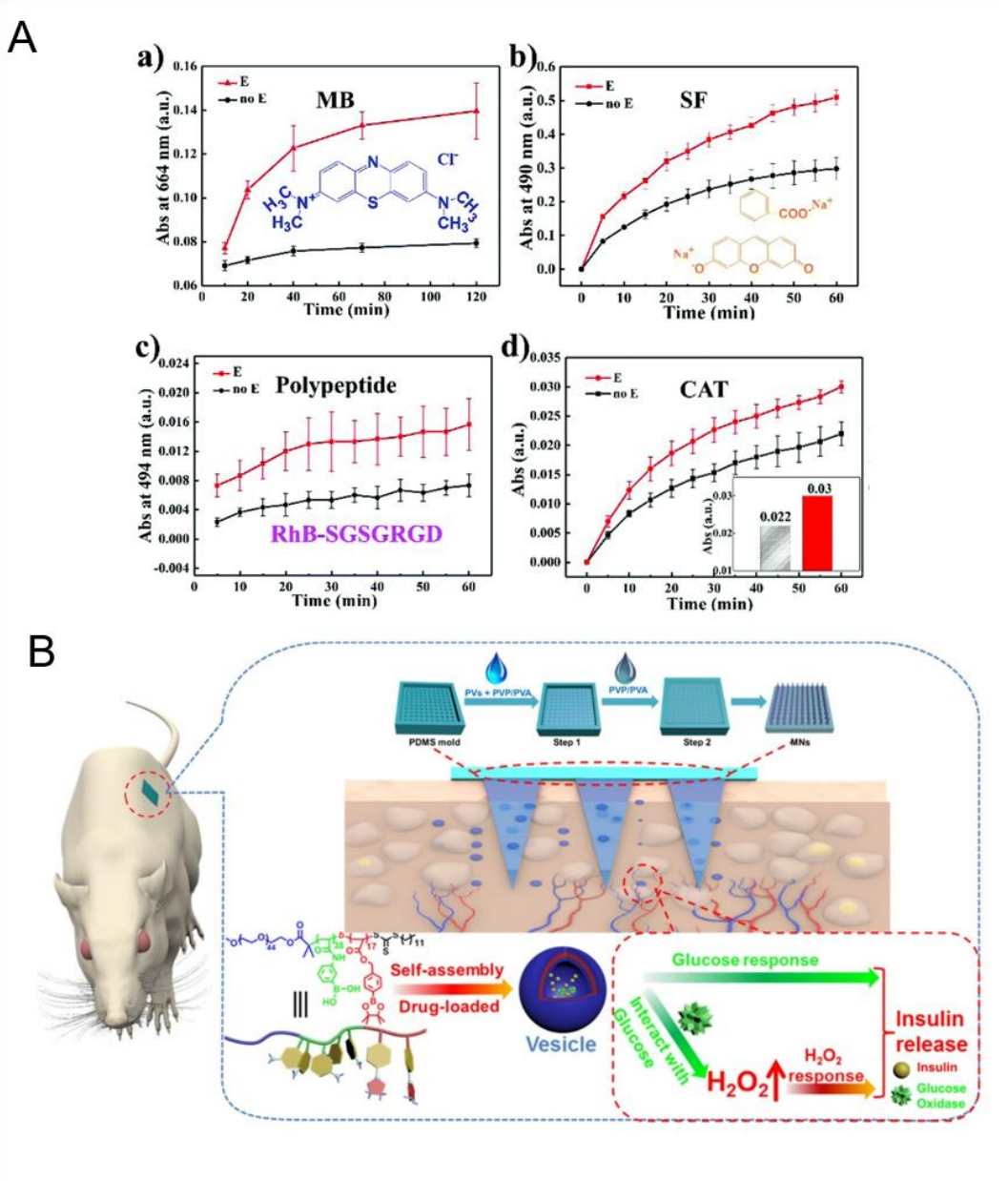

Figure 6: A. Release of several proteins by a piezoelectric-dielectric film with and without finger-pressing (adapted from article [126]). B. Schematic illustration of the fabrication of the patch and the release pathways (reproduced from article [95]).

VI.1.3 Hydrogels

A study reported the development of liposome/gelatin methacrylate composite HG for the delivery of SDF-1α to induce cells migration to the wound site [171]. The use of type B gelatin assured the biocompatibility of the system, as it is a denatured form of COL, and its protease-induced degradability. As for the use of liposome to encapsulate SDF-1α, it was operated to better control the release of the protein drug. *In vitro* experiment showed that the system retained SDF-1α activity as it enhanced hMSCs migration and induced mTOR signalling activity. This was interesting as the mTOR pathway is involved in the stimulation of cells metabolism, migration and pro-healing protein production.

VI.1.4 Macroporous scaffolds

A MacPS scaffold has been designed for wound healing, combining the ability of silk fibroin particles to protect sensitive molecules, the ability of silk fibroin scaffold to promote wound healing by supporting cell growth and several functionalities of insulin [105]. Indeed, insulin can stimulate the migration and proliferation of keratinocytes as well as tube formation of endothelial cells, a typical angiogenesis phenomenon improving wound healing. The system was made by LBL of silk fibroin solution and insulin core-silk fibroin shell MPs and showed improved wound closure in scratch assay operated with HaCaT cells and EA. Hy926 cells, which are human keratinocyte cell line and human endothelial cell line respectively.

VI.2 Transdermal drug delivery

MNs patches are widely developed for transdermal delivery, and notably for the treatment of diabetes as it allows the delivery of drugs without damaging the tissue, bleeding and pain. The protein drug can then be directly loaded in the system, as proposed by Seong *et al.* who designed an MNs patch with bullet-shaped MNs made of two layers [93]. The external layer was made of swellable PS-PAA while the internal layer was made of non-swellable PS. *In vitro* experiment showed that 60 % of the loaded insulin was released and that 70 % of the released insulin retained its structure integrity.

In another study, the release of loaded proteins was ensured by a charge-invertible polymer micelle [88]. The MNs patch was made with PLLA and was then coated with the charge-invertible polymeric micelles made of poly(2-(diisopropylamino) ethyl methacrylate – block – methacrylic acid) (P(DPAEMA-b-MAA)). Then, LBL was operated with proteins (lysozyme, OVA or Cy5-OVA) and polymer (polyamine or PAA). This system was able to deliver the LBL film within one minute to the epidermis due to the charge-inversion of the micelle which disrupts the cohesion between the MNs patch and the LBL film.

The therapeutic protein can also be loaded into particles embedded in the MNs patch. For example, Liu *et al.* simply loaded insulin in $CaCO_3$ MPs that they embedded in a PVP MNs patch [94]. But more complex system has also been reported: Chen *et al.* proposed an alginate MNs patch integrating mineralized particles loaded with either GOx or Ex4, a glucagon-like peptide-1 receptor agonist able to induce insulin production by β-cells [119]. More precisely, GOx was immobilized in copper phosphate mineralized particles, while Ex4 was loaded in calcium phosphate mineralized particles. These different integrations of the protein drugs allowed the release of Ex4 while keeping the glucose-responsive GOx inside the MNs patch. Another example is illustrated in Erreur ! Source du renvoi introuvable.**B**. In this example, insulin and GOx were loaded in glucose- and H_2O_2-responsive particles made of PEG, poly(phenylboronic acid) (glucose-sensitive block), and poly(phenylboronic acid pinacol ester) (H_2O_2-sensitive block). These particles were then embedded in the MNs of a PVP/PVA MNs patch [95].

At last, a light responsive system has also been reported for transdermal protein delivery. Indeed, Haine *et al.* added PSS/PAH-coated gold nanorods to a transparent HG film made of gellan gum, chondroitin sulfate and HA. The objective was to use the photothermal property of gold nanorods to enhance the protein delivery to the skin under NIR irradiation [123].

VI.3 Transbuccal drug delivery

The buccal mucosa is a great route for drug administration as it is easy to reach, allows the use of non-invasive systems and is estimated to be 4,000 more permeable than skin. Delivering drug through buccal mucosa also avoid losing drug because of the enzymatic activity and different pH conditions met through the gastrointestinal tract. These properties have been exploited by Lancina *et al.* to design a transbuccal delivery system for insulin as a solution to avoid subcutaneous injection or infusion pump in the treatment of diabetes [211]. The delivery system consisted of CHI/PEO/insulin electrospun fibers and the authors notably studied the impact of PEO quantity on fibers characteristics. The increase of PEO content induced a decrease of the diameter of the fibers and an increase of the release kinetics. The activity of released insulin was assessed by checking the AKT phosphorylation of 3T3-L1 preadipocyte cells, which was significantly increased.

Delivery through the buccal mucosa has also been exploited for the delivery of anti-hypertensive peptide (AhP) by the group of M. Pintado. In a first study, they loaded AhP in PLGA NPs further embedded in a guar-gum film (GfNP) [155]. The permeability of the system was assessed in an *in vitro* model of the epithelium of buccal mucosa using TR146 buccal cells. The results showed that the free AhP had a faster permeation than AhP-loaded GfNP but that the final amount of AhP found within the cell monolayer was higher for the GfNP system. In another study, they loaded the AhP in CHI MPs further embedded in CHI film [91]. Experimental designs were used to obtain optimal CHI MPs and CHI film and TR146 cells were also used as human buccal epithelium model. The optimal MPs had a diameter of 2.5 µm and a loading efficiency of 76 % and the optimal film was composed of 0.79 % of CHI, 6.74 % of sorbitol and 0.82 % of citric acid (w/v). The viability assay on TR146 cells showed no cytotoxicity of the system.

The systems and their major *in vitro* results are summarized in **Table 5**.

Table 5: Interesting *in vitro* results obtained with covering systems

System/ Application	Material	Protein / therapeutic moeity	Therapeutic ability	*In vitro* cell line model	Main result	Ref
Fiber Tissue healing	Coacervate-coated PLGA fibers	VEGF TGF-β3	VEGF: angiogenesis, reduction of necrosis TGF- β3: angiogenesis	CCL-64, hDFBs, HUVECs	Bioactivity of growth factors retained	[163]
Fiber Tissue healing	CHI NPs in PCL fibers	PDGF-BB	PDGF-BB: cell proliferation, fibroblast migration CHI: anti-inflammatory	Fibroblast cells	Improved cell mass growth and cell movement	[213]
Film Tissue healing	CHI and Sodium alginate organized in layers	EGF and/or TGF-β siRNA	EGF: growth promoting TGF-β siRNA: reduction of COL production	A431 cells, *E. coli*, *S. aureus*	Cytocompatible, prevents bacterial colony formation	[214]
HG Tissue healing	Nanosilicate in κ-carrageenan	VEGF	Angiogenesis	hMSCs, HUVECs	Enhanced wound healing in a scratch assay	[72]
MacPS Tissue healing	Silk fibroin MPs in silk fibroin sponge	Insulin	Angiogenesis, migration and proliferation of keratinocytes	HaCaT cells, EA. hy926 cells	Stimulation of cell migration	[105]
Patch Transdermal drug delivery	Polymeric vesicles in PVP/PVA patch	Insulin and GOx	Insulin: hypoglycemic effect	MCF-7 cells	Cytocompatibility of the loaded polymeric vesicles	[95]
Film Transbuccal drug delivery	PLGA NPs in guar-gum film	AhP	Anti-hypertensive	TR146 cell line	Improved permeation through cell multilayer	[155]

PLGA poly(lactic-co-glycolic acid); VEGF vascular endothelial growth factor; TGF-β3 transforming growth factor-β3; CCL-64 Mink lung epithelial cell line; hDFBs human dermal fibroblasts; HUVECs human umbilical vein endothelial cells; CHI chitosan; NPs nanoparticles; PCL polycaprolactone; PDGF-BB platelet-derived growth factor-BB; EGF epidermal growth factor; TGF-β

siRNA transforming growth factor-β small interfering ribonucleic acid; A431 human epidermoid carcinoma cells; *E. coli Escherichia coli*; *S. aureus Staphylococcus aureus*; hMSCs human mesenchymal stem cells; MPs microparticles; HaCaT immortal human keratinocyte line; EA. hy926 human endothelial cell line; PVP poly(vinylpyrrolidone); PVA poly(vinylalcohol); GOx glocuse oxidase; MCF-7 cells human breast adenocarcinoma cells; AhP anti-hypetensive peptideTR146 human buccal carcinoma cell line

VII *In vivo* studies

VII.1 Circulating systems

VII.1.1 Cancer treatment

The use of cancerous-cells xenograft tumour-bearing mice is the dominant model to evaluate the efficiency of particle systems on tumours. Then, several cell lines can be used. For example, 4T1 xenograft tumour-bearing BALB/c mice were used as a model to test the efficiency of RNBC-loaded KPEI nanocomplex coated with HA-hematoporphyrin (KHHR) [122]. As illustrated in Erreur ! Source du renvoi introuvable.**A**, the KHHR system stopped the tumour growth, compared to KHHB where RNBC is replaced by BSA, KHR where there is no hematoporphyrin, and PBS. This model has also been used to test the efficiency of PH20-ExSM together with PC3 xenograft tumour-bearing BALBc nu/nu mice. The results showed 83 % inhibition of the PC3 tumour growth and a reduction of the 4T1 tumour volume [56].

HeLa xenograft has also been used and showed the enhanced anti-cancer efficiency of diselenide bridge-containing MSNs when there were coated with cancer cell membrane [35]. Unzueta *et al.* chose the subcutaneous CXCR4+ colorectal cancer xenograft model applied in female Swiss nu/nu mice to confirm the specific accumulation of their T22-GFP-H6 BIB *in vivo* (study presented in perspective due to its originality) [158].

HT29 xenograft tumour-bearing male BALB/c nu/nu mice and CT26.CL25 xenograft tumour-bearing BALB/c mice were also used by Cho *et al.* to evaluate the anti-cancer activity of their SIRPα-ExSM, showing a delayed tumour growth in the HT29 xenograft model and the inhibition of the CT26.CL25 xenograft tumour growth [57].

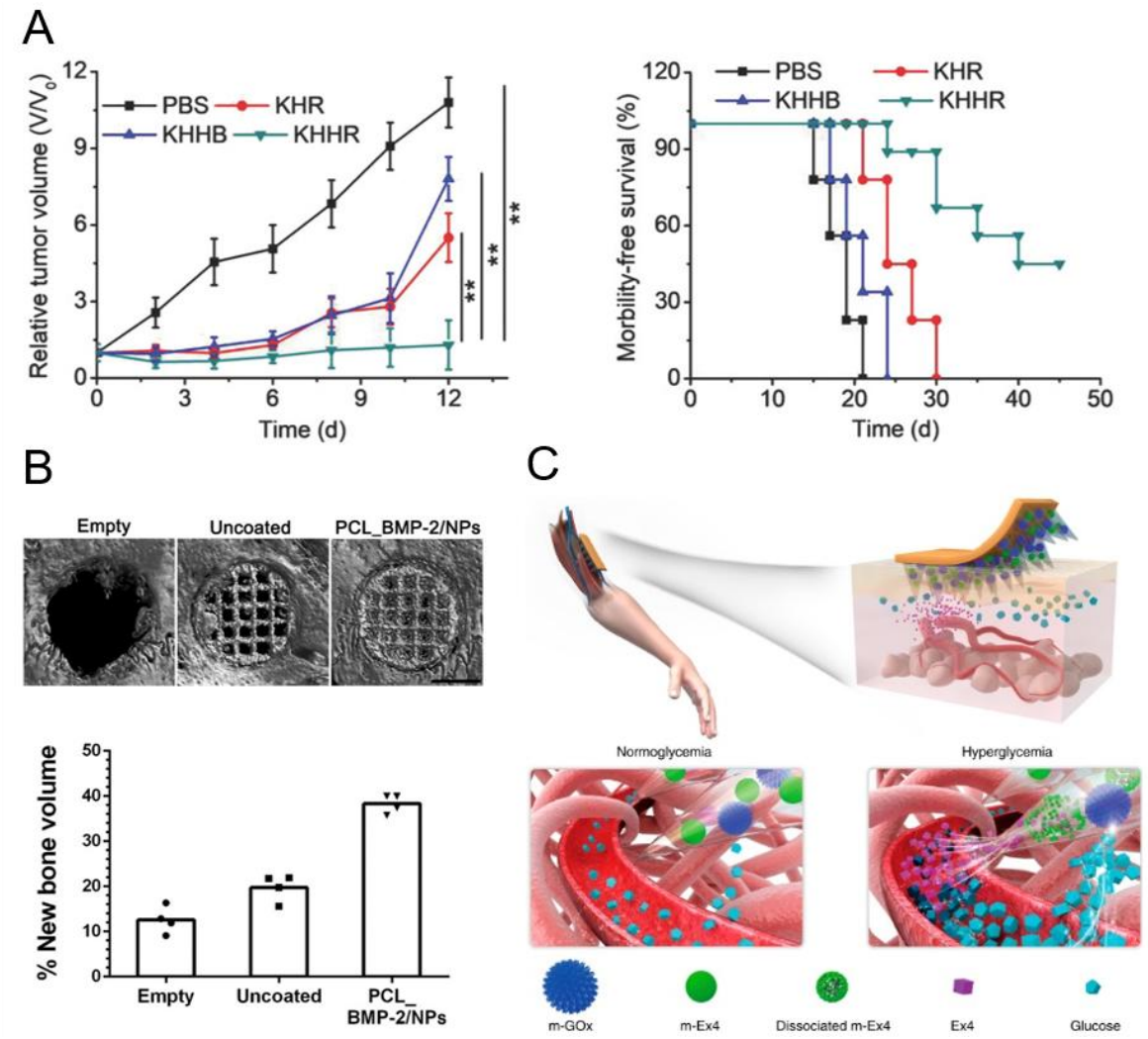

Figure 7: A. Tumor volume and survival rate of mice treated with different particle systems (adapted from article [122]). B. Micro-CT images of calvarial defect 8 weeks post-implantation and volume of new bone (adapted from article [138]). C. Schematic representation of the glucose-responsive MNs patch (reproduced from Article [119])

VII.1.2 Diabetes treatment

In the case of diabetes, the disease is usually induced by injection of a chemical. For example, Meneguin *et al.* used alloxan to induce diabetes in Wistar rats to test the efficiency of their insulin-loaded gellan gum MPs coated with retrograded starch and pectin. The results showed a reduction of glucose up to 7 h post-injection with a maximum reduction up to 51.02 % [22]. Another example is the study of Fan *et al.*, who induced diabetes in Sprague-Dawley (SD) rats with streptozotocin to confirm the absorption mechanism of their insulin-loaded deoxycholic acid-modified CHI NPs. The mechanism was confirmed and the study showed a slower but longer reduction of blood glucose level notably compared to free insulin [182].

VII.1.3 Tissue engineering

A medial meniscal transection (MTT) injury has been reported in SD rats to test the ability of TSG-6-loaded heparin MPs to reduce cartilage damage for osteoarthritis treatment. TSG-6 is the tumour necrosis factor-alpha stimulated gene 6, it has anti-inflammatory property as well as the capacity to inhibits the plasmin responsible for

ECM degradation in osteoarthritis joints. The evaluation of cartilage thickness, volume and attenuation showed the higher efficiency of TSG-6 when released by the heparin MPs compared to free TSG-6 [215].

In the domain of nerve tissue engineering, Santhosh *et al.* applied severe clip-compression SCI at mid-thoracic level in SD rats to test their rhNrg-1β1-loaded PLGA MPs. The results showed that the system reduced scar formation and neuroinflammation and promoted oligodendrocytes and axons preservation [185].

For cardiac tissue engineering application, the ligation of the left anterior descending (LAD) coronary artery is quite common for *in vivo* experiment. This model has been applied in SD rats to check the efficiency of liraglutide-loaded PLGA-PEG NPs [157]. The injection of these NPs led to the improvement of cardiac functions, the attenuation of infarct size, the preservation of wall thickness, the promotion of angiogenesis and the prevention of cardiomyocyte apoptosis. Of course, it is not the only model used. For example, Díaz-Herráez *et al.* used a chronic MI model applied in SD rats to study their system, which was Nrg-1-loaded PLGA/COL/PDL MPs with adipose-derived stem cells adhered on their surface [159]. The study showed the synergistic effect of the stem cells and the Nrg-1, leading to better neovascularization. The presence of Nrg-1 also stimulated cardiomyocyte proliferation and altogether, these effects led to better heart regeneration.

VII.1.4 Inflammatory bowel disease

Ling *et al.* tested their alginate/CHI MPs in two *in vivo* models [116]. They first used C57BL/6 mice to check the small intestine uptake of eGFP NPs-loaded MPs and this showed that the system could reach the total gastrointestinal tract. Then, they checked the efficiency of the AvrA-NPs-loaded MPs in a dextran sulfate sodium (DSS) colitis mouse model. This study showed the efficiency of the system by showing the reduction of weight loss and of Disease Activity Index.

VII.2 Implantable matrices

VII.2.1 Bone tissue engineering

VII.2.1.1 Macroporous scaffolds

Bone defect is the most common model used to evaluate the ability of MacPSs to induce bone regeneration, and among the possible ones, calvarial defect seems to be the most chosen. It has for example been used in SD rats to check the co-delivery of rhBMP2 and alendronate by COL sponge. The results showed a greater regeneration with the co-delivery system, with the new bone presenting a dense structure with less fatty marrow tissue compared to the rhBMP2 only-loaded COL sponge [102]. This model has also been applied in Wistar rats by Quinlan *et al.* [167] and by Kuttapan *et al.* [152]. Indeed, Quinlan *et al.* chose this model to study the effect of their COL/HAP system containing VEGF-loaded alginate MPs. The implantation of the system led to the enhancement of angiogenesis and thus to better osteogenesis [167].As for Kuttappan *et al.* they chose it to study their gelatin scaffold containing silica-coated nanoHAP and oriented PLLA yarns. As said previously, the authors studied the delivery of VEGF+BMP2 and FGF2+BMP2. The *in vivo* studies showed that both co-delivery induced angiogenesis and bone formation without differences between the two groups [152].

Finally, the calvarial bone defect model has been applied in New Zealand (NZ) white rabbit by Kim *et al.* to check their system: a 3D-printed HAP scaffold coated with a PCL solution containing rhBMP2-loaded PLGA NPs. The study showed

improved bone regeneration as it can be seen in Erreur ! Source du renvoi introuvable.**B** [138]. NZ white rabbits have been used in other studies with a radius critical bone defect. Bone regeneration with this model has been observed after implantation of true bone ceramic containing P28-loaded enlarged pores MSNs [156] and after implantation of BMP2/IL-8-loaded mesoporous bioactive glass. This system was also implanted in tight muscle pouches of mice as an ectopic bone formation model [191]. This study showed the ability of the system to recruit stem cells and to have the formation of cartilage due to IL-8 and the formation of bone due to BMP2.

Other bones can support osteotomy. Thus, Hettiaratchi *et al.* used a femoral defect in SASCO SD rats to study the effect of their COL sponge surrounded by PCL nanofiber mesh containing BMP2-loaded heparin MPs. The result showed no difference in heterotopic ossification, probably due to interactions between heparin and BMP2 and heparin and proteins present in the serum [192]. As for Xue *et al.*, they created a radial defect in SD rats to study their HMGB1-loaded gelatin sponge combined with MSCs sheets. The implantation of the system showed an enhanced fracture healing promoted by HMGB1 via the STAT3 pathway [193].

MacPSs implantation can also be realized in other tissues. For example, implantation in muscle has already been mentioned above. The abdominal muscle pouch model has been used in SD rats to check the osteoconductivity and osteoinductivity of rhBMP2/zoledronic acid-loaded gelatin/HAP/calcium sulphate cryogel. The results showed that zoledronic acid allowed the reduction of the rhBMP2 dose and that their co-delivery led to bone formation [151]. It has also been used to check the osteoinductive property of SDF-1/Dex@CDMs-loaded HAP scaffold [14]. This scaffold was notably implanted in dorsal muscle of beagles and the results showed the cell recruitment and vascularization into the scaffold and the cell differentiation leading to the formation of mineralized tissue. Subcutaneous implantation has also been used in Wistar rats and athymic nude mice. In the first case, a PLLA nanofibrous scaffold, coated with HAP and grafted with BMP2-loaded liposomes, was implanted and induced bone formation [75]. In the second case, a CHI/agarose/gelatin scaffold containing CHI/heparin NPs was implanted after loading with SDF-1 to check its ability to recruit MSCs [106].

Finally, the ACL reconstruction model has been used in NZ white rabbit to check the ability of osteoprotegerin/BMP2-loaded COL sponge to promote tendon-bone healing [189]. This tendon-bone healing was improved with the reduction of bone tunnel enlargement and an enhanced formation of fibrocartilage and COL fibers at the tendon-bone interface.

VII.2.1.2 Fibers

The ability of some fibrous systems to promote bone formation has been tested *in vivo* with subcutaneous implantation or implantation in a calvarial bone defect. Both models were used by Cheng *et al.* to test CTGF/CHI-coated BMP2/PVA core-silk fibroin/PCL sheath fibers [197]. The first experiment was subcutaneous implantation in the abdominal midline of nude mice and showed the ability of the system to promote angiogenesis and osteogenesis. Then, the system was implanted in calvarial bone defect created in C57BL/6 mice and showed its ability to promote osteogenesis with ~ 70 % of newly formed bone compared to other groups who presented maximum ~ 50 %. The calvarial bone defect model has also been used by Bhattarai *et al.* in NZ white rabbits to check their BMP2/PLA core-TDCU/PLA sheath fibers. The results showed higher blood vessel and bone formation after the implantation of the loaded fibers [196].

VII.2.1.3 Hydrogels

HGs were also tested *in vivo*. A femoral bone defect created in SD rats has notably been used by Krishnan *et al.* and by Hettiaratchi *et al*. In the first case, the authors have assessed their alginate HG in comparison with commercial COL sponge to deliver rhBMP2 [198]. Their goal was to evaluate if the alginate HG could prevent heterotopic bone formation when a high dose of rhBMP2 is delivered. The results showed that the implantation of the alginate HG, compared to COL sponge, led to the formation of a higher volume of bone but with the same volume of heterotopic bone. The authors suggested that the high dose of rhBMP2 may be sufficient to induce the heterotopic bone formation. In the second case, the system studied was an alginate HG loaded with BMP2-loaded heparin MPs and contained in a PCL nanofiber mesh tube [71]. The study notably compared this system with BMP2-loaded alginate HG. The results showed that the loading in the heparin MPs allowed higher retention of BMP2 in the bone defect but led to a lower volume of newly formed bone. It is interesting to notice that this system was primarily tested *in vivo* by subcutaneous implantation in SD rats to evaluate some properties of the scaffold, such as the retention of BMP2 in the system *in vivo* and the ability of the system to form mineral tissue.

Subcutaneous implantation was also the model chosen by Olthof *et al.* to check their OPF-BP HG containing BMP2-loaded PLGA MPs [61]. More precisely, they did a comparison between this system, BMP2-loaded PLGA MPs and BMP2-loaded OPF-BP HG. The systems showed different release profiles and the HG alone, with its burst release, showed better bone formation. Last model presented here, the sheep drill hole defect model applied in Merino-mix sheep by Huber *et al.* to test their BMP2-loaded demineralized bone matrix putty. The results confirmed the ability of the system to induce bone healing [199].

VII.2.2 Cartilage tissue engineering

The ACL reconstruction model has been applied in NZ white rabbit to check the ability of SDF-1-loaded COL sponge surrounded by silk mesh to regenerate bone-tendon in combination with intra-articular injection of LSPCs. The experiment showed tendon regeneration and bone tunnel healing with reduction of osteoarthritis [104].

VII.2.3 Nerve tissue engineering

A common way to test if a system is efficient for nerve tissue regeneration is to induce nerve defect. For example, B. Xia and Y. Lv created critical sized defect in SD rats' sciatic nerve to test their VEGF/β-NGF-loaded PLLA fibrous nerve conduit [162]. The results showed a synergistic effect of both protein drugs leading to neovascularization and nerve healing. Another example is the hemi-incision model at cervical level 5 in SD rats' spinal cord created by Nguyen *et al*. [76]. Their system was an NT-3-loaded COL scaffold containing aligned PCLEEP nanofibers in which miR-222-loaded micelles were embedded. The results showed direct axon regeneration and remyelination without inflammation or scar tissue formation.

VII.2.4 Cardiac tissue engineering

The previously described LBL patch containing endothelial cells, VEGF-loaded PLGA NPs and DEX-loaded PLGA NPs was tested *in vivo*. More precisely, it was

implanted subcutaneously in SD rats' back. The results confirmed the angiogenesis of the system by showing infiltration of new blood vessels inside the patch [209].

Two HGs were also tested in an *in vivo* MI model induced by ligation of the LAD coronary artery in rats. The first system, tested in SD rats, consisted of fibrin HG loaded with TIMP-3 and two types of coacervate, containing either FGF2 or SDF-1α [195]. The results showed good tissue repair thanks to revascularization, stem cell homing and preservation of cardiomyocytes. The implantation of the system also led to the reduction of inflammation, fibrosis, ECM degradation and ventricular dilation. The second system, tested in Wistar rats, was the HGFdf-loaded SHIELD HG. The results showed that the implantation of the system could improve angiogenesis and reduce fibrosis, limiting adverse remodelling [144].

VII.2.5 Other applications: cancer and diabetes treatment

Like for particles systems, the efficiency of implantable matrices against cancer can be evaluated in xenograft tumour-bearing mice. Thus, Jiang *et al.* tested their hirudin/TRAIL-loaded oligopeptide HG in such tumour model, induced by injection of MDA-MB-231 cells in nude mice. [145]. The synergistic anti-tumour effect of the co-delivery system was assessed, with a tumour inhibition ratio of ~ 64 % compared to saline treatment.

In the fate of diabetes treatment, IL-33-loaded PLGA scaffolds were implanted in C57BL/6 mice after induction of diabetes by injection of streptozotocin [210]. The results showed that the transplantation of allogeneic islet led to the increase of graft protective T cell population, the decrease of destructive T cell population but delayed the islet engraftment.

VII.3 Covering systems

VII.3.1 Tissue healing

VII.3.1.1 Fibers

A first nanofiber system was tested *in vivo* by applying the skin flap model in mice [163]. This system consisted of coacervate-coated PLGA nanofibers, with the coacervate containing PEAD, heparin and VEGF and/or TGF-β3. The experiment showed a synergistic effect with the co-delivery leading to better skin flap survival with reduction of necrosis and improvement of blood perfusion. Another system consisting of VEGF/PEO core-PCL/PEG sheath fibers was tested *in vivo* by subcutaneous implantation in severe combined immunodeficiency (SCID) mice. This experiment confirmed the ability of the system to promote cell migration and improve angiogenesis [212].

VII.3.1.2 Film

A CHI/sodium alginate film was tested in an excisional wound healing model in C57BL/6 mice to check the effect of TGF-β siRNA and EGF alone or together [214]. The single delivery of the siRNA could reduce the TGF-β protein expression and thus reduce COL production while the single delivery of EGF improved wound contraction. The co-delivery of these proteins accelerated wound healing and decreased scar formation due to the reduction of COL production.

VII.3.1.3 Macroporous scaffold

A MacPS made by LBL of silk fibroin sponge and insulin-loaded silk fibroin MPs was tested in diabetic SD rats [105]. The diabetes was induced by injection of

streptozotocin and full-thickness wounds were created on rats' back for the treatment with the scaffold. The experiment showed that the system significantly accelerated the wound closure healing by accelerating wound closure, COL deposition and vascularization.

VII.3.2 Transdermal drug delivery

As said before, transdermal delivery is widely looked for the treatment of diabetes. Thus, streptozotocin-induced diabetic SD rats were used to test several systems. The first one was the PVP/PVA MNs patch containing insulin/GOx-loaded glucose-and H_2O_2-responsive vehicles [95]. This experiment showed that the system could reduce the blood glucose level with a slower rate but could maintain it in the normoglycemic level for 4 h, against 1 h for injection of insulin. In addition, the return to the initial blood glucose level was also slower than for injection of insulin (more than 12 h post-treatment against 7 h post-injection). This model was also used to test PVP MNs patch containing insulin-loaded $CaCO_3$ MPs. [94]. Here again, the blood regulation was slower but longer with the system. The insulin relative bioavailability, which is the percentage of insulin absorbed intact by the circulatory system when delivered by the DDS compared to subcutaneous injection, was evaluated at 96.6 %. Another possibility to study the efficiency of a delivery system to treat diabetes is to use C57BL/6 db/db mice, as it is an *in vivo* model for diabetes type II. This model has been chosen by Chen *et al.* to test their system illustrated in Erreur ! Source du renvoi introuvable.**C**: an alginate MNs patch containing GOx and Ex4 loaded in mineralized particles. This study confirmed the ability of the system to regulate blood glucose level [119].

Healthy animals were also used to test MNs patches. For example, Seong *et al.* used both SD rats and C57BL/6 J mice to evaluate the ability of their double-layered MNs patch to deliver insulin [93]. The results confirmed the possibility to use the patch as painless transdermal delivery system as it showed a prolonged release of insulin and the decrease of blood glucose level. Another system was tested by application on the ear of healthy C57BL/6 mice [88]. The system was PLLA MNs patch coated with a charge-invertible polymer and an LBL film of OVA and polymer. The results showed that the film was delivered to the epidermis in only 1 min and that OVA was delivered in a sustained manner over 3 days, leading to an increased immune response. Male ddY mice were also used without any induced disease to confirm the improved transdermal delivery of FITC-OVA, used as a model protein, due to the photothermal property of PSS/PAH-coated gold nanorods embedded in gellan gum/chondroitin sulfate/HA film [123].

Some systems and their major results obtained by *in vivo* experiments are summarized in **Table 6**.

Table 6: Interesting *in vivo* results

System/ Application	Material	Protein / therapeutic moeity	Therapeutic ability	*In vivo* model	Main result	Ref
CIRCULATING SYSTEMS						
NPs Cancer	RNBC in KPEI nanocomplex coated PS-HA	RNase A Hematopor-phyrin	RNase A: cleaves RNA Hematoporphyrin: ROS production	4T1 tumour in mice	Tumour growth stopped	[122]
ExSM	Exosome from	SIRPα	CD47 antagonist	HT29 or	Tumour growth	[57]

Cancer	HEKT293T cells			CT26.CL25 tumor in mice	delayed (HT29) or inhibited (CT26.CL25)	
MPs Diabetes	Retrograded start/ pectin-coated Gellan gum MPs	Insulin	Hypoglycemic effect	Alloxan diabetes in rats	Maximum glucose reduction up to 51 %	[22]
MPs Bone tissue eng.	Desulfated heparin	TSG-6	Anti-plasmin and anti-inflammatory properties	MMT injury in rats	Reduction of cartilage damage	[215]
MPs Nerve tissue eng.	PLGA	rhNrh-1β1	Differentiation of NPCs into myelin-forming oligodendrocytes	Severe clip-compression SCI in rats	Reduction of scar formation, axons preservation	[185]
MPs Cardiac tissue eng.	Adipose-derived SCs on PLGA/ COL/PDL MPs	Nrg-1	Angiogenesis, cardiomyocyte proliferation, cell survival	Chronic MI model in rats	Synergistic effect inducing better heart regeneration	[159]
IMPLANTABLE MATRICES						
MacPS Bone tissue eng.	Alginate MPs in COL/HAP scaffold	rhVEGF$_{165}$	rhVEGF$_{165}$: angiogenesis HAP: osteoinductive	Calvarial BD in rats	Enhanced angiogenesis and osteogenesis	[167]
MacPS Bone tissue eng.	CDMs-loaded HAP scaffold	DEX SDF-1	DEX: osteogenesis SDF-1: osteogenesis and cell migration	Implantation in dorsal muscle of beagles	Synergic effect: acceleration of bone formation	[14]
Fiber Bone tissue eng.	PVA core – silk fibroin/PCL sheath	BMP2 CTGF	BMP2: osteogenesis CTGF: angiogenesis	Calvarial BD model in mice	Improvement of bone regeneration by 43 %	[197]
HG Bone tissue eng.	Demineralized Bone Matrix putty	BMP2	Osteoinduction	Sheep drill hole defect model in Merino-mix sheep	Complete bone healing	[199]
MacPS Cartilage tissue eng.	Knitted silk mesh cross-linked to COL sponge	SDF-1 LSPCs	SDF-1: cell recruitment LSPCs: tendon-forming cells	ACL model in rabbits	Bone and tendon healing, osteo-arthritis reduction	[104]
Fiber Nerve tissue eng.	PLLA fibers used as nerve conduit	VEGF$_{165}$ β-NGF	VEGF: angiogenesis β-NGF: neurogenesis	Defect in rat sciatic nerve model	Enhanced neovascularization and nerve healing	[162]
HG Cardiac tissue eng.	Coacervate in fibrin gel	TIMP-3, FGF-2, SDF-1α	TIMP-3: reduction of ECM degradation FGF-2: angiogenesis SDF-1α: recruitment of progenitor cells	MI model in rats by LADCA ligation	Heart tissue regeneration	[195]
COVERING SYSTEMS						
Fiber Tissue healing	PEO core – PCL/PEG sheath	rhVEGF$_{165}$	Angiogenesis	Subcutane-ous mouse model in SCID mice	Cell migration and significant improvement of angiogenesis	[212]
Film Tissue healing	CHI and Sodium alginate organized in layers	EGF and/or TGF-β siRNA	EGF: growth promoting TGF-β siRNA: reduction of COL production	Excisional wound healing in mice	Synergistic effect: reduction of COL deposition and faster wound healing	[214]
MacPS Tissue healing	Silk fibroin MPs in silk fibroin sponge	Insulin	Angiogenesis, migration and proliferation of keratinocytes	Wound in rats Streptozoto-cin-induced diabetes	Accelerated wound healing	[105]
Patch Transdermal drug delivery	$CaCO_3$ MPs in PVP microneedles	Insulin	Hypoglycemic effect	Streptozocin diabete in rats	Slower and longer blood glucose regulation	[94]
Film Transdermal drug delivery	PSS/PAH-coated gold nanorods in gellan gum/chondroitin sulfate/HA film	FITC-ovalbumin	Model protein	ddY mice	Improved protein transdermal delivery thanks to skin heating	[123]

NPs nanoparticles; RNBC 4-nitrophenyl 4-(4,4,5,5-tetramethyl-1,3,2-dioxaborolan-2-yl)benzylcarbonate-modified RNase; KPEI ketal cross-linked polyethylenimine; PS-HA photosensitizer-hyaluronic acid; RNase A ribonuclease A; RNA ribonucleic acid; ROS Reactive Oxygen Species; 4T1 mouse mammary carcinoma cells; ExSM exosome; SIRPα signal regulatory protein α; HT29 human colon adenocarcinoma HT29 cells; MPs microparticles; TSG-6 tumor necrosis factor-alpha stimulated gene 6; MMT medial meniscal transection; PLGA poly(lactic-co-glycolic acid); rhNrh-1β1 recombinant human neuregulin-1β1 peptide; NPCs neural progenitor cells; SCI spinal cord injury; SCs stem cells; COL collagen; PDL poly(-D-lysine); Nrg neuregulin; MI

myocardial infarction; MacPS MacroPorous Scaffold; eng. Engineering; HAP hydroxyapatite; rhVEGF recombinant human vascular endothelial growth factor; BD bone defect; CDMs hydroxypropyl- β-cyclodextrin microspheres; DEX dexamethasone; SDF stromal cell-derived factor 1; PVA poly(vinylalcohol); PCL polycaprolactone; BMP2 bone morphongenetic protein 2; CTGF connective tissue growth factor; LSPCs ligament-derived stem/progenitor cells; ACL anterior cruciate ligament; PLLA poly(L-lactic acid); β-NGF β-nerve growth factor; TIMP-3 tissue inhibitor of metalloproteinases-3; FGF-2 basic fibroblast growth factor; SDF-1α stromal cell-derived factor 1-α; LADCA left anterior descending coronary artery; PEO poly(ethylene oxide); PEG poly(ethylene glycol); SCID severe combined immunodeficiency; CHI chitosan; EGF epidermal growth factor; TGF-β siRNA transforming growth factor-β small interfering ribonucleic acid; PVP poly(vinylpyrrolidone); PSS poly(sodium 4-styrenesulfonate); PAH poly(allylamine hydrochloride); FITC fluorescein isothiocyanate

VIII Perspectives

New strategies have emerged in the last years in the protein delivery system domain. A first one is to use protein-rich materials in order to deliver a pool of proteins instead of only one or two isolated proteins. Such a strategy should lead to the activation of all the required phenomena to treat a disease such as tissue regeneration for example. On other one is to deliver plasmid DNA to induce the production of proteins by cells or RNA to modulate the expression of a specific gene. Finally, some authors studied the possibility to develop systems able to sequester proteins, to deliver them and recharge for the next delivery. These three strategies will be presented in this section, with the last part presenting other applications for which protein delivery systems can be designed.

VIII.1 Protein-rich materials

The use of protein-rich materials allows the delivery of a cocktail of proteins to the disease site, which can lead to the activation of several phenomena necessary to obtain proper healing. They can be used as a building block for the formulation of the material or only as the cargo.

VIII.2.1 Implantable systems for tissue regeneration

Platelet-rich plasma (PRP) has already been studied to treat several types of injury, and has recently been investigated for the regeneration of bone tissue as it contains several useful growth factors. Among these, it is possible to find platelet-derived growth factor (PDGF) which is a chemotactic signal for MSCs, VEGF that promotes angiogenesis, TGF-β1 that promotes MSCs osteogenic differentiation and COL expression and IGF-1, able to promote cell proliferation, and notably osteoblast proliferation. In a first study, PRP was integrated into a calcium deficient HAP/COL scaffold obtained by 3D-printing [113]. The release of TGF- β1 and PDGF were notably monitored during 35 days and showed a sustained release of both growth factors. *In vitro* studies were also conducted by seeding preosteoblasts MC3T3-E1 on the PRP-loaded scaffold and this showed a better cell growth and differentiation compared to seeding on the empty scaffold. In another study, PRP was integrated into coaxial fibers [216]. More precisely, the fibers were composed of PRP and PVA in the core and silk fibroin and PCL in the sheath. The release profiles of VEGF, IGF, PDGF-BB and TGF- β were evaluated for 30 days and showed the delivery of a higher dose of PDGF-BB in a sustained manner after a burst release of one day. The system was tested *in vitro* on bone MSCs and showed the highest migration, proliferation and differentiation of cells. Indeed, the number of mineralized nodules was the highest in the sample treated with the PRP-loaded fibers. The system was also implanted in a calvarial bone defect created in C57BL/6 mice, confirming the ability of the fibers to enhance bone regeneration.

A platelet rich in growth factor (PRGF-Endoret) was used as building block to prepare an injectable HG for tissue regeneration to avoid the potential undesirable fibrin retraction [217]. PRGF-Endoret was chosen as the material for the HG due to its biocompatibility and biodegradability but also because it is a growth factor reservoir able to release them. The release profiles of EGF, IGF-1, PDGF-AB and TGF- β1 were notably studied and primary human dermal fibroblasts were used to test its cytotoxicity and ability to promote cell proliferation. This study showed the ability of the system to promote cell differentiation when seeded inside the HG as well as its ability to promote matrix production such as HA and COL type I.

Another possibility is to use secretome which is a pool of bioactive molecules released by cells. Thus, Waters *et al.* loaded secretome secreted by human adipose-derived stem cells in a gelatin HG containing Laponite® for the treatment of MI [218]. This system was tested *in vitro* and in an *in vivo* MI model in Fischer rats. The results showed the increase of angiogenesis, the reduction of scar formation and cardioprotection, enhancing cardiac functions.

VIII.2.2 Wound healing

Soy protein hydrolysate (SPH) has been used as building block with cellulose acetate to produce fibers for skin regeneration due to several reasons. First, soy protein contains several ECM-mimetic peptides that support tissue regeneration. Second, both materials are plant-based, not animal-derived or synthetic. And finally, they are able to mimic the ECM structure. The ability of the system to promote cell proliferation, migration and infiltration was tested with dermal fibroblast and its ability to enhance wound healing was assessed in an excisional wound splinting model applied in C57BL/6NCrl mice [82]. Human platelet lysate (hPL) is another material containing a pool of growth factors and cytokines able to induce regeneration. Thus, Pignatelli *et al.* integrated hPL in a silk fibroin solution to obtain a fibrous patch by electrospinning [219]. The study showed the possibility to control hPL release by controlling fibroin crystallinity and the bioactivity of the release hPL was showed by the increased cell viability and proliferation of primary human dermal fibroblasts. Last example, Tansathien *et al.* used a Deer Antler Velvet (DAV) extract to treat skin [220]. More precisely, the DAV extract was integrated into a cream containing sponge microspicules. The ability of the system to promote cell proliferation was assessed *in vitro* with human normal foreskin fibroblasts and positive effect were observed by application on the skin of healthy human volunteers.

VIII.2.3 Cancer treatment

A specific protein can also be used to synthesize a DDS, as proposed by Unzueta *et al*. with their “death star-like approach” [158]. More precisely, they reported the synthesis of bacterial inclusion body (BIB) made of protein-based NPs (pNPs) to deliver the protein inside cancer cells as presented in **Figure 8A**. The pNPs were formed by the self-assembling proteins T22-GFP-H6 or R9-GFP-H6, as T22 and R9 parts target CXCR4 receptor, which is overexpressed in colorectal cancer. The segments encoding for these proteins were transfected in *E. coli*, the bacteria then produced these proteins, which self-assembled in pNPs and then in BIB. The specific CXCR4-mediated cellular uptake was assessed in HeLa cells treated with CXCR4 inhibitor AMD3100. A clear inhibition of the cellular uptake was observed, as the median fluorescence intensity decreased from ~ 200 F.U to ~ 0 F.U in presence of AMD3100 for the T22-GFP-H6 system. This system was tested only with GFP as a proof of concept but this part of it the self-assembling proteins could be adapted with other therapeutic proteins to have specific effect.

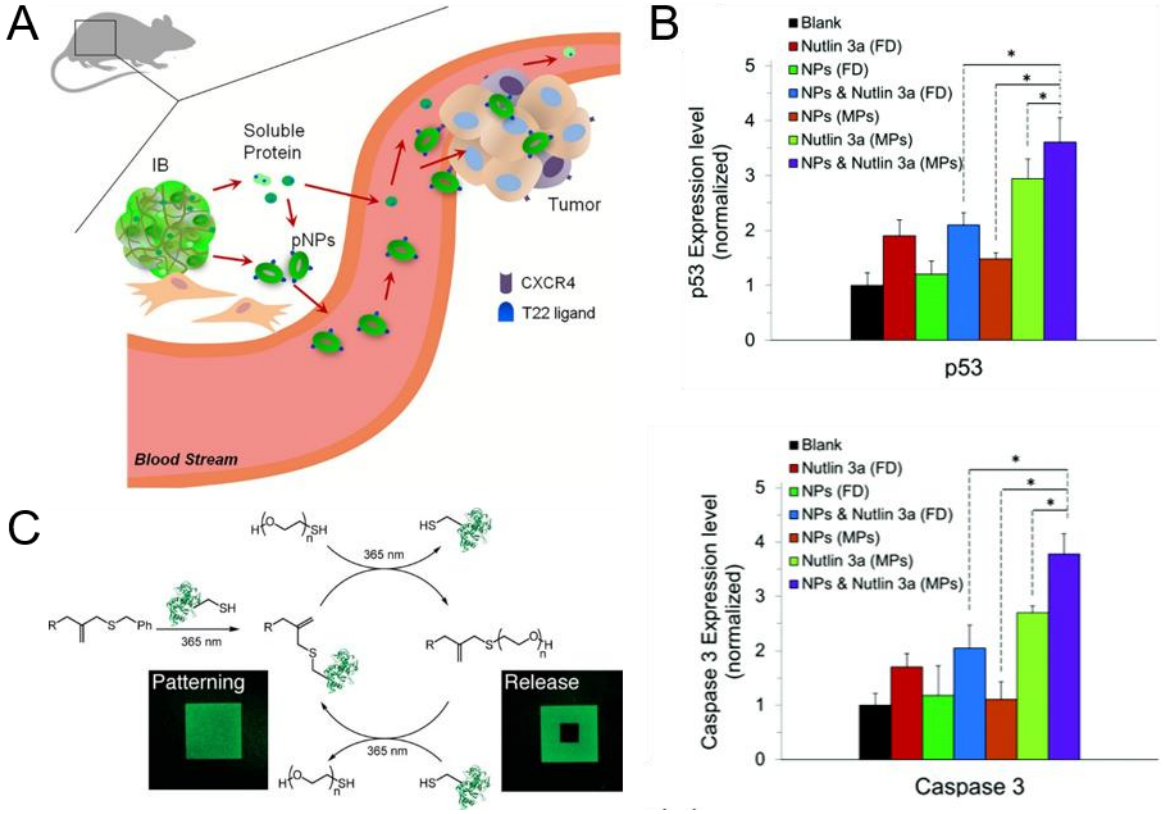

Figure 8 : A. Schematic presentation of the BIB and the protein delivery to cancer cell (reproduced from [158]). B. p53 and Caps-3 cell expression depending the delivery system (adapted from [221]). C. Schematic representation of the release and self-reloading of hydrogel (reproduced from [222])

VIII.2 Bioinduction of protein release through gene therapy (DNA, plasmid DNA, siRNA)

An emerging strategy is the transfection of cells with DNA, plasmid DNA (pDNA) or RNA. It is important to note that in this case, it is not a direct release of protein, but a way to make the organism produce the desired protein or to prevent it from producing some when the corresponding gene is silenced.

VIII.1.1 Gene delivery (poofs of concept)

Several materials can be used to deliver such molecules. For example, pEGFP-LUC, a plasmid encoding for firefly luciferase and GFP, was loaded in CHI NPs, themselves loaded in zein MPs [153]. Lipids are also designed to obtain gene delivery systems. For example, Colombani *et al.* studied the influence of the linker function in the two lipids used to obtain lipoplexes when mixed with this type of molecule [173]. More precisely, they used parommomycin-based cationic lipid and imidazole-based helper lipid, both presenting a dioleyl backbone as the hydrophobic tail. The linker was an amide function or a phosphoramide function and they studied the effect of the linker nature on the lipoplexe (same or hybrid). They studied the formation of lipoplexes using pGWIZ-Luc (encoding for luciferase), pGWIZ-eGFP, mRNA (encoding for luciferase and GFP) and human anti-laminA/C siRNA. As for Patel *et al.*, they tested 11 cationic and ionisable lipids to obtain lipid NPs able to deliver mRNA to the retina [169].

Fibers were also designed for gene delivery or gene silencing. For example, Zhang *et al.* designed a gene vector made of a lipophilic tail, tetraphenylethene and a peptide containing four arginines named TR4 to self-assemble with pDNA, leading to the obtention of nanofibers [223]. As for Pinese *et al.*, they chose the load siRNA in MSNs-PEI and to coat PCL fibers with these NPs [224].

If these systems were tested for general gene delivery or gene silencing application, some systems have been designed for specific applications.

VIII.1.2 Bone tissue engineering

As BMP2 is very used for bone regeneration, delivering pDNA encoding for this protein completely makes sense when exploring gene delivery for this application. Thus, different scaffolds were developed to do so. For example, Tenkumo *et al.* proposed a nanoHAP/COL scaffold containing pBMP2-functionalized calcium phosphate NPs to enhance bone regeneration [225]. The system was subcutaneously implanted in Wistar rats' back and the results showed that it induced the release of a higher quantity of BMP2 and for a longer time compared to the system containing naked pBMP2 and BMP2 in solution. Raftery *et al.*, on their side, evaluated if modified pBMP2 could be more efficient in enhancing bone formation [226]. Thus, they first evaluated the release of the plasmid from CHI NPs and its activity and then embedded these loaded CHI NPs in a COL/HAP scaffold for implantation in a calvarial bone defect created in Wistar rats. The results showed that the modification of the plasmid led to a higher production of BMP2 from cells and thus to a higher bone formation.

Particles were also designed for such application: McMillan *et al.* integrated nanocomplexes composed of mineral-coated HAP MPs and lipofectamine/pDNA into MSC aggregates [227]. This work was based on the fact that MSC aggregates can form bone-like tissues when guided by addition of certain proteins in the culture media. The pDNAs were pBMP2 and pTGF-β1, delivered alone or in combination, and three porcine donors were used to form the bone-marrow-derived MSC aggregates due to possible variation of properties among donors. Globally speaking, the results showed the ability of the nanocomplexes to promote osteogenesis in the different MSC aggregates.

VIII.1.3 Cancer treatment

Specific pDNA can be used for cancer treatment. For example, Davoodi *et al.* designed core-shell particles to deliver p53 pDNA together with nultin-3a [221]. The p53 gene is the most inactivated or mutated gene in tumour tissues, which is problematic as the p53 protein activity leads to the apoptosis of tumour cells. Intracellularly, the p53 protein activity is regulated by the murine double minute 2 (MDM2) protein which forms a complex with it to stop the apoptotic activity. However, MDM2 can be upregulated in cancer cells. Thus, the strategy adopted by Davoodi *et al.* was to use nutlin-3a to disrupt the MDM2-p53 protein complex and to deliver p53 pDNA to promote p53 protein production. To deliver these therapeutics, they designed PLGA core-PDLLA (poly(D,L-lactic acid)) shell MPs. Prior to fabrication, nutlin-3a and p53 pDNA-loaded β-cyclodextrin-graft-CHI NPs were mixed in the PLGA solution. The *in vitro* experiment showed a synergistic anti-tumour effect of nutlin-3a and p53 pDNA by a high production of p53 protein and Casp3 as presented in **Figure 8B** and a high intracellular ROS level.

Another circulating system was proposed for anti-cancer application: poly(styrene-alt-maleic anhydride) was grafted with PEG and two amino acids via disulphide bond

to obtain a molecule able to self-assemble into micelles [165]. The disulphide bond was bringing reduction-responsiveness and the two amino acids were histidine to bring pH-responsiveness and arginine to bind to nucleic acids. The micelle was loaded with doxorubicin and coated with polo like kinase 1 siRNA (PLK-1 siRNA). The dual responsiveness and anti-cancer effect were then tested *in vitro* and *in vivo.*

An MNs patch has also been designed for cancer treatment [160]. The MNs patch was made with polycarbonate and was first immersed in dopamine solution to obtain a polydopamine coating. LBL was then operated with the adjuvant polyriboinosinic:polyribocytidylic (poly(I:C)), a TLR3 agonist able to activate natural cancer cell killer, and oligo sulfamethazine conjugated poly(β-amino ester urethane) (OSM-(PEG-PAEU)). The last layer was a coating of polyplexe made with pOVA as vaccine DNA and bPEI-deoxycholic acid (DA3) conjugate. The system was also tested *in vitro* and *in vivo* and the experiment showed its ability to induce OVA expression and to inhibit tumour growth in a metastatic cancer model.

VIII.3 Sequestration of proteins

Some systems are designed to sequester proteins secreted by cells to better control the cellular environment. Such a strategy has been adopted by Rinker *et al.* to modulate chondrocytic differentiation [228]. They synthesized heparin MPs and PEG MPs and incubated them in ATDC5 cells transwell culture (2D) and in ATDC5 spheroid culture (3D). A delay in differentiation was observed in presence of heparin MPS, and the analysis of the proteins contained in the MPs revealed that they sequestered insulin-like growth factor binding proteins (IGFBP)-3 and 5. An additional experiment consisting of incubating the cells with an inhibitor of IGFBPs confirmed that the delayed differentiation in presence of heparin MPs was due to protein sequestration.

An HG was also designed for protein sequestration [222]. The goal was to obtain an HG able to deliver protein and to recharge itself with fresh protein. To do so, they added an allyl sulfide moiety to an HG, which allowed the immobilization and release of protein via a thiol-ene reaction as showed by **Figure 8C**. More precisely, the HG was made with an eight-armed PEG-dibenzylcyclooctyne functionalized with a cell adhesive azido-RGDS peptide and the azido allyl sulphide. The ability of the HG to release protein and to recharge itself has been assessed, notably with TGF-β1 which bioactivity was retained.

VIII.4 Other possible applications

Delivery to the retina has already been mentioned once, with a system delivering mRNA. Delplace *et al.*, on their side, designed an HA/methylcellulose HG to deliver the ciliary neurotrophic factor (CNTF), known for its neuroprotective effect on retina [229]. More precisely, they modified CNTF with Src homology 3 (SH3) and methylcellulose with SH3 binding peptide to assure the immobilization of CNTF in the HG. *In vitro* experiment performed with TF1-α cells assessed the bioactivity of the released CNTF and experiment performed on C57BL/6 J mice confirmed the release of bioactive CNTF *in vivo* with the quantification of numerous markers.

Dai *et al.* proposed a system for inner ear therapy [230]. The systems consisted of interferon α-2b (IFN α-2b)-loaded PLGA NPs embedded in a CHI/β-glycerophosphate thermosensitive HG. IFN α-2b was chosen as interferons showed anti-viral and immunomodulatory effect in the treatment of sudden deafness. *In vivo* experiment was conducted by injecting the HG in the inner ear of albino guinea pigs

and the results showed that the system increased the IFN α-2b residence time in the inner ear by 3-fold compared to IFN α-2b-loaded HG.

A protein delivery system has also been proposed for the treatment of short stature children, and more precisely for the delivery of rhGH [24]. Indeed, this disease can be caused by a deficiency in growth hormone and this one is known to promote longitudinal bone growth. Thus, Gao *et al.* synthesized poly(ester urea) nanofibers to deliver it and used sugar-glass NPs to stabilize it. The results showed that the nanofibers could release rhGH in a sustained manner for up to six weeks without production of acid degradation products. The bioactivity of the released rhGH was also assessed by checking the proliferation of rat node lymphoma cells (Nb2 cells).

The last example presented here has been developed to treat MI. If the application has already been seen before, the authors developed a quite original system. They used MSC as the initial material and performed LBL on it with alginate and VEGF-loaded gelatin [161]. The objective was to exploit the tropism of MSCs to myocardial infarct zone to be sure that the system would go to the heart and deliver the cells and the encapsulated VEGF, thus enhancing angiogenesis and cardiac function. The *in vitro* experiment showed that the system was able to deliver VEGF in a sustained manner and had a tropism to SDF-1. An MI model was created in SD rats by punctually blocking the left coronary artery to check the system *in vivo*. The results showed that the system migrated to the myocardial infarct site, promoting angiogenesis and enhancing cardiac function, confirming that it is a promising material to treat MI.

IX Conclusions

As seen through this review, a large range of delivery systems have been developed these last years for the specific delivery of proteins: MPs, NPs, HGs, fibers, films, patches and MacPSs, in a monolithic or composite formulation. All these systems can be formulated using very well-established techniques, such as emulsion for NPs, layer-by-layer for films and patches or freeze-drying for MacPSs. Noteworthy, other techniques are emerging, such as the rotary jet spinning for the formulation of fibers, which is interesting as it does not necessitate the application of an electrical field to the polymer solution and thus, eliminates a stress applied to the protein cargo.

These protein cargos can be loaded via three different techniques, which are diffusion, immersion and immobilization, and can then be released via three major mechanisms: diffusion, natural erosion via local stimuli (pH, ROS, redox, glucose, protease) and triggered degradation via external stimuli (visible and NIR light, magnetic field, mechanical stress). A wide range of characterization techniques is available to measure the amount of loaded and released proteins. In simple samples, techniques such as light absorption or fluorimetry can be sufficient. The ELISA test is also widely used for sensitive proteins due to its high specificity and high sensitivity. However, in case of more complex samples, such as biologic ones, composed of several proteins, a first separation step can be necessary, which notably led to the development of the Western blot technique. The release mechanism can then be modelled more finely thanks to mathematical methods.

In this review, the DDSs have been categorized into three main types: circulating systems, implantable systems and covering systems. Circulating systems - which are MPs, NPs, capsules and exosomes - have mainly been developed for the treatment of cancer, and more precisely for the delivery of RNase A to cancer cells. However, some systems have been developed for the treatment of diabetes and tissue engineering. Regarding implantable systems, they are mostly developed for tissue engineering (bone, cartilage, nerve, heart) even if some systems were designed for the treatment of diabetes, cancer or internal wound healing. The formulations types found in this category are MacPSs, fibers, HGs, films and patches. As for covering systems - which often consist of films and patches, but can also be fibers and HGs - they are mainly used for skin regeneration but are also used for transdermal and transbuccal delivery.

At last, many of these systems have been tested *in vivo*, and the most common models have been presented here, such as xenograft tumour-bearing mice for cancer or bone critical defect for bone tissue engineering, as well as the major results associated to the experiment.

Finally, emerging routes for the design of new protein delivery systems have been presented in this review such as the use of protein-rich materials, to deliver a pool of proteins rather than a single protein, and the delivery of plasmid DNA or RNA to induce the production of proteins by cells directly at the injury site. Some interesting unusual applications of such delivery systems have also been shown in this last part.

As seen here, the main systems for therapeutic protein delivery were developed to respond by natural leaking or upon local biochemical stimuli. We expect that an emerging domain for future development in this field will be the remote release of

proteins (or other fragile biomacromolecules) that may be induced remotely by external fields applied (magnetic field, near infra-red light or ultra sounds). In such approaches, a common mechanism is to convert the magnetic/phtonic/acoustic wave energy into a local heat. To achieve this, important developments should be achieved considered in the design of thermo-responsive interface suitable specifically for proteins immobilization/and release.

Author contributions

Joëlle Bizeau: Conceptualization, Methodology, Writing - Original Draft**, Damien Mertz:** Conceptualization, Methodology, Writing - Review & Editing, Supervision, Funding acquisition**.**

Acknowledgements

D.M. acknowledges the Materials Institute Carnot Alsace (project ProtRemote) and the Agence Nationale de la Recherche (grant ANR-19-CE09-0004 – Corelmag) for financial supports.

Bibliography

[1] Vermonden T, Censi R, Hennink WE. Hydrogels for Protein Delivery. Chem Rev 2012;112:2853–88. https://doi.org/10.1021/cr200157d.

[2] Yu M, Wu J, Shi J, Farokhzad OC. Nanotechnology for protein delivery: Overview and perspectives. Journal of Controlled Release 2016;240:24–37. https://doi.org/10.1016/j.jconrel.2015.10.012.

[3] Lu Y, Sun W, Gu Z. Stimuli-responsive nanomaterials for therapeutic protein delivery. Journal of Controlled Release 2014;194:1–19. https://doi.org/10.1016/j.jconrel.2014.08.015.

[4] Sinha VR, Trehan A. Biodegradable microspheres for protein delivery. Journal of Controlled Release 2003;90:261–80. https://doi.org/10.1016/S0168-3659(03)00194-9.

[5] Medlicott NJ, Tucker IG. Pulsatile release from subcutaneous implants. Advanced Drug Delivery Reviews 1999;38:139–49. https://doi.org/10.1016/S0169-409X(99)00013-7.

[6] Kikuchi A, Okano T. Pulsatile drug release control using hydrogels. Advanced Drug Delivery Reviews 2002;54:53–77. https://doi.org/10.1016/S0169-409X(01)00243-5.

[7] Chen L, Mei L, Feng D, Huang D, Tong X, Pan X, et al. Anhydrous reverse micelle lecithin nanoparticles/PLGA composite microspheres for long-term protein delivery with reduced initial burst. Colloids and Surfaces B: Biointerfaces 2018;163:146–54. https://doi.org/10.1016/j.colsurfb.2017.12.040.

[8] Sedyakina NE, Zakharov AN, Krivoshchepov AF, Pribytkova AP, Bogdanova YA, Feldman NB, et al. Effect of carbon chain length of dicarboxylic acids as cross-linking agents on morphology, encapsulation, and release features of protein-loaded chitosan microparticles. Colloid Polym Sci 2017;295:1915–24. https://doi.org/10.1007/s00396-017-4171-0.

[9] Rinker TE, Philbrick BD, Temenoff JS. Core-shell microparticles for protein sequestration and controlled release of a protein-laden core. Acta Biomaterialia 2017;56:91–101. https://doi.org/10.1016/j.actbio.2016.12.042.

[10] Kumar A, Montemagno C, Choi H-J. Smart Microparticles with a pH-responsive Macropore for Targeted Oral Drug Delivery. Scientific Reports 2017;7:1–15. https://doi.org/10.1038/s41598-017-03259-x.

[11] Galliani M, Tremolanti C, Signore G. Nanocarriers for Protein Delivery to the Cytosol: Assessing the Endosomal Escape of Poly(Lactide-co-Glycolide)-Poly(Ethylene Imine) Nanoparticles. Nanomaterials 2019;9:652. https://doi.org/10.3390/nano9040652.

[12] Hsiao L-W, Lai Y-D, Lai J-T, Hsu C-C, Wang N-Y, Wang S SS, et al. Cross-linked polypeptide-based gel particles by emulsion for efficient protein encapsulation. Polymer 2017;115:261–72. https://doi.org/10.1016/j.polymer.2017.03.055.

[13] Rahmani V, Elshereef R, Sheardown H. Optimizing electrostatic interactions for controlling the release of proteins from anionic and cationically modified alginate. European Journal of Pharmaceutics and Biopharmaceutics 2017;117:232–43. https://doi.org/10.1016/j.ejpb.2017.04.025.

[14] Zhang B, Li H, He L, Han Z, Zhou T, Zhi W, et al. Surface-decorated hydroxyapatite scaffold with on-demand delivery of dexamethasone and stromal cell derived factor-1 for enhanced osteogenesis. Materials Science and Engineering: C 2018;89:355–70. https://doi.org/10.1016/j.msec.2018.04.008.

[15] Fröhlich K, Hartzke D, Schmidt F, Eucker J, Gurlo A, Sittinger M, et al. Delayed release of chemokine CCL25 with bioresorbable microparticles for mobilization of human mesenchymal stem cells. Acta Biomaterialia 2018;69:290–300. https://doi.org/10.1016/j.actbio.2018.01.036.
[16] Wu C, Baldursdottir S, Yang M, Mu H. Lipid and PLGA hybrid microparticles as carriers for protein delivery. Journal of Drug Delivery Science and Technology 2018;43:65–72. https://doi.org/10.1016/j.jddst.2017.09.006.
[17] Saengruengrit C, Ritprajak P, Wanichwecharungruang S, Sharma A, Salvan G, Zahn DRT, et al. The combined magnetic field and iron oxide-PLGA composite particles: Effective protein antigen delivery and immune stimulation in dendritic cells. Journal of Colloid and Interface Science 2018;520:101–11. https://doi.org/10.1016/j.jcis.2018.03.008.
[18] Lv J, He B, Yu J, Wang Y, Wang C, Zhang S, et al. Fluoropolymers for intracellular and in vivo protein delivery. Biomaterials 2018;182:167–75. https://doi.org/10.1016/j.biomaterials.2018.08.023.
[19] Yang X, Tang Q, Jiang Y, Zhang M, Wang M, Mao L. Nanoscale ATP-Responsive Zeolitic Imidazole Framework-90 as a General Platform for Cytosolic Protein Delivery and Genome Editing. J Am Chem Soc 2019;141:3782–6. https://doi.org/10.1021/jacs.8b11996.
[20] Ardeshirylajimi A, Ghaderian SM-H, Omrani MD, Moradi SL. Biomimetic scaffold containing PVDF nanofibers with sustained TGF-β release in combination with AT-MSCs for bladder tissue engineering. Gene 2018;676:195–201. https://doi.org/10.1016/j.gene.2018.07.046.
[21] Song M, Li L, Zhang Y, Chen K, Wang H, Gong R. Carboxymethyl-β-cyclodextrin grafted chitosan nanoparticles as oral delivery carrier of protein drugs. Reactive and Functional Polymers 2017;117:10–5. https://doi.org/10.1016/j.reactfunctpolym.2017.05.008.
[22] Meneguin AB, Beyssac E, Garrait G, Hsein H, Cury BSF. Retrograded starch/pectin coated gellan gum-microparticles for oral administration of insulin: A technological platform for protection against enzymatic degradation and improvement of intestinal permeability. European Journal of Pharmaceutics and Biopharmaceutics 2018;123:84–94. https://doi.org/10.1016/j.ejpb.2017.11.012.
[23] Meng X, Liu J, Yu X, Li J, Lu X, Shen T. Pluronic F127 and D-α-Tocopheryl Polyethylene Glycol Succinate (TPGS) Mixed Micelles for Targeting Drug Delivery across The Blood Brain Barrier. Scientific Reports 2017;7:1–12. https://doi.org/10.1038/s41598-017-03123-y.
[24] Gao Y, Xu Y, Land A, Harris J, Policastro GM, Childers EP, et al. Sustained Release of Recombinant Human Growth Hormone from Bioresorbable Poly(ester urea) Nanofibers. ACS Macro Lett 2017;6:875–80. https://doi.org/10.1021/acsmacrolett.7b00334.
[25] Yuan D, Jacquier JC, O'Riordan ED. Entrapment of proteins and peptides in chitosan-polyphosphoric acid hydrogel beads: A new approach to achieve both high entrapment efficiency and controlled in vitro release. Food Chemistry 2018;239:1200–9. https://doi.org/10.1016/j.foodchem.2017.07.021.
[26] Wu C, van de Weert M, Baldursdottir SG, Yang M, Mu H. Effect of excipients on encapsulation and release of insulin from spray-dried solid lipid microparticles. International Journal of Pharmaceutics 2018;550:439–46. https://doi.org/10.1016/j.ijpharm.2018.09.007.
[27] Tavares M, Cabral RP, Costa C, Martins P, Fernandes AR, Casimiro T, et al. Development of PLGA dry powder microparticles by supercritical CO2-assisted

spray-drying for potential vaccine delivery to the lungs. The Journal of Supercritical Fluids 2017;128:235–43. https://doi.org/10.1016/j.supflu.2017.06.004.
[28] Chen N, Johnson MM, Collier MA, Gallovic MD, Bachelder EM, Ainslie KM. Tunable degradation of acetalated dextran microparticles enables controlled vaccine adjuvant and antigen delivery to modulate adaptive immune responses. Journal of Controlled Release 2018;273:147–59. https://doi.org/10.1016/j.jconrel.2018.01.027.
[29] Hao N, Nie Y, Xu Z, Closson AB, Usherwood T, Zhang JXJ. Microfluidic continuous flow synthesis of functional hollow spherical silica with hierarchical sponge-like large porous shell. Chemical Engineering Journal 2019;366:433–8. https://doi.org/10.1016/j.cej.2019.02.095.
[30] Foster GA, Headen DM, González-García C, Salmerón-Sánchez M, Shirwan H, García AJ. Protease-degradable microgels for protein delivery for vascularization. Biomaterials 2017;113:170–5. https://doi.org/10.1016/j.biomaterials.2016.10.044.
[31] Yu L, Sun Q, Hui Y, Seth A, Petrovsky N, Zhao C-X. Microfluidic formation of core-shell alginate microparticles for protein encapsulation and controlled release. Journal of Colloid and Interface Science 2019;539:497–503. https://doi.org/10.1016/j.jcis.2018.12.075.
[32] Stöber W, Fink A, Bohn E. Controlled growth of monodisperse silica spheres in the micron size range. Journal of Colloid and Interface Science 1968;26:62–9. https://doi.org/10.1016/0021-9797(68)90272-5.
[33] Omar H, Croissant JG, Alamoudi K, Alsaiari S, Alradwan I, Majrashi MA, et al. Biodegradable Magnetic Silica@Iron Oxide Nanovectors with Ultra-Large Mesopores for High Protein Loading, Magnetothermal Release, and Delivery. Journal of Controlled Release 2017;259:187–94. https://doi.org/10.1016/j.jconrel.2016.11.032.
[34] Deng C, Zhang Q, Fu C, Zhou F, Yang W, Yi D, et al. Template-Free Synthesis of Chemically Asymmetric Silica Nanotubes for Selective Cargo Loading and Sustained Drug Release. Chem Mater 2019;31:4291–8. https://doi.org/10.1021/acs.chemmater.9b01530.
[35] Shao D, Li M, Wang Z, Zheng X, Lao Y-H, Chang Z, et al. Bioinspired Diselenide-Bridged Mesoporous Silica Nanoparticles for Dual-Responsive Protein Delivery. Advanced Materials 2018;30:1801198. https://doi.org/10.1002/adma.201801198.
[36] Tian Z, Xu Y, Zhu Y. Aldehyde-functionalized dendritic mesoporous silica nanoparticles as potential nanocarriers for pH-responsive protein drug delivery. Materials Science and Engineering: C 2017;71:452–9. https://doi.org/10.1016/j.msec.2016.10.039.
[37] Mertz D, Tan P, Wang Y, Goh TK, Blencowe A, Caruso F. Bromoisobutyramide as an Intermolecular Surface Binder for the Preparation of Free-standing Biopolymer Assemblies. Advanced Materials 2011;23:5668–73. https://doi.org/10.1002/adma.201102890.
[38] Mertz D, Cui J, Yan Y, Devlin G, Chaubaroux C, Dochter A, et al. Protein Capsules Assembled via Isobutyramide Grafts: Sequential Growth, Biofunctionalization, and Cellular Uptake. ACS Nano 2012;6:7584–94. https://doi.org/10.1021/nn302024t.
[39] Li B, Harlepp S, Gensbittel V, Wells CJR, Bringel O, Goetz JG, et al. Near infra-red light responsive carbon nanotubes@mesoporous silica for photothermia

and drug delivery to cancer cells. Materials Today Chemistry 2020;17:100308. https://doi.org/10.1016/j.mtchem.2020.100308.
[40] Perton F, Tasso M, Muñoz Medina GA, Ménard M, Blanco-Andujar C, Portiansky E, et al. Fluorescent and magnetic stellate mesoporous silica for bimodal imaging and magnetic hyperthermia. Applied Materials Today 2019;16:301–14. https://doi.org/10.1016/j.apmt.2019.06.006.
[41] Perton F, Harlepp S, Follain G, Parkhomenko K, Goetz JG, Bégin-Colin S, et al. Wrapped stellate silica nanocomposites as biocompatible luminescent nanoplatforms assessed in vivo. Journal of Colloid and Interface Science 2019;542:469–82. https://doi.org/10.1016/j.jcis.2019.01.098.
[42] Wang Y, Wise AK, Tan J, Maina JW, Shepherd RK, Caruso F. Mesoporous Silica Supraparticles for Sustained Inner-Ear Drug Delivery. Small 2014;10:4244–8. https://doi.org/10.1002/smll.201401767.
[43] Yang Y, Zhu H, Wang J, Fang Q, Peng Z. Enzymatically Disulfide-Crosslinked Chitosan/Hyaluronic Acid Layer-by-Layer Self-Assembled Microcapsules for Redox-Responsive Controlled Release of Protein. ACS Appl Mater Interfaces 2018;10:33493–506. https://doi.org/10.1021/acsami.8b07120.
[44] Ramalapa B, Crasson O, Vandevenne M, Gibaud A, Garcion E, Cordonnier T, et al. Protein–polysaccharide complexes for enhanced protein delivery in hyaluronic acid templated calcium carbonate microparticles. J Mater Chem B 2017;5:7360–8. https://doi.org/10.1039/C7TB01538K.
[45] Wang J, Kumeria T, Bezem MT, Wang J, Sailor MJ. Self-Reporting Photoluminescent Porous Silicon Microparticles for Drug Delivery. ACS Appl Mater Interfaces 2018;10:3200–9. https://doi.org/10.1021/acsami.7b09071.
[46] Zuidema JM, Kumeria T, Kim D, Kang J, Wang J, Hollett G, et al. Oriented Nanofibrous Polymer Scaffolds Containing Protein-Loaded Porous Silicon Generated by Spray Nebulization. Advanced Materials 2018;30:1706785. https://doi.org/10.1002/adma.201706785.
[47] Bae S-E, Lyu SK, Kim K-J, Shin HJ, Kwon H, Huh S. Intracellular delivery of a native functional protein using cell-penetrating peptide functionalized cubic MSNs with ultra-large mesopores. J Mater Chem B 2018;6:3456–65. https://doi.org/10.1039/C8TB00330K.
[48] Mout R, Ray M, Tay T, Sasaki K, Yesilbag Tonga G, Rotello VM. General Strategy for Direct Cytosolic Protein Delivery via Protein–Nanoparticle Co-engineering. ACS Nano 2017;11:6416–21. https://doi.org/10.1021/acsnano.7b02884.
[49] Volodkin DV, Larionova NI, Sukhorukov GB. Protein Encapsulation via Porous CaCO3 Microparticles Templating. Biomacromolecules 2004;5:1962–72. https://doi.org/10.1021/bm049669e.
[50] Volodkin DV, von Klitzing R, Möhwald H. Pure Protein Microspheres by Calcium Carbonate Templating. Angewandte Chemie 2010;122:9444–7. https://doi.org/10.1002/ange.201005089.
[51] Tan J, Wang Y, Yip X, Glynn F, Shepherd RK, Caruso F. Nanoporous Peptide Particles for Encapsulating and Releasing Neurotrophic Factors in an Animal Model of Neurodegeneration. Advanced Materials 2012;24:3362–6. https://doi.org/10.1002/adma.201200634.
[52] Ménard M, Meyer F, Parkhomenko K, Leuvrey C, Francius G, Bégin-Colin S, et al. Mesoporous silica templated-albumin nanoparticles with high doxorubicin payload for drug delivery assessed with a 3-D tumor cell model. Biochimica et

Biophysica Acta (BBA) - General Subjects 2019;1863:332–41. https://doi.org/10.1016/j.bbagen.2018.10.020.
[53] Mertz D, Wu H, Wong JS, Cui J, Tan P, Alles R, et al. Ultrathin, bioresponsive and drug-functionalized protein capsules. J Mater Chem 2012;22:21434–42. https://doi.org/10.1039/C2JM33737A.
[54] Mertz D, Affolter-Zbaraszczuk C, Barthès J, Cui J, Caruso F, Baumert TF, et al. Templated assembly of albumin-based nanoparticles for simultaneous gene silencing and magnetic resonance imaging. Nanoscale 2014;6:11676–80. https://doi.org/10.1039/C4NR02623C.
[55] Dutta K, Hu D, Zhao B, Ribbe AE, Zhuang J, Thayumanavan S. Templated Self-Assembly of a Covalent Polymer Network for Intracellular Protein Delivery and Traceless Release. J Am Chem Soc 2017;139:5676–9. https://doi.org/10.1021/jacs.7b01214.
[56] Hong Y, Nam G-H, Koh E, Jeon S, Kim GB, Jeong C, et al. Exosome as a Vehicle for Delivery of Membrane Protein Therapeutics, PH20, for Enhanced Tumor Penetration and Antitumor Efficacy. Advanced Functional Materials 2018;28:1703074. https://doi.org/10.1002/adfm.201703074.
[57] Cho E, Nam G-H, Hong Y, Kim YK, Kim D-H, Yang Y, et al. Comparison of exosomes and ferritin protein nanocages for the delivery of membrane protein therapeutics. Journal of Controlled Release 2018;279:326–35. https://doi.org/10.1016/j.jconrel.2018.04.037.
[58] Lima DS, Tenório-Neto ET, Lima-Tenório MK, Guilherme MR, Scariot DB, Nakamura CV, et al. pH-responsive alginate-based hydrogels for protein delivery. Journal of Molecular Liquids 2018;262:29–36. https://doi.org/10.1016/j.molliq.2018.04.002.
[59] Wei W, Li J, Qi X, Zhong Y, Zuo G, Pan X, et al. Synthesis and characterization of a multi-sensitive polysaccharide hydrogel for drug delivery. Carbohydrate Polymers 2017;177:275–83. https://doi.org/10.1016/j.carbpol.2017.08.133.
[60] Qi X, Wei W, Li J, Zuo G, Pan X, Su T, et al. Salecan-Based pH-Sensitive Hydrogels for Insulin Delivery. Mol Pharmaceutics 2017;14:431–40. https://doi.org/10.1021/acs.molpharmaceut.6b00875.
[61] Olthof MGL, Kempen DHR, Liu X, Dadsetan M, Tryfonidou MA, Yaszemski MJ, et al. Bone morphogenetic protein-2 release profile modulates bone formation in phosphorylated hydrogel. Journal of Tissue Engineering and Regenerative Medicine 2018;12:1339–51. https://doi.org/10.1002/term.2664.
[62] McAvan BS, Khuphe M, Thornton PD. Polymer hydrogels for glutathione-mediated protein release. European Polymer Journal 2017;87:468–77. https://doi.org/10.1016/j.eurpolymj.2016.09.032.
[63] Ma X, Xu T, Chen W, Qin H, Chi B, Ye Z. Injectable hydrogels based on the hyaluronic acid and poly (γ-glutamic acid) for controlled protein delivery. Carbohydrate Polymers 2018;179:100–9. https://doi.org/10.1016/j.carbpol.2017.09.071.
[64] Koshy ST, Zhang DKY, Grolman JM, Stafford AG, Mooney DJ. Injectable nanocomposite cryogels for versatile protein drug delivery. Acta Biomaterialia 2018;65:36–43. https://doi.org/10.1016/j.actbio.2017.11.024.
[65] Dai L, Cheng T, Wang Y, Lu H, Nie S, He H, et al. Injectable all-polysaccharide self-assembling hydrogel: a promising scaffold for localized therapeutic proteins. Cellulose 2019;26:6891–901. https://doi.org/10.1007/s10570-019-02579-7.

[66] Shigemitsu H, Fujisaku T, Tanaka W, Kubota R, Minami S, Urayama K, et al. An adaptive supramolecular hydrogel comprising self-sorting double nanofibre networks. Nature Nanotechnology 2018;13:165–72. https://doi.org/10.1038/s41565-017-0026-6.
[67] Phan VHG, Thambi T, Gil MS, Lee DS. Temperature and pH-sensitive injectable hydrogels based on poly(sulfamethazine carbonate urethane) for sustained delivery of cationic proteins. Polymer 2017;109:38–48. https://doi.org/10.1016/j.polymer.2016.12.039.
[68] Ozel B, Cikrikci S, Aydin O, Oztop MH. Polysaccharide blended whey protein isolate-(WPI) hydrogels: A physicochemical and controlled release study. Food Hydrocolloids 2017;71:35–46. https://doi.org/10.1016/j.foodhyd.2017.04.031.
[69] Khang MK, Zhou J, Huang Y, Hakamivala A, Tang L. Preparation of a novel injectable in situ-gelling nanoparticle with applications in controlled protein release and cancer cell entrapment. RSC Adv 2018;8:34625–33. https://doi.org/10.1039/C8RA06589F.
[70] Wang R, Yang Z, Luo J, Hsing I-M, Sun F. B12-dependent photoresponsive protein hydrogels for controlled stem cell/protein release. PNAS 2017;114:5912–7. https://doi.org/10.1073/pnas.1621350114.
[71] Hettiaratchi MH, Rouse T, Chou C, Krishnan L, Stevens HY, Li M-TA, et al. Enhanced in vivo retention of low dose BMP-2 via heparin microparticle delivery does not accelerate bone healing in a critically sized femoral defect. Acta Biomaterialia 2017;59:21–32. https://doi.org/10.1016/j.actbio.2017.06.028.
[72] Lokhande G, Carrow JK, Thakur T, Xavier JR, Parani M, Bayless KJ, et al. Nanoengineered injectable hydrogels for wound healing application. Acta Biomaterialia 2018;70:35–47. https://doi.org/10.1016/j.actbio.2018.01.045.
[73] Wongkanya R, Chuysinuan P, Pengsuk C, Techasakul S, Lirdprapamongkol K, Svasti J, et al. Electrospinning of alginate/soy protein isolated nanofibers and their release characteristics for biomedical applications. Journal of Science: Advanced Materials and Devices 2017;2:309–16. https://doi.org/10.1016/j.jsamd.2017.05.010.
[74] Machado-Paula MM, Corat MAF, Lancellotti M, Mi G, Marciano FR, Vega ML, et al. A comparison between electrospinning and rotary-jet spinning to produce PCL fibers with low bacteria colonization. Materials Science and Engineering: C 2020;111:110706. https://doi.org/10.1016/j.msec.2020.110706.
[75] Mohammadi M, Alibolandi M, Abnous K, Salmasi Z, Jaafari MR, Ramezani M. Fabrication of hybrid scaffold based on hydroxyapatite-biodegradable nanofibers incorporated with liposomal formulation of BMP-2 peptide for bone tissue engineering. Nanomedicine: Nanotechnology, Biology and Medicine 2018;14:1987–97. https://doi.org/10.1016/j.nano.2018.06.001.
[76] Nguyen LH, Gao M, Lin J, Wu W, Wang J, Chew SY. Three-dimensional aligned nanofibers-hydrogel scaffold for controlled non-viral drug/gene delivery to direct axon regeneration in spinal cord injury treatment. Scientific Reports 2017;7:1–12. https://doi.org/10.1038/srep42212.
[77] Jha BS, Colello RJ, Bowman JR, Sell SA, Lee KD, Bigbee JW, et al. Two pole air gap electrospinning: Fabrication of highly aligned, three-dimensional scaffolds for nerve reconstruction. Acta Biomaterialia 2011;7:203–15. https://doi.org/10.1016/j.actbio.2010.08.004.
[78] Wang J, Windbergs M. Controlled dual drug release by coaxial electrospun fibers – Impact of the core fluid on drug encapsulation and release.

International Journal of Pharmaceutics 2019;556:363–71. https://doi.org/10.1016/j.ijpharm.2018.12.026.
[79] Wen P, Wen Y, Huang X, Zong M-H, Wu H. Preparation and Characterization of Protein-Loaded Electrospun Fiber Mat and Its Release Kinetics. J Agric Food Chem 2017;65:4786–96. https://doi.org/10.1021/acs.jafc.7b01830.
[80] Wang M, Zhou Y, Shi D, Chang R, Zhang J, Keidar M, et al. Cold atmospheric plasma (CAP)-modified and bioactive protein-loaded core–shell nanofibers for bone tissue engineering applications. Biomater Sci 2019;7:2430–9. https://doi.org/10.1039/C8BM01284A.
[81] Aragón J, Salerno S, De Bartolo L, Irusta S, Mendoza G. Polymeric electrospun scaffolds for bone morphogenetic protein 2 delivery in bone tissue engineering. Journal of Colloid and Interface Science 2018;531:126–37. https://doi.org/10.1016/j.jcis.2018.07.029.
[82] Ahn S, Chantre CO, Gannon AR, Lind JU, Campbell PH, Grevesse T, et al. Soy Protein/Cellulose Nanofiber Scaffolds Mimicking Skin Extracellular Matrix for Enhanced Wound Healing. Advanced Healthcare Materials 2018;7:1701175. https://doi.org/10.1002/adhm.201701175.
[83] Straeten A vander, Bratek-Skicki A, Germain L, D'Haese C, Eloy P, Fustin C-A, et al. Protein–polyelectrolyte complexes to improve the biological activity of proteins in layer-by-layer assemblies. Nanoscale 2017;9:17186–92. https://doi.org/10.1039/C7NR04345G.
[84] vander Straeten A, Dupont-Gillain C. Self-Reorganizing Multilayer to Release Free Proteins from Self-Assemblies. Langmuir 2020;36:972–8. https://doi.org/10.1021/acs.langmuir.9b03547.
[85] Cho Y, Hong J. Sustained release of therapeutic proteins from multilayers adsorbed on the sidewalls of porous membranes. Colloids and Surfaces A: Physicochemical and Engineering Aspects 2019;562:296–303. https://doi.org/10.1016/j.colsurfa.2018.11.010.
[86] Park S, Choi D, Jeong H, Heo J, Hong J. Drug Loading and Release Behavior Depending on the Induced Porosity of Chitosan/Cellulose Multilayer Nanofilms. Mol Pharmaceutics 2017;14:3322–30. https://doi.org/10.1021/acs.molpharmaceut.7b00371.
[87] Zhao Y-N, Xu X, Wen N, Song R, Meng Q, Guan Y, et al. A Drug Carrier for Sustained Zero-Order Release of Peptide Therapeutics. Scientific Reports 2017;7:1–9. https://doi.org/10.1038/s41598-017-05898-6.
[88] He Y, Hong C, Li J, Howard MT, Li Y, Turvey ME, et al. Synthetic Charge-Invertible Polymer for Rapid and Complete Implantation of Layer-by-Layer Microneedle Drug Films for Enhanced Transdermal Vaccination. ACS Nano 2018;12:10272–80. https://doi.org/10.1021/acsnano.8b05373.
[89] Choi M, Choi D, Han U, Hong J. Inkjet-based multilayered growth factor-releasing nanofilms for enhancing proliferation of mesenchymal stem cells in vitro. Journal of Industrial and Engineering Chemistry 2017;50:36–40. https://doi.org/10.1016/j.jiec.2017.02.014.
[90] Ageitos JM, Pulgar A, Csaba N, Garcia-Fuentes M. Study of nanostructured fibroin/dextran matrixes for controlled protein release. European Polymer Journal 2019;114:197–205. https://doi.org/10.1016/j.eurpolymj.2019.02.028.
[91] Batista P, Castro P, Madureira AR, Sarmento B, Pintado M. Development and Characterization of Chitosan Microparticles-in-Films for Buccal Delivery of Bioactive Peptides. Pharmaceuticals 2019;12:32. https://doi.org/10.3390/ph12010032.

[92] Uz M, Sharma AD, Adhikari P, Sakaguchi DS, Mallapragada SK. Development of multifunctional films for peripheral nerve regeneration. Acta Biomaterialia 2017;56:141–52. https://doi.org/10.1016/j.actbio.2016.09.039.
[93] Seong K-Y, Seo M-S, Hwang DY, O'Cearbhaill ED, Sreenan S, Karp JM, et al. A self-adherent, bullet-shaped microneedle patch for controlled transdermal delivery of insulin. Journal of Controlled Release 2017;265:48–56. https://doi.org/10.1016/j.jconrel.2017.03.041.
[94] Liu D, Yu B, Jiang G, Yu W, Zhang Y, Xu B. Fabrication of composite microneedles integrated with insulin-loaded CaCO3 microparticles and PVP for transdermal delivery in diabetic rats. Materials Science and Engineering: C 2018;90:180–8. https://doi.org/10.1016/j.msec.2018.04.055.
[95] Tong Z, Zhou J, Zhong J, Tang Q, Lei Z, Luo H, et al. Glucose- and H2O2-Responsive Polymeric Vesicles Integrated with Microneedle Patches for Glucose-Sensitive Transcutaneous Delivery of Insulin in Diabetic Rats. ACS Appl Mater Interfaces 2018;10:20014–24. https://doi.org/10.1021/acsami.8b04484.
[96] Zhang Z, Liu C, Yang C, Wu Y, Yu F, Chen Y, et al. Aptamer-Patterned Hydrogel Films for Spatiotemporally Programmable Capture and Release of Multiple Proteins. ACS Appl Mater Interfaces 2018;10:8546–54. https://doi.org/10.1021/acsami.8b00191.
[97] Qi H, Cao J, Xin Y, Mao X, Xie D, Luo J, et al. Dual responsive zein hydrogel membrane with selective protein adsorption and sustained release property. Materials Science and Engineering: C 2017;70:347–56. https://doi.org/10.1016/j.msec.2016.09.010.
[98] Cacicedo ML, Islan GA, Drachemberg MF, Alvarez VA, Bartel LC, Bolzán AD, et al. Hybrid bacterial cellulose–pectin films for delivery of bioactive molecules. New J Chem 2018;42:7457–67. https://doi.org/10.1039/C7NJ03973E.
[99] Economidou SN, Pere CPP, Reid A, Uddin MJ, Windmill JFC, Lamprou DA, et al. 3D printed microneedle patches using stereolithography (SLA) for intradermal insulin delivery. Materials Science and Engineering: C 2019;102:743–55. https://doi.org/10.1016/j.msec.2019.04.063.
[100] M. Czekanska E, Geng J, Glinka M, White K, Kanczler J, D Evans N, et al. Combinatorial delivery of bioactive molecules by a nanoparticle-decorated and functionalized biodegradable scaffold. Journal of Materials Chemistry B 2018;6:4437–45. https://doi.org/10.1039/C8TB00474A.
[101] Marciello M, Rossi S, Caramella C, Remuñán-López C. Freeze-dried cylinders carrying chitosan nanoparticles for vaginal peptide delivery. Carbohydrate Polymers 2017;170:43–51. https://doi.org/10.1016/j.carbpol.2017.04.051.
[102] Cho TH, Kim IS, Lee B, Park S-N, Ko J-H, Hwang SJ. Early and Marked Enhancement of New Bone Quality by Alendronate-Loaded Collagen Sponge Combined with Bone Morphogenetic Protein-2 at High Dose: A Long-Term Study in Calvarial Defects in a Rat Model. Tissue Engineering Part A 2017;23:1343–60. https://doi.org/10.1089/ten.tea.2016.0557.
[103] Cai Y, Tong S, Zhang R, Zhu T, Wang X. In vitro evaluation of a bone morphogenetic protein- 2 nanometer hydroxyapatite collagen scaffold for bone regeneration. Molecular Medicine Reports 2018;17:5830–6. https://doi.org/10.3892/mmr.2018.8579.
[104] Hu Y, Ran J, Zheng Z, Jin Z, Chen X, Yin Z, et al. Exogenous stromal derived factor-1 releasing silk scaffold combined with intra-articular injection of

progenitor cells promotes bone-ligament-bone regeneration. Acta Biomaterialia 2018;71:168–83. https://doi.org/10.1016/j.actbio.2018.02.019.
[105] Li X, Liu Y, Zhang J, You R, Qu J, Li M. Functionalized silk fibroin dressing with topical bioactive insulin release for accelerated chronic wound healing. Materials Science and Engineering: C 2017;72:394–404. https://doi.org/10.1016/j.msec.2016.11.085.
[106] Wang B, Guo Y, Chen X, Zeng C, Hu Q, Yin W, et al. Nanoparticle-modified chitosan-agarose-gelatin scaffold for sustained release of SDF-1 and BMP-2. Int J Nanomedicine 2018;13:7395–408. https://doi.org/10.2147/IJN.S180859.
[107] Azizian S, Hadjizadeh A, Niknejad H. Chitosan-gelatin porous scaffold incorporated with Chitosan nanoparticles for growth factor delivery in tissue engineering. Carbohydrate Polymers 2018;202:315–22. https://doi.org/10.1016/j.carbpol.2018.07.023.
[108] Wang B, Lv X, Chen S, Li Z, Yao J, Peng X, et al. Use of heparinized bacterial cellulose based scaffold for improving angiogenesis in tissue regeneration. Carbohydrate Polymers 2018;181:948–56. https://doi.org/10.1016/j.carbpol.2017.11.055.
[109] Yao Q, Liu Y, Selvaratnam B, Koodali RT, Sun H. Mesoporous silicate nanoparticles/3D nanofibrous scaffold-mediated dual-drug delivery for bone tissue engineering. Journal of Controlled Release 2018;279:69–78. https://doi.org/10.1016/j.jconrel.2018.04.011.
[110] Bastami F, Paknejad Z, Jafari M, Salehi M, Rezai Rad M, Khojasteh A. Fabrication of a three-dimensional β-tricalcium-phosphate/gelatin containing chitosan-based nanoparticles for sustained release of bone morphogenetic protein-2: Implication for bone tissue engineering. Materials Science and Engineering: C 2017;72:481–91. https://doi.org/10.1016/j.msec.2016.10.084.
[111] Cheng C-H, Chen Y-W, Kai-Xing Lee A, Yao C-H, Shie M-Y. Development of mussel-inspired 3D-printed poly (lactic acid) scaffold grafted with bone morphogenetic protein-2 for stimulating osteogenesis. J Mater Sci: Mater Med 2019;30:78. https://doi.org/10.1007/s10856-019-6279-x.
[112] Huang K-H, Lin Y-H, Shie M-Y, Lin C-P. Effects of bone morphogenic protein-2 loaded on the 3D-printed MesoCS scaffolds. Journal of the Formosan Medical Association 2018;117:879–87. https://doi.org/10.1016/j.jfma.2018.07.010.
[113] Lee J, Kim G. Calcium-Deficient Hydroxyapatite/Collagen/Platelet-Rich Plasma Scaffold with Controlled Release Function for Hard Tissue Regeneration. ACS Biomater Sci Eng 2018;4:278–89. https://doi.org/10.1021/acsbiomaterials.7b00640.
[114] Unagolla JM, Jayasuriya AC. Drug transport mechanisms and in vitro release kinetics of vancomycin encapsulated chitosan-alginate polyelectrolyte microparticles as a controlled drug delivery system. European Journal of Pharmaceutical Sciences 2018;114:199–209. https://doi.org/10.1016/j.ejps.2017.12.012.
[115] Maciel VBV, Yoshida CMP, Pereira SMSS, Goycoolea FM, Franco TT. Electrostatic Self-Assembled Chitosan-Pectin Nano- and Microparticles for Insulin Delivery. Molecules 2017;22:1707. https://doi.org/10.3390/molecules22101707.
[116] Ling K, Wu H, Neish AS, Champion JA. Alginate/chitosan microparticles for gastric passage and intestinal release of therapeutic protein nanoparticles. Journal of Controlled Release 2019;295:174–86. https://doi.org/10.1016/j.jconrel.2018.12.017.

[117] Wu D-Y, Ma Y, Hou X-S, Zhang W-J, Wang P, Chen H, et al. Co-delivery of antineoplastic and protein drugs by chitosan nanocapsules for a collaborative tumor treatment. Carbohydrate Polymers 2017;157:1470–8. https://doi.org/10.1016/j.carbpol.2016.11.027.
[118] Zhang Y, Chi C, Huang X, Zou Q, Li X, Chen L. Starch-based nanocapsules fabricated through layer-by-layer assembly for oral delivery of protein to lower gastrointestinal tract. Carbohydrate Polymers 2017;171:242–51. https://doi.org/10.1016/j.carbpol.2017.04.090.
[119] Chen W, Tian R, Xu C, Yung BC, Wang G, Liu Y, et al. Microneedle-array patches loaded with dual mineralized protein/peptide particles for type 2 diabetes therapy. Nature Communications 2017;8:1–11. https://doi.org/10.1038/s41467-017-01764-1.
[120] Mumcuoglu D, de Miguel L, Jekhmane S, Siverino C, Nickel J, Mueller TD, et al. Collagen I derived recombinant protein microspheres as novel delivery vehicles for bone morphogenetic protein-2. Materials Science and Engineering: C 2018;84:271–80. https://doi.org/10.1016/j.msec.2017.11.031.
[121] Ménard M, Meyer F, Affolter-Zbaraszczuk C, Rabineau M, Adam A, Ramirez PD, et al. Design of hybrid protein-coated magnetic core-mesoporous silica shell nanocomposites for MRI and drug release assessed in a 3D tumor cell model. Nanotechnology 2019;30:174001. https://doi.org/10.1088/1361-6528/aafe1c.
[122] He H, Chen Y, Li Y, Song Z, Zhong Y, Zhu R, et al. Effective and Selective Anti-Cancer Protein Delivery via All-Functions-in-One Nanocarriers Coupled with Visible Light-Responsive, Reversible Protein Engineering. Advanced Functional Materials 2018;28:1706710. https://doi.org/10.1002/adfm.201706710.
[123] Haine AT, Koga Y, Hashimoto Y, Higashi T, Motoyama K, Arima H, et al. Enhancement of transdermal protein delivery by photothermal effect of gold nanorods coated on polysaccharide-based hydrogel. European Journal of Pharmaceutics and Biopharmaceutics 2017;119:91–5. https://doi.org/10.1016/j.ejpb.2017.06.005.
[124] Tuncaboylu DC, Friess F, Wischke C, Lendlein A. A multifunctional multimaterial system for on-demand protein release. Journal of Controlled Release 2018;284:240–7. https://doi.org/10.1016/j.jconrel.2018.06.022.
[125] Mertz D, Sandre O, Bégin-Colin S. Drug releasing nanoplatforms activated by alternating magnetic fields. Biochimica et Biophysica Acta (BBA) - General Subjects 2017;1861:1617–41. https://doi.org/10.1016/j.bbagen.2017.02.025.
[126] Zhang Y, Tong C, Ma Z, Lu L, Fu H, Pan S, et al. A self-powered delivery substrate boosts active enzyme delivery in response to human movements. Nanoscale 2019;11:14372–82. https://doi.org/10.1039/C9NR04673A.
[127] Xu C, Wei Z, Gao H, Bai Y, Liu H, Yang H, et al. Bioinspired Mechano-Sensitive Macroporous Ceramic Sponge for Logical Drug and Cell Delivery. Advanced Science 2017;4:1600410. https://doi.org/10.1002/advs.201600410.
[128] Mertz D, Vogt C, Hemmerlé J, Debry C, Voegel J-C, Schaaf P, et al. Tailored design of mechanically sensitive biocatalytic assemblies based on polyelectrolyte multilayers. J Mater Chem 2011;21:8324–31. https://doi.org/10.1039/C0JM03496G.
[129] Mertz D, Vogt C, Hemmerlé J, Mutterer J, Ball V, Voegel J-C, et al. Mechanotransductive surfaces for reversible biocatalysis activation. Nature Materials 2009;8:731–5. https://doi.org/10.1038/nmat2504.

[130] Aitken A, Learmonth MP. Protein Determination by UV Absorption. The Protein Protocols Handbook, Humana Press, Totowa, NJ; 2009, p. 3–6. https://doi.org/10.1007/978-1-59745-198-7_1.
[131] Bradford MM. A rapid and sensitive method for the quantitation of microgram quantities of protein utilizing the principle of protein-dye binding. Analytical Biochemistry 1976;72:248–54. https://doi.org/10.1016/0003-2697(76)90527-3.
[132] Kruger NJ. The Bradford Method For Protein Quantitation. In: Walker JM, editor. The Protein Protocols Handbook, Totowa, NJ: Humana Press; 2009, p. 17–24. https://doi.org/10.1007/978-1-59745-198-7_4.
[133] Brady PN, Macnaughtan MA. Evaluation of Colorimetric Assays for Analyzing Reductively Methylated Proteins: Biases and Mechanistic Insights. Anal Biochem 2015;491:43–51. https://doi.org/10.1016/j.ab.2015.08.027.
[134] Smith PK, Krohn RI, Hermanson GT, Mallia AK, Gartner FH, Provenzano MD, et al. Measurement of protein using bicinchoninic acid. Analytical Biochemistry 1985;150:76–85. https://doi.org/10.1016/0003-2697(85)90442-7.
[135] Walker JM. The Bicinchoninic Acid (BCA) Assay for Protein Quantitation. In: Walker JM, editor. The Protein Protocols Handbook, Totowa, NJ: Humana Press; 2009, p. 11–5. https://doi.org/10.1007/978-1-59745-198-7_3.
[136] Wang X, Li Y, Li Q, Neufeld CI, Pouli D, Sun S, et al. Hyaluronic acid modification of RNase A and its intracellular delivery using lipid-like nanoparticles. Journal of Controlled Release 2017;263:39–45. https://doi.org/10.1016/j.jconrel.2017.01.037.
[137] Cao Q, He Z, Sun WQ, Fan G, Zhao J, Bao N, et al. Improvement of calcium phosphate scaffold osteogenesis in vitro via combination of glutamate-modified BMP-2 peptides. Materials Science and Engineering: C 2019;96:412–8. https://doi.org/10.1016/j.msec.2018.11.048.
[138] Kim B-S, Yang S-S, Kim CS. Incorporation of BMP-2 nanoparticles on the surface of a 3D-printed hydroxyapatite scaffold using an ε-polycaprolactone polymer emulsion coating method for bone tissue engineering. Colloids and Surfaces B: Biointerfaces 2018;170:421–9. https://doi.org/10.1016/j.colsurfb.2018.06.043.
[139] Gobeaux F, Bizeau J, Samson F, Marichal L, Grillo I, Wien F, et al. Albumin-driven disassembly of lipidic nanoparticles: the specific case of the squalene-adenosine nanodrug. Nanoscale 2020;12:2793–809. https://doi.org/10.1039/C9NR06485K.
[140] Bhakuni V, Gupta CM. Interactions of tuftsin with bovine serum albumin. FEBS Letters 1986;205:347–50. https://doi.org/10.1016/0014-5793(86)80926-7.
[141] Tian J, Liu J, Hu Z, Chen X. Interaction of wogonin with bovine serum albumin. Bioorganic & Medicinal Chemistry 2005;13:4124–9. https://doi.org/10.1016/j.bmc.2005.02.065.
[142] Jahanban-Esfahlan A, Panahi-Azar V. Interaction of glutathione with bovine serum albumin: Spectroscopy and molecular docking. Food Chemistry 2016;202:426–31. https://doi.org/10.1016/j.foodchem.2016.02.026.
[143] Qu Y, Wei T, Zhan W, Hu C, Cao L, Yu Q, et al. A reusable supramolecular platform for the specific capture and release of proteins and bacteria. J Mater Chem B 2017;5:444–53. https://doi.org/10.1039/C6TB02821G.
[144] Steele AN, Cai L, Truong VN, Edwards BB, Goldstone AB, Eskandari A, et al. A novel protein-engineered hepatocyte growth factor analog released via a shear-thinning injectable hydrogel enhances post-infarction ventricular function.

Biotechnology and Bioengineering 2017;114:2379–89. https://doi.org/10.1002/bit.26345.
[145] Jiang T, Shen S, Wang T, Li M, He B, Mo R. A Substrate-Selective Enzyme-Catalysis Assembly Strategy for Oligopeptide Hydrogel-Assisted Combinatorial Protein Delivery. Nano Lett 2017;17:7447–54. https://doi.org/10.1021/acs.nanolett.7b03371.
[146] Udenfriend S, Stein S, Böhlen P, Dairman W, Leimgruber W, Weigele M. Fluorescamine: A Reagent for Assay of Amino Acids, Peptides, Proteins, and Primary Amines in the Picomole Range. Science 1972;178:871–2. https://doi.org/10.1126/science.178.4063.871.
[147] fluorescamine , Chemical Structures , Manuals & Protocols | Thermo Fisher Scientific n.d. https://www.thermofisher.com/search/results?query=fluorescamine&persona=DocSupport&navId=4294959583%2B4294959596&refinementAction=true&focusarea=Rechercher (accessed June 8, 2020).
[148] Engvall E, Perlmann P. Enzyme-linked immunosorbent assay (ELISA) quantitative assay of immunoglobulin G. Immunochemistry 1971;8:871–4. https://doi.org/10.1016/0019-2791(71)90454-X.
[149] Systems in ELISA. Methods Mol Biol 2009;516:9–42. https://doi.org/10.1007/978-1-60327-254-4_2.
[150] Overview of ELISA - FR n.d. https://www.thermofisher.com/fr/fr/home/life-science/protein-biology/protein-biology-learning-center/protein-biology-resource-library/pierce-protein-methods/overview-elisa.html (accessed June 9, 2020).
[151] Raina DB, Larsson D, Mrkonjic F, Isaksson H, Kumar A, Lidgren L, et al. Gelatin- hydroxyapatite- calcium sulphate based biomaterial for long term sustained delivery of bone morphogenic protein-2 and zoledronic acid for increased bone formation: In-vitro and in-vivo carrier properties. Journal of Controlled Release 2018;272:83–96. https://doi.org/10.1016/j.jconrel.2018.01.006.
[152] Kuttappan S, Mathew D, Jo J, Tanaka R, Menon D, Ishimoto T, et al. Dual release of growth factor from nanocomposite fibrous scaffold promotes vascularisation and bone regeneration in rat critical sized calvarial defect. Acta Biomaterialia 2018;78:36–47. https://doi.org/10.1016/j.actbio.2018.07.050.
[153] Farris E, Brown DM, Ramer-Tait AE, Pannier AK. Chitosan-zein nano-in-microparticles capable of mediating in vivo transgene expression following oral delivery. Journal of Controlled Release 2017;249:150–61. https://doi.org/10.1016/j.jconrel.2017.01.035.
[154] da Silva TN, Gonçalves RP, Rocha CL, Archanjo BS, Barboza CAG, Pierre MBR, et al. Controlling burst effect with PLA/PVA coaxial electrospun scaffolds loaded with BMP-2 for bone guided regeneration. Materials Science and Engineering: C 2019;97:602–12. https://doi.org/10.1016/j.msec.2018.12.020.
[155] Castro PM, Baptista P, Madureira AR, Sarmento B, Pintado ME. Combination of PLGA nanoparticles with mucoadhesive guar-gum films for buccal delivery of antihypertensive peptide. International Journal of Pharmaceutics 2018;547:593–601. https://doi.org/10.1016/j.ijpharm.2018.05.051.
[156] Cui W, Liu Q, Yang L, Wang K, Sun T, Ji Y, et al. Sustained Delivery of BMP-2-Related Peptide from the True Bone Ceramics/Hollow Mesoporous Silica Nanoparticles Scaffold for Bone Tissue Regeneration. ACS Biomater Sci Eng 2018;4:211–21. https://doi.org/10.1021/acsbiomaterials.7b00506.

[157] Qi Q, Lu L, Li H, Yuan Z, Chen G, Lin M, et al. Spatiotemporal delivery of nanoformulated liraglutide for cardiac regeneration after myocardial infarction. Int J Nanomedicine 2017;12:4835–48. https://doi.org/10.2147/IJN.S132064.
[158] Unzueta U, Cespedes MV, Sala R, Alamo P, Sánchez-Chardi A, Pesarrodona M, et al. Release of targeted protein nanoparticles from functional bacterial amyloids: A death star-like approach. Journal of Controlled Release 2018;279:29–39. https://doi.org/10.1016/j.jconrel.2018.04.004.
[159] Díaz-Herráez P, Saludas L, Pascual-Gil S, Simón-Yarza T, Abizanda G, Prósper F, et al. Transplantation of adipose-derived stem cells combined with neuregulin-microparticles promotes efficient cardiac repair in a rat myocardial infarction model. Journal of Controlled Release 2017;249:23–31. https://doi.org/10.1016/j.jconrel.2017.01.026.
[160] Duong HTT, Yin Y, Thambi T, Nguyen TL, Giang Phan VH, Lee MS, et al. Smart vaccine delivery based on microneedle arrays decorated with ultra-pH-responsive copolymers for cancer immunotherapy. Biomaterials 2018;185:13–24. https://doi.org/10.1016/j.biomaterials.2018.09.008.
[161] Liu G, Li L, Huo D, Li Y, Wu Y, Zeng L, et al. A VEGF delivery system targeting MI improves angiogenesis and cardiac function based on the tropism of MSCs and layer-by-layer self-assembly. Biomaterials 2017;127:117–31. https://doi.org/10.1016/j.biomaterials.2017.03.001.
[162] Xia B, Lv Y. Dual-delivery of VEGF and NGF by emulsion electrospun nanofibrous scaffold for peripheral nerve regeneration. Materials Science and Engineering: C 2018;82:253–64. https://doi.org/10.1016/j.msec.2017.08.030.
[163] Lee MS, Ahmad T, Lee J, Awada HK, Wang Y, Kim K, et al. Dual delivery of growth factors with coacervate-coated poly(lactic-co-glycolic acid) nanofiber improves neovascularization in a mouse skin flap model. Biomaterials 2017;124:65–77. https://doi.org/10.1016/j.biomaterials.2017.01.036.
[164] Marvin M. Microscopy apparatus. US3013467A, 1961.
[165] Aji Alex MR, Nehate C, Veeranarayanan S, Kumar DS, Kulshreshtha R, Koul V. Self assembled dual responsive micelles stabilized with protein for co-delivery of drug and siRNA in cancer therapy. Biomaterials 2017;133:94–106. https://doi.org/10.1016/j.biomaterials.2017.04.022.
[166] Dutta D, Fauer C, Hickey K, Salifu M, Stabenfeldt SE. Tunable delayed controlled release profile from layered polymeric microparticles. J Mater Chem B 2017;5:4487–98. https://doi.org/10.1039/C7TB00138J.
[167] Quinlan E, López-Noriega A, Thompson EM, Hibbitts A, Cryan SA, O'Brien FJ. Controlled release of vascular endothelial growth factor from spray-dried alginate microparticles in collagen–hydroxyapatite scaffolds for promoting vascularization and bone repair. Journal of Tissue Engineering and Regenerative Medicine 2017;11:1097–109. https://doi.org/10.1002/term.2013.
[168] Kelly SM, Jess TJ, Price NC. How to study proteins by circular dichroism. Biochimica et Biophysica Acta (BBA) - Proteins and Proteomics 2005;1751:119–39. https://doi.org/10.1016/j.bbapap.2005.06.005.
[169] Patel S, Ryals RC, Weller KK, Pennesi ME, Sahay G. Lipid nanoparticles for delivery of messenger RNA to the back of the eye. Journal of Controlled Release 2019;303:91–100. https://doi.org/10.1016/j.jconrel.2019.04.015.
[170] Wang A, Yang T, Fan W, Yang Y, Zhu Q, Guo S, et al. Protein Corona Liposomes Achieve Efficient Oral Insulin Delivery by Overcoming Mucus and Epithelial Barriers. Advanced Healthcare Materials 2019;8:1801123. https://doi.org/10.1002/adhm.201801123.

[171] Yu JR, Janssen M, Liang BJ, Huang H-C, Fisher JP. A liposome/gelatin methacrylate nanocomposite hydrogel system for delivery of stromal cell-derived factor-1α and stimulation of cell migration. Acta Biomaterialia 2020;108:67–76. https://doi.org/10.1016/j.actbio.2020.03.015.
[172] Chatzikleanthous D, Schmidt ST, Buffi G, Paciello I, Cunliffe R, Carboni F, et al. Design of a novel vaccine nanotechnology-based delivery system comprising CpGODN-protein conjugate anchored to liposomes. Journal of Controlled Release 2020;323:125–37. https://doi.org/10.1016/j.jconrel.2020.04.001.
[173] Colombani T, Peuziat P, Dallet L, Haudebourg T, Mével M, Berchel M, et al. Self-assembling complexes between binary mixtures of lipids with different linkers and nucleic acids promote universal mRNA, DNA and siRNA delivery. Journal of Controlled Release 2017;249:131–42. https://doi.org/10.1016/j.jconrel.2017.01.041.
[174] Costa P, Sousa Lobo JM. Modeling and comparison of dissolution profiles. European Journal of Pharmaceutical Sciences 2001;13:123–33. https://doi.org/10.1016/S0928-0987(01)00095-1.
[175] Korsmeyer RW, Gurny R, Doelker E, Buri P, Peppas NA. Mechanisms of solute release from porous hydrophilic polymers. International Journal of Pharmaceutics 1983;15:25–35. https://doi.org/10.1016/0378-5173(83)90064-9.
[176] Alfrey T, Gurnee EF, Lloyd WG. Diffusion in glassy polymers. Journal of Polymer Science Part C: Polymer Symposia 1966;12:249–61. https://doi.org/10.1002/polc.5070120119.
[177] Kosmidis K, Rinaki E, Argyrakis P, Macheras P. Analysis of Case II drug transport with radial and axial release from cylinders. International Journal of Pharmaceutics 2003;254:183–8. https://doi.org/10.1016/S0378-5173(03)00030-9.
[178] Ritger PL, Peppas NA. A simple equation for description of solute release I. Fickian and non-fickian release from non-swellable devices in the form of slabs, spheres, cylinders or discs. Journal of Controlled Release 1987;5:23–36. https://doi.org/10.1016/0168-3659(87)90034-4.
[179] Ritger PL, Peppas NA. A simple equation for description of solute release II. Fickian and anomalous release from swellable devices. Journal of Controlled Release 1987;5:37–42. https://doi.org/10.1016/0168-3659(87)90035-6.
[180] Peppas NA, Sahlin JJ. A simple equation for the description of solute release. III. Coupling of diffusion and relaxation. International Journal of Pharmaceutics 1989;57:169–72. https://doi.org/10.1016/0378-5173(89)90306-2.
[181] Matoušek J. Ribonucleases and their antitumor activity. Comparative Biochemistry and Physiology Part C: Toxicology & Pharmacology 2001;129:175–91. https://doi.org/10.1016/S1532-0456(01)90202-9.
[182] Fan W, Xia D, Zhu Q, Li X, He S, Zhu C, et al. Functional nanoparticles exploit the bile acid pathway to overcome multiple barriers of the intestinal epithelium for oral insulin delivery. Biomaterials 2018;151:13–23. https://doi.org/10.1016/j.biomaterials.2017.10.022.
[183] Cross LM, Carrow JK, Ding X, Singh KA, Gaharwar AK. Sustained and Prolonged Delivery of Protein Therapeutics from Two-Dimensional Nanosilicates. ACS Appl Mater Interfaces 2019;11:6741–50. https://doi.org/10.1021/acsami.8b17733.
[184] Porter AG, Jänicke RU. Emerging roles of caspase-3 in apoptosis. Cell Death Differ 1999;6:99–104. https://doi.org/10.1038/sj.cdd.4400476.

[185] Santhosh KT, Alizadeh A, Karimi-Abdolrezaee S. Design and optimization of PLGA microparticles for controlled and local delivery of Neuregulin-1 in traumatic spinal cord injury. Journal of Controlled Release 2017;261:147–62. https://doi.org/10.1016/j.jconrel.2017.06.030.
[186] Fakhoury M. Microglia and Astrocytes in Alzheimer's Disease: Implications for Therapy. Curr Neuropharmacol 2018;16:508–18. https://doi.org/10.2174/1570159X15666170720095240.
[187] Zeng W, Liu Z, Li Y, Zhu S, Ma J, Li W, et al. Development and characterization of cores–shell poly(lactide-co-glycolide)-chitosan microparticles for sustained release of GDNF. Colloids and Surfaces B: Biointerfaces 2017;159:791–9. https://doi.org/10.1016/j.colsurfb.2017.08.052.
[188] Rosini R, Rinaudo CD, Soriani M, Lauer P, Mora M, Maione D, et al. Identification of novel genomic islands coding for antigenic pilus-like structures in Streptococcus agalactiae. Molecular Microbiology 2006;61:126–41. https://doi.org/10.1111/j.1365-2958.2006.05225.x.
[189] Wei B, Wang C, Yan C, Tang B, Yu X, Zhang H, et al. Osteoprotegerin/bone morphogenetic protein 2 combining with collagen sponges on tendon-bone healing in rabbits. J Bone Miner Metab 2020. https://doi.org/10.1007/s00774-019-01078-w.
[190] Fujioka-Kobayashi M, Schaller B, Saulacic N, Pippenger BE, Zhang Y, Miron RJ. Absorbable collagen sponges loaded with recombinant bone morphogenetic protein 9 induces greater osteoblast differentiation when compared to bone morphogenetic protein 2. Clinical and Experimental Dental Research 2017;3:32–40. https://doi.org/10.1002/cre2.55.
[191] Lin D, Chai Y, Ma Y, Duan B, Yuan Y, Liu C. Rapid initiation of guided bone regeneration driven by spatiotemporal delivery of IL-8 and BMP-2 from hierarchical MBG-based scaffold. Biomaterials 2019;196:122–37. https://doi.org/10.1016/j.biomaterials.2017.11.011.
[192] Hettiaratchi MH, Chou C, Servies N, Smeekens JM, Cheng A, Esancy C, et al. Competitive Protein Binding Influences Heparin-Based Modulation of Spatial Growth Factor Delivery for Bone Regeneration. Tissue Engineering Part A 2017;23:683–95. https://doi.org/10.1089/ten.tea.2016.0507.
[193] Xue D, Zhang W, Chen E, Gao X, Liu L, Ye C, et al. Local delivery of HMGB1 in gelatin sponge scaffolds combined with mesenchymal stem cell sheets to accelerate fracture healing. Oncotarget 2017;8:42098–115. https://doi.org/10.18632/oncotarget.16887.
[194] Whitehead TJ, Avila COC, Sundararaghavan HG. Combining growth factor releasing microspheres within aligned nanofibers enhances neurite outgrowth. Journal of Biomedical Materials Research Part A 2018;106:17–25. https://doi.org/10.1002/jbm.a.36204.
[195] Awada HK, Long DW, Wang Z, Hwang MP, Kim K, Wang Y. A single injection of protein-loaded coacervate-gel significantly improves cardiac function post infarction. Biomaterials 2017;125:65–80. https://doi.org/10.1016/j.biomaterials.2017.02.020.
[196] Bhattarai DP, Kim MH, Park H, Park WH, Kim BS, Kim CS. Coaxially fabricated polylactic acid electrospun nanofibrous scaffold for sequential release of tauroursodeoxycholic acid and bone morphogenic protein2 to stimulate angiogenesis and bone regeneration. Chemical Engineering Journal 2020;389:123470. https://doi.org/10.1016/j.cej.2019.123470.

[197] Cheng G, Yin C, Tu H, Jiang S, Wang Q, Zhou X, et al. Controlled Co-delivery of Growth Factors through Layer-by-Layer Assembly of Core–Shell Nanofibers for Improving Bone Regeneration. ACS Nano 2019;13:6372–82. https://doi.org/10.1021/acsnano.8b06032.
[198] Krishnan L, Priddy LB, Esancy C, Klosterhoff BS, Stevens HY, Tran L, et al. Delivery vehicle effects on bone regeneration and heterotopic ossification induced by high dose BMP-2. Acta Biomaterialia 2017;49:101–12. https://doi.org/10.1016/j.actbio.2016.12.012.
[199] Huber E, Pobloth A-M, Bormann N, Kolarczik N, Schmidt-Bleek K, Schell H, et al. Demineralized Bone Matrix as a Carrier for Bone Morphogenetic Protein-2: Burst Release Combined with Long-Term Binding and Osteoinductive Activity Evaluated In Vitro and In Vivo. Tissue Engineering Part A 2017;23:1321–30. https://doi.org/10.1089/ten.tea.2017.0005.
[200] Enezei HH, Ahmad A, Takeuchi K, Suzuki J, Khamis MF, Razak NHA, et al. Osteoinductive Activity of Bone Scaffold Bioceramic Companied with Control Release of VEGF Protein Treated Dental stem cells as A New Concept for Bone Regeneration: Part II. Journal of Hard Tissue Biology 2018;27:69–78. https://doi.org/10.2485/jhtb.27.69.
[201] Qu D, Zhu JP, Childs HR, Lu HH. Nanofiber-based transforming growth factor-β3 release induces fibrochondrogenic differentiation of stem cells. Acta Biomaterialia 2019;93:111–22. https://doi.org/10.1016/j.actbio.2019.03.019.
[202] Sydow S, Cassan D de, Hänsch R, R. Gengenbach T, D. Easton C, Thissen H, et al. Layer-by-layer deposition of chitosan nanoparticles as drug-release coatings for PCL nanofibers. Biomaterials Science 2019;7:233–46. https://doi.org/10.1039/C8BM00657A.
[203] Wang J, Sun B, Tian L, He X, Gao Q, Wu T, et al. Evaluation of the potential of rhTGF- β3 encapsulated P(LLA-CL)/collagen nanofibers for tracheal cartilage regeneration using mesenchymal stems cells derived from Wharton's jelly of human umbilical cord. Materials Science and Engineering: C 2017;70:637–45. https://doi.org/10.1016/j.msec.2016.09.044.
[204] Henry N, Clouet J, Visage CL, Weiss P, Gautron E, Renard D, et al. Silica nanofibers as a new drug delivery system: a study of the protein–silica interactions. J Mater Chem B 2017;5:2908–20. https://doi.org/10.1039/C7TB00332C.
[205] Tapeinos C, Larrañaga A, Tomatis F, Bizeau J, Marino A, Battaglini M, et al. Advanced Functional Materials and Cell-Based Therapies for the Treatment of Ischemic Stroke and Postischemic Stroke Effects. Advanced Functional Materials 2020;30:1906283. https://doi.org/10.1002/adfm.201906283.
[206] Bruggeman KF, Wang Y, Maclean FL, Parish CL, Williams RJ, Nisbet DR. Temporally controlled growth factor delivery from a self-assembling peptide hydrogel and electrospun nanofibre composite scaffold. Nanoscale 2017;9:13661–9. https://doi.org/10.1039/C7NR05004F.
[207] Sivak WN, White JD, Bliley JM, Tien LW, Liao HT, Kaplan DL, et al. Delivery of chondroitinase ABC and glial cell line-derived neurotrophic factor from silk fibroin conduits enhances peripheral nerve regeneration. Journal of Tissue Engineering and Regenerative Medicine 2017;11:733–42. https://doi.org/10.1002/term.1970.
[208] O'Neill HS, O'Sullivan J, Porteous N, Ruiz-Hernandez E, Kelly HM, O'Brien FJ, et al. A collagen cardiac patch incorporating alginate microparticles permits the controlled release of hepatocyte growth factor and insulin-like growth factor-1 to

enhance cardiac stem cell migration and proliferation. Journal of Tissue Engineering and Regenerative Medicine 2018;12:e384–94. https://doi.org/10.1002/term.2392.
[209] Fleischer S, Shapira A, Feiner R, Dvir T. Modular assembly of thick multifunctional cardiac patches. PNAS 2017;114:1898–903. https://doi.org/10.1073/pnas.1615728114.
[210] Liu JMH, Zhang X, Joe S, Luo X, Shea LD. Evaluation of biomaterial scaffold delivery of IL-33 as a localized immunomodulatory agent to support cell transplantation in adipose tissue. Journal of Immunology and Regenerative Medicine 2018;1:1–12. https://doi.org/10.1016/j.regen.2018.01.003.
[211] Lancina MG, Shankar RK, Yang H. Chitosan nanofibers for transbuccal insulin delivery. Journal of Biomedical Materials Research Part A 2017;105:1252–9. https://doi.org/10.1002/jbm.a.35984.
[212] Zigdon-Giladi H, Khutaba A, Elimelech R, Machtei EE, Srouji S. VEGF release from a polymeric nanofiber scaffold for improved angiogenesis. Journal of Biomedical Materials Research Part A 2017;105:2712–21. https://doi.org/10.1002/jbm.a.36127.
[213] Piran M, Vakilian S, Piran M, Mohammadi-Sangcheshmeh A, Hosseinzadeh S, Ardeshirylajimi A. In vitro fibroblast migration by sustained release of PDGF-BB loaded in chitosan nanoparticles incorporated in electrospun nanofibers for wound dressing applications. Artificial Cells, Nanomedicine, and Biotechnology 2018;46:511–20. https://doi.org/10.1080/21691401.2018.1430698.
[214] Mandapalli PK, Labala S, Jose A, Bhatnagar S, Janupally R, Sriram D, et al. Layer-by-Layer Thin Films for Co-Delivery of TGF-β siRNA and Epidermal Growth Factor to Improve Excisional Wound Healing. AAPS PharmSciTech 2017;18:809–20. https://doi.org/10.1208/s12249-016-0571-6.
[215] Tellier LE, Treviño EA, Brimeyer AL, Reece DS, Willett NJ, Guldberg RE, et al. Intra-articular TSG-6 delivery from heparin-based microparticles reduces cartilage damage in a rat model of osteoarthritis. Biomater Sci 2018;6:1159–67. https://doi.org/10.1039/C8BM00010G.
[216] Cheng G, Ma X, Li J, Cheng Y, Cao Y, Wang Z, et al. Incorporating platelet-rich plasma into coaxial electrospun nanofibers for bone tissue engineering. International Journal of Pharmaceutics 2018;547:656–66. https://doi.org/10.1016/j.ijpharm.2018.06.020.
[217] Anitua E, Pino A, Troya M, Jaén P, Orive G. A novel personalized 3D injectable protein scaffold for regenerative medicine. J Mater Sci: Mater Med 2017;29:7. https://doi.org/10.1007/s10856-017-6012-6.
[218] Waters R, Alam P, Pacelli S, Chakravarti AR, Ahmed RPH, Paul A. Stem cell-inspired secretome-rich injectable hydrogel to repair injured cardiac tissue. Acta Biomaterialia 2018;69:95–106. https://doi.org/10.1016/j.actbio.2017.12.025.
[219] Pignatelli C, Perotto G, Nardini M, Cancedda R, Mastrogiacomo M, Athanassiou A. Electrospun silk fibroin fibers for storage and controlled release of human platelet lysate. Acta Biomaterialia 2018;73:365–76. https://doi.org/10.1016/j.actbio.2018.04.025.
[220] Tansathien K, Suriyaaumporn P, Charoenputtakhun P, Ngawhirunpat T, Opanasopit P, Rangsimawong W. Development of Sponge Microspicule Cream as a Transdermal Delivery System for Protein and Growth Factors from Deer Antler Velvet Extract. Biological and Pharmaceutical Bulletin 2019;42:1207–15. https://doi.org/10.1248/bpb.b19-00158.

[221] Davoodi P, P. Srinivasan M, Wang C-H. Effective co-delivery of nutlin-3a and p53 genes via core–shell microparticles for disruption of MDM2–p53 interaction and reactivation of p53 in hepatocellular carcinoma. Journal of Materials Chemistry B 2017;5:5816–34. https://doi.org/10.1039/C7TB00481H.
[222] Grim JC, Brown TE, Aguado BA, Chapnick DA, Viert AL, Liu X, et al. A Reversible and Repeatable Thiol–Ene Bioconjugation for Dynamic Patterning of Signaling Proteins in Hydrogels. ACS Cent Sci 2018;4:909–16. https://doi.org/10.1021/acscentsci.8b00325.
[223] Zhang C, Zhang T, Jin S, Xue X, Yang X, Gong N, et al. Virus-Inspired Self-Assembled Nanofibers with Aggregation-Induced Emission for Highly Efficient and Visible Gene Delivery. ACS Appl Mater Interfaces 2017;9:4425–32. https://doi.org/10.1021/acsami.6b11536.
[224] Pinese C, Lin J, Milbreta U, Li M, Wang Y, Leong KW, et al. Sustained delivery of siRNA/mesoporous silica nanoparticle complexes from nanofiber scaffolds for long-term gene silencing. Acta Biomaterialia 2018;76:164–77. https://doi.org/10.1016/j.actbio.2018.05.054.
[225] Tenkumo T, Vanegas Sáenz JR, Nakamura K, Shimizu Y, Sokolova V, Epple M, et al. Prolonged release of bone morphogenetic protein-2 in vivo by gene transfection with DNA-functionalized calcium phosphate nanoparticle-loaded collagen scaffolds. Materials Science and Engineering: C 2018;92:172–83. https://doi.org/10.1016/j.msec.2018.06.047.
[226] Raftery RM, Mencía-Castaño I, Sperger S, Chen G, Cavanagh B, Feichtinger GA, et al. Delivery of the improved BMP-2-Advanced plasmid DNA within a gene-activated scaffold accelerates mesenchymal stem cell osteogenesis and critical size defect repair. Journal of Controlled Release 2018;283:20–31. https://doi.org/10.1016/j.jconrel.2018.05.022.
[227] McMillan A, Nguyen MK, Gonzalez-Fernandez T, Ge P, Yu X, Murphy WL, et al. Dual non-viral gene delivery from microparticles within 3D high-density stem cell constructs for enhanced bone tissue engineering. Biomaterials 2018;161:240–55. https://doi.org/10.1016/j.biomaterials.2018.01.006.
[228] Rinker TE, Philbrick BD, Hettiaratchi MH, Smalley DM, McDevitt TC, Temenoff JS. Microparticle-mediated sequestration of cell-secreted proteins to modulate chondrocytic differentiation. Acta Biomaterialia 2018;68:125–36. https://doi.org/10.1016/j.actbio.2017.12.038.
[229] Delplace V, Ortin-Martinez A, Tsai ELS, Amin AN, Wallace V, Shoichet MS. Controlled release strategy designed for intravitreal protein delivery to the retina. Journal of Controlled Release 2019;293:10–20. https://doi.org/10.1016/j.jconrel.2018.11.012.
[230] Dai J, Long W, Liang Z, Wen L, Yang F, Chen G. A novel vehicle for local protein delivery to the inner ear: injectable and biodegradable thermosensitive hydrogel loaded with PLGA nanoparticles. Drug Development and Industrial Pharmacy 2018;44:89–98. https://doi.org/10.1080/03639045.2017.1373803.